AD_____

Award Number: W81XWH-11-1-0459

TITLE: Innovative T Cell-Targeted Therapy for Ovarian Cancer

PRINCIPAL INVESTIGATOR: Laurence JN Cooper, MD, PhD

CONTRACTING ORGANIZATION: The University of Texas MD Anderson Cancer Center

Houston, Texas 77030-4009

REPORT DATE: October 2013

TYPE OF REPORT: Annual

PREPARED FOR: U.S. Army Medical Research and Materiel Command
Fort Detrick, Maryland 21702-5012

REPORT DOCUMENTATION PAGE

Form Approved
OMB No. 0704-0188

1. REPORT DATE *(DD-MM-YYYY)*	2. REPORT TYPE	3. DATES COVERED *(From - To)*
October 2013	Annual	30 Sep 2013 - 29 Sep 2014

4. TITLE AND SUBTITLE

Innovative T Cell-Targeted Therapy for Ovarian Cancer

5a. CONTRACT NUMBER

5b. GRANT NUMBER
W81XWH-11-1-0459

5c. PROGRAM ELEMENT NUMBER

6. AUTHOR(S)

Laurence James Neil Cooper, MD, PhD

E-MAIL: ljncooper@mdanderson.org

5d. PROJECT NUMBER

5e. TASK NUMBER

5f. WORK UNIT NUMBER

7. PERFORMING ORGANIZATION NAME(S) AND ADDRESS(ES)

University of Texas MD Anderson Cancer Center

Houston, Texas 77030-4009

8. PERFORMING ORGANIZATION REPORT NUMBER

9. SPONSORING / MONITORING AGENCY NAME(S) AND ADDRESS(ES)
U.S. Army Medical Research and Materiel Command
Fort Detrick, Maryland 21702-5012

10. SPONSOR/MONITOR'S ACRONYM(S)

11. SPONSOR/MONITOR'S REPORT NUMBER(S)

12. DISTRIBUTION / AVAILABILITY STATEMENT

Approved for Public Release; Distribution Unlimited

13. SUPPLEMENTARY NOTES

14. ABSTRACT

Major advances have been made in two main areas. Firstly, Receptor tyrosine kinase-like orphan receptor-1 (ROR1) was identified as a tumor antigen expressed on ovarian cancer (OvCa), but not expressed on normal tissue(s). Second generation chimeric antigen receptors (CARs) were designed with CD3z and either CD28 or CD137 endodomains fused to the antigen-binding region of a ROR1-specific monoclonal antibody (clone 4A5). CARs were stably expressed in T cells following *Sleeping Beauty* transposition and propagation on ROR1$^+$ artificial antigen presenting cells (aAPC). Re-directed cytolysis of ROR1$^+$ OvCa cell lines by CAR$^+$ T cells was demonstrated. Secondly, the anti-tumor activity of γδ T cells was harnessed to kill OvCa. Our aAPC were used to massively expand for the first time a polyclonal population of γδ T cells for immunotherapy. OvCa cell lines and xenografts were eliminated by these massively expanded polyclonal γδ T cells. γδ T cells are HLA-unrestricted and rapid expansion with our novel aAPCs may also have utility as off the shelf therapy for Ebola and other virus and bacteria mediated outbreaks.

15. SUBJECT TERMS

ROR1, γδ T cells, adoptive T cell therapy, ovarian cancer, chimeric antigen receptor (CAR)

16. SECURITY CLASSIFICATION OF:			17. LIMITATION OF ABSTRACT	18. NUMBER OF PAGES	19a. NAME OF RESPONSIBLE PERSON
a. REPORT	b. ABSTRACT	c. THIS PAGE			USAMRMC,
U	U	U	UU	102	19b. TELEPHONE NUMBER *(include area code)*

TABLE OF CONTENTS

INTRODUCTION

Ovarian cancer, hypoxia, and tumor antigens. Relapsed ovarian cancer (OvCa) is refractory to current therapies in many cases and remains a lethal disease for women worldwide.[1, 2] Advanced ovarian tumors have significant areas that are hypoxic (low O_2 concentration), which can lead to therapeutic escape and relapse in women who initially respond to therapy.[3-5] Therapies targeting tumor-associated antigens (TAAs) expressed in both hypoxic and normoxic regions of ovarian tumors could dramatically increase survivorship in women with advanced disease. c-Met, hepatocyte growth factor receptor (HGFR), has been identified as a candidate TAA because of its well-described expression on OvCa that increases in hypoxia.[6-8] However, c-Met is also expressed on normal tissues, such as liver and lung,[9] thereby complicating its utility as a TAA for cell-based therapy. In contrast to c-Met, the TAA receptor tyrosine kinase-like orphan receptor-1 (ROR1) is not expressed on normal adult tissues, but is expressed on a variety of cancers, including OvCa.[10-12] ROR1 expression was maintained in hypoxia in OvCa cell lines (**Figure 1**), suggesting that targeting ROR1 may be a safe and effective strategy for OvCa immunotherapy.

Chimeric Antigen Receptors. Chimeric antigen receptors (CARs) are employed to re-direct T-cell specificity to TAAs. They are fashioned by fusing T-cell signaling endodomains (CD3ζ, CD28, and CD137) to a single chain variable fragment (scFv) derived from a monoclonal antibody (mAb) with specificity to a cell surface TAA. Upon docking with TAA the introduced CAR activates genetically modified T cells outside of the constraints of major histocompatibility complex (MHC) interaction with the endogenous T-cell receptor (TCR). The CAR contains both signal 1 (CD3ζ) and signal 2 (CD28 or CD137) to achieve full T-cell activation. Clinical trials are investigating the therapeutic efficacy of CAR-based therapies.[13] Patients with refractory B-cell malignancies who were recently treated with CD19-specific CAR^+ T cells employing a CD137 endodomain achieved complete responses.[14, 15] Thus, ROR1 was targeted in this study with CAR^+ T cells expressing either CD28 (ROR1RCD28) or CD137 (ROR1RCD137) endodomains (**Appendix 1**).

Adoptive T-cell therapy, graft-versus-host disease, and γδ T cells. Allogeneic adoptive T-cell therapy (allo-ACT) is a cancer treatment modality used in clinical trials. Allo-ACT is particularly useful when autologous T cells cannot be generated, *e.g.*, after/during chemotherapy.[16, 17] However, there is the risk of graft-versus-host disease (GvHD) in allo-ACT, where donor TCRαβ inappropriately recognizes the host MHC leading the infused T cells to attack normal tissues. It is difficult to predict GvHD incidence because specificity of the donort-derived TCRαβ chains are uniquely educated within individuals.[18] T cells can be dichotomized into two main subsets based on their TCRs. The conventional αβ T cells express TCRαβ and constitute ~95% of the circulating T-cell pool. In contrast, γδ T cells are less frequent (1-10% of peripheral-blood-derived T cells) and are characterized by TCRγδ. While αβ T cells recognize peptides in the context of MHC, γδ T cells do not necessarily recognize MHC and most of the antigens they recognize are outside of MHC presentation altogether. Therefore, γδ T cells have a reduced risk for GvHD and appear to be a safer option for allogeneic allo-ACT compared with T cells expressing αβTCR.[19]

γδ T-cell numeric expansion and utility in cancer therapy. Bisphosphonates have been used to propagate mono- and oligo-clonal subsets of human peripheral blood-derived γδ T cells. The utility of clinical-grade bisphosphonates in γδ T-cell expansion was serendipitously discovered when patients with bone diseases, e.g. osteoporosis, sarcoma, etc…, were treated with bisphosphonates to regenerate their bone and sizeable expansions of γδ T cells were subsequently observed *in vivo*.[20] The bisphosphonate-derived Vδ2 T cells are reactive to metabolites in the cholesterol synthesis pathway and display natural anti-tumor reactivity, because tumors are commonly dependent upon cholesterol-rich lipid rafts for growth factor signaling. Moreover, γδ T cells are regarded in general as a critical part of the natural anti-tumor response.[21, 22] Clinical trials have investigated the efficacy of bisphosphonates in tumor therapy with some promising results in both hematological and solid cancers, including OvCa, but were not curative.[23] In contrast, long term survivorship of patients following allogeneic TCRαβ-depleted hematopoietic stem-cell transplantation (HSCT) was predictive based on increased frequency of peripheral γδ T cells that were primarily of Vδ1 origin.[24-26] Polyclonal γδ T cell expansion has not been achieved, which limits the ability to use both anti-tumor subsets of γδ T cells in anti-cancer therapy. A major problem with attempting to *ex vivo* propagate γδ T cells to clinically-appealing numbers is that conventional strategies to expand αβ T cells, *e.g.*, with high-dose IL-2 and OKT3 (anti-CD3), do not support long-term growth of γδ T cells in tissue culture. Furthermore, there are very limited starting

quantities of γδ T cells (1-10% of peripheral T cells). The expansion schema used in our lab centers around using K562-derived artificial antigen presenting cells (aAPC) that express cytokines, co-stimulatory molecules, and TAA as feeder cells to support T-cell growth to clinically relevant numbers. K562 cells are natural targets for allogeneic γδ T cells, and for the first time, our K562 genetically modified aAPC enables massive expansion of all three subsets of γδ T cells, with similar kinetics as αβ T cells. Our γδ T cells can now be massively expanded on our aAPC in compliance with current good laboratory practice (cGLP) and current good manufacturing practices (cGMP) and thus can be rapidly translated into clinical trials. The first clinical trials using *Sleeping Beauty* transposition and aAPC technology is currently open at MD Anderson for treating B cell leukemia with allogeneic αβ T cells re-directed to leukemia with a CD19-specific CAR.

***Sleeping Beauty* transposition and aAPC-based T-cell expansion.** As with the CD19-specific CAR, ROR1 CARs can be expressed in T cells with the *Sleeping Beauty* transposase/transposon gene transfer system. *Sleeping Beauty* transposition is a non-viral gene cut-and-paste mechanism where the transposase enzyme is transiently expressed in the cell, makes excisions at inverted repeats flanking the transposon containing the CAR, and integrates the excised transposon into TA repeats within the genome.[27] After a few days, the transposase enzyme is no longer expressed, and long-term stability and expression of the transposon can be readily achieved. Nucleofection is used to electroporate peripheral blood mononuclear cells (PBMC) with CAR transposon and *Sleeping Beauty* transposase, and stimulations with γ-irradiated aAPC are applied weekly to the cells along with recombinant interleukin-2 (IL-2) and interleukin-21 (IL-21).[28] The aAPC culture imposes selective pressure for selective CAR^+ T-cell propagation through (i) corresponding antigen expression, (ii) co-stimulation, and (iii) cytokine support, and after four weeks the culture contains >90% CAR^+ T cells at clinically relevant numbers (**Appendix 2**). The electroporated/propagated CAR^+ T cells kill tumors and secrete pro-inflammatory cytokines in a CAR- and antigen-restricted manner, and can allow for conditional production of pro-inflammatory molecules in a canonically immunosuppressive tumor microenvironment.

IL-17 and ovarian cancer. IL-17-polarized T cells exhibit anti-tumor efficacy and are sought after cell lineage for adoptive T cell therapy. More specifically, IL-17 expression and presence of IL-17 producing cell types in tumors are positively associated with survivorship in ovarian cancer.[29, 30] IL-17 is well described to induce pro-inflammatory processes, which can be advantageous in cancer therapy.[31] $CD4^+$ T cells, $CD8^+$ T cells, and γδ T cells have been described as IL-17 producers, and are named Th17, Tc17, and Tγδ17, respectively.[32] Importantly, Th17 cells are inversely correlated with regulatory T cells (Tregs), and Tregs often promote tumor growth.[33, 34] It was recently shown that inducible co-stimulator (ICOS) polarized $CD4^+$ T cells towards Th17 lineage, and that CD28 co-stimulation reversed the polarization and made the $CD4^+$ T cells express interferon-γ (IFNγ).[35] This is important for the current aAPC expansion strategy because the aAPC express CD86, a ligand for CD28, and most aAPC-expanded T cells are restricted to IFNγ production and not IL-17. γδ T cells are also known to polarize towards either IFNγ or IL-17 producing lineages, although the co-stimulatory requirements are unknown. CD27 expression predicts for IFNγ producing γδ T cells, whereas $CD27^{neg}$ γδ T cells are commonly IL-17 producing lineages.[36] Optimization of the co-stimulatory molecules on the aAPC could allow skewing towards ideal cytokine production and anti-tumor effect that can be induced in the hypoxic environment by T cells.

Summary. This project accomplished (i) targeting of ovarian cancer with ROR1-specific T cells under conditions of normoxia and hypoxia and (ii) optimization of the co-stimulation requirements for maximum anti-tumor efficacy and pro-inflammatory cytokine production by the T cells, especially IL-17, in the ovarian tumors. Our *Sleeping Beauty* gene transfer and aAPC technology were integral in evaluating the hypotheses, and data generated by this study will serve as the basis for initiating a ROR1 CAR T-cells clinical trial for the safe and effective treatment of disease-resistant ovarian cancer. Furthermore, for human γδ T cells, we (iii) massively expanded three γδ T cells subsets in culture with our aAPC, and (iv) showed our expanded human γδ T cells killed OvCa tumor cells in vitro. T-cells expanded on aAPC are in clinical trials so we have a direct path to clinical translation of our γδ T cells for ovarian cancer.

KEYWORDS

ROR1, γδ T cells, adoptive T cell therapy, ovarian cancer (OvCa), chimeric antigen receptor (CAR), artificial antigen presenting cells (aAPC)

BODY

We **hypothesized** that cell-based therapies for OvCa can be generated by (i) targeting ROR1 with CAR$^+$ T cells and (ii) expanding polyclonal γδ T cells for clinical use where optimization of their endogenous co-stimulation would maximize anti-tumor efficacy.

Specific Aim #1: To evaluate the ability of ROR1-specific CAR to re-direct the specificity of T cells to kill OvCa. Recent clinical trials treating refractory B-cell malignancies with CD19-specific CAR$^+$ T cells achieved complete responses using a CD137 endodomain instead of chimeric CD28.[15] It is unknown whether the same would apply to targeting ROR1. Two second generation CAR transposons were generated with CD28 (ROR1RCD28) and CD137 (ROR1RCD137) endodomains[14, 15]. The following ovarian cancer cell lines were kindly given to us by Dr. Bast (UTMDACC): A2780, EFO21, EFO27, IGROV1, OC314, and UPN251. Identities of all cell lines were confirmed by STR Fingerprinting (Characterized Cell Line Core, UTMDACC) and were found to be mycoplasma free. Flow cytometry was used to analyze ROR1 antigen levels on the available OvCa cell lines following three days growth in normoxia (20% O_2) or hypoxia (1% O_2). As anticipated, ROR1 was expressed on 5 of 6 cell lines tested and expression was maintained or increased in hypoxic conditions (Figure 1). This was the first report of ROR1 expression in hypoxia to our knowledge, and corroborated previous reports of ROR1 expression in OvCa.[12] After establishing that ROR1 is expressed in both high and low oxygen tension, OvCa was targeted with ROR1-specific CAR$^+$ T cells. Healthy donor-derived peripheral blood mononuclear cells (PBMC) were electroporated with *Sleeping Beauty* transposase and either ROR1RCD28 or ROR1RCD137 transposons (Appendix 1) then stimulated with ROR1$^+$ aAPC, IL-2, and IL-21 (Appendix 2). Sham electroporations were be sorted and stimulated in parallel with OKT3 (agonistic CD3 antibody)-loaded aAPC to propagate CAR^{neg} T cells for negative controls. aAPC were phenotyped for antigens (CD19 and ROR1), membrane bound IL15 (fused to IL-15Rα), co-stimulatory molecules (CD86 and CD137L), and Fc receptors (CD32 and CD64) before stimulations (Appendix 3). After 36 days of expansion on aAPC, >10^9 CAR$^+$ T cells were propagated from 10^6 CAR$^+$ T cells at the start of the culture (Figure 2). Stable CAR expression was observed with both ROR1RCD28 and ROR1RCD137 indicating that there was imposed selective pressure for CAR expression though cognate antigen expression on aAPC (Figure 3). Extended phenotypic analysis for CD3, CD4, CD8, CD56, CD27, CD28, CD62L, CCR7, CD38, CD95, TCRγδ, and TCRαβ were evaluated by flow cytometry. Interferon-γ (IFNγ) expression were evaluated by intracellular cytokine staining following TCR stimulation (PMA/Ionomycin) and CAR stimulation from co-culture with EL4-ROR1^{neg} and EL4-ROR1$^+$ tumor targets. Ovarian cancer cell lines (A2780, EFO21, EFO27, IGROV1, OC314, and UPN251) were profiled for ROR1 expression in normoxia (20% O_2) and hypoxia (1% O_2). Four-hour CRA was used to evaluate cytotoxicity against the OvCa and EL4 tumor targets in normoxia and hypoxia. OC314 (ROR1$^+$) cell line was genetically modified to express mKate ewd fluorescent protein and *firefly Luciferase* (*ffLuc*) to measure tumor burden by fluorescence and bioluminescent imaging (BLI), respectively. *In vivo* tumor clearance of established OC314-mKate-*ffLuc* xenografts (intraperitoneal, i.p.) by CAR$^+$ T cells (i.p.) in immunocompromised (NOD.*scid*.γc$^{-/-}$; NSG) mice were monitored by non-invasive BLI following subcutaneous (s.c.) D-Luciferin administration. Immunohistochemistry and fluorescence were used to corroborate BLI data post-mortem. Both ROR1RCD28 and ROR1RCD137 displayed minimal killing of EL4-ROR1^{neg} cells (**Figure 4A**) but significantly higher killing of EL4-ROR1$^+$ cells compared to CAR^{neg} T cells (**Figure 4B**). Similarly, A2780 (ROR1^{neg}) OvCa cells were lysed at the same levels by CAR$^+$ T cells as CAR^{neg} T cells (**Figure 4C**), whereas EFO27 (ROR1$^+$) OvCa cells were significantly killed by CAR$^+$ cells compared to CAR^{neg} T cells (**Figure 4D**). Thus, CAR$^+$ T cells were specifically re-directed to ROR1 expressed on OvCa. As ROR1 expression on OvCa has only recently been elucidated and has not yet been tested as a target for OvCa, ROR1-specific CAR T cells can thus be used for the first time in OvCa treatment.

Specific Aim #2: To assess the inherent cytolysis of γδ T cells against OvCa. We established that γδ T cells propagated on aAPC in parallel with CD19-specific CAR$^+$ γδ T cells and maintained a polyclonal distribution of γ and δ TCR chains.[37] This was a major advance as only one subset (Vγ9Vδ2) of γδ T cells had been previously expanded for human application, yet other γδ T-cell subsets exhibit anti-tumor immunity. Thus, studies were initiated to evaluate whether aAPC would drive γδ T-cell proliferation in the absence of CAR$^+$ T cells and if these γδ T cell would express polyclonal TCRγδ repertoire.

Healthy donor-derived PBMC were first depleted of NK cells with CD56 microbeads on paramagnetic columns, and then paramagnetically sorted for γδ T cells with TCRγ/δ–ιsolation kit then stimulated weekly with aAPC feeder cells and exogenous IL-2 and IL-21. The other fraction of the paramagnetic bead sorting, comprising mainly of αβ T cells, were stimulated with OKT3-loaded aAPC to propagate αβ T cells for negative staining controls. Extended phenotypic analysis of cell surface markers (as in Aim#1 with TCRδ1, TCRδ2, and TCRγ9) was performed at the end of the culture period by flow cytometry to assess TCR distribution and T cell, homing, and memory phenotype in the culture. TCRγδ allele expression was evaluated by our direct TCR expression array (DTEA[46]) using digital probes to quantify mRNA expressing TCR chains and validated by flow cytometry. Cytokine release following TCR stimulation (PMA/Ionomycin) and co-culture with OvCa cell lines was assessed by Luminex. Standard 4-hour CRA was used to evaluate cytotoxicity towards OvCa cell lines detailed in Aim#1 with healthy donor-derived B cells serving as negative controls. CAOV3 cell line was genetically modified to express mKate and *firefly Luciferase* (*ffLuc*) as done for OC314 in Aim#1. The ability of i.p. injected γδ T cells to eliminate i.p. established CAOV3-mKate-*ffLuc* xenografts in NSG mice was evaluated by BLI during the course of the experiment then immunohistochemistry and fluorescence were used to corroborate BLI data post-mortem.

γδ T cells were in limited quantities in the starting PBMC (3.2% ± 1.2%; mean ± SD; n=4), but after sorting and expansion for 22 days on aAPC the cultures were highly pure for γδ T cells (97.9% ± 0.6%) as assessed by co-expression of $CD3^+$ and $TCR\gamma\delta^+$ (**Figure 5A**). Cultures yielded $>10^9$ γδ T cells from $<10^6$ total cells in three weeks of co-culture (**Figure 5B**), which represented $4.9x10^3 \pm 1.7x10^3$ fold change over the culture period (**Figure 5C**). Similar results were seen with γδ T cells sorted from umbilical cord blood (UCB) by fluorescence activated cell sorting (FACS) and stimulated as was done with PBMC (data not shown). Altogether this suggested the aAPC, not CAR, led to growth of γδ T cells in the culture system.
Only three TCRγδ chain-specific antibodies are commercially available limiting the detection of γδ T cell repertoire outside of Vδ1, Vδ2, and Vγ9. Thus, the direct T cell expression array "DTEA[46]" was utilized to detect TCR mRNA in the γδ T-cell cultures and flow cytometry was used to corroborate mRNA data, when applicable. All three Vδ alleles, i.e. Vδ1, Vδ2, and Vδ3, were detected by both flow cytometry (**Figure 6A**) and DTEA (**Figure 6C**) with similar frequencies following the trend of Vδ1>Vδ3>Vδ2. The Vδ3 subset was shown to be present within the $V\delta1^{neg}V\delta2^{neg}$ population with DTEA analysis which allowed for inferential detection by flow cytometry.[37] Most Vδ2 cells paired with Vγ9 (**Figure 6B**), as expected, and DTEA revealed that Vγ2, Vγ5, Vγ7, Vγ8 (two alleles), Vγ10, and Vγ11 mRNA were expressed along with Vγ9 in the aAPC-expanded γδ T cell cultures (**Figure 6D**). All work was performed under GLP for direct clinical translation. Thus, we report the first clinically-relevant expansion of polyclonal γδ T cells for human use.

To determine whether γδ T cells would foster an inflammatory environment during therapy, a multiplex analysis (27-Plex Luminex) of cytokines and chemokines was performed on T cells following culture on aAPC. Phorbol myristate acetate (PMA) and Ionomycin mimic TCR activation by stimulating protein kinase C (PKC) and increasing intracellular Ca^{2+} to activate phospholipase C (PLC), respectively.[38, 39] There was no significant production of anti-inflammatory Th2 cytokines IL-4, IL-5, and IL-13, and there was only a small increase in IL-10 production from baseline (**Figure 7A**). In contrast, IL-1Ra, IL-6, and IL-17 were significantly secreted by γδ T cells and have roles together for IL-17 inflammatory responses important γδ T cells in killing OvCa (**Figure 7B**).[31, 40] Moreover, pro-inflammatory Th1 cytokines IL-2, IL-12 (p70), interferon-γ (IFNγ), and tumor necrosis factor-α (TNFα) were all significantly produced by γδ T cells when TCR was stimulated compared to mock stimulated controls (**Figure 7C**). Extremely high expression of chemokines CCL3 (macrophage inflammatory protein-1α; MIP1α), CCL4 (MIP1β), and CCL5 (regulated and normal T cell expressed and secreted; RANTES) were also detected (**Figure 7D**). In aggregate, TCR stimulation in γδ T cells led to a largely pro-inflammatory response desired for cell-based OvCa therapy.

It is of interest to employ γδ T cells for adoptive T cell therapy because they have less risk for graft-versus-host disease (GvHD). γδ T cells did not proliferate or produce IFNγ in response to healthy donor B cells (selected for their relative abundance in PBMC and ability to function as APC) nor did they have any significant killing of normal cells (**Figure 8; upper left**). Proliferation, IFNγ production, and killing were observed in positive controls, which attests to their functional capacity while leaving healthy cells untouched (data not shown). In addition to having fewer responses to normal cells, γδ T cells displayed an inherent ability to kill ovarian cancer. All OvCa cell lines tested in standard 4-hour chromium release assays were lysed by γδ T cells but

healthy B cells were not killed (**Figure 8**). The order of killing tumor cell lines was cell line and donor dependent, which could not be directly correlated to a particular Vδ subset of deference to a certain combination of Vδ lineages (**Figure 8**). In aggregate, γδ T cells showed broad anti-tumor effects with limited reactivity to healthy cells.

Lastly, the ability of γδ T cells to target and eliminate established OvCa xenografts *in vivo* was evaluated. NSG mice were used for their ability to accept human tumor xenografts well and were injected with CAOV3-*ffLuc*-mKate tumor cells i.p. then randomized into treatment groups. Stable disease was established after 8 days of engraftment and either PBS (negative control) or γδ T cells (escalating doses) were administered i.p. to the mice. Tumor burden was monitored during the experiment with non-invasive bioluminescence imaging (BLI) following D-luciferin administration (**Figure 9A**). γδ T cells significantly ($p = 0.0005$) eliminated established CAOV3 tumors during the course of the experiment whereas mice treated with vehicle (PBS) retained high tumor burden (**Figure 9B-C**). Persistent OvCa disease was evident in the PBS group by (i) flux maintenance to day 43 (**Figure 9B**), (ii) increase in flux to day 79 (**Figure 9D**), and (iii) death of mice (n=3). In contrast, mice treated with γδ T cells displayed significantly lower CAOV3-*ffLuc*-mKate flux after 79 days post-engraftment compared to the day prior to treatment (day 7 post-engraftment) and no mice died in this group (**Figure 9D**). Thus, polyclonal γδ T cells were effective in treating OvCa *in vivo* and represent an attractive approach to cell-based OvCa treatment.

Specific Aim #3: Examine the role of endogenous co-stimulation for pro-inflammatory γδ T cell expansion in both normoxia and hypoxia. In order to maximize the anti-tumor efficacy of γδ T cells for OvCa therapy, it is important to distinguish what molecules on aAPC drive their proliferation. The aAPC discussed in Aims #1 and #2 co-expressed CD86 and 4-1BBL co-stimulatory molecules, which were high value targets for these studies. It was also advantageous to examine IL-17/IFNγ polarization and growth in hypoxia in the same studies. Reports in αβ T cells show that CD70 and CD86 led to IFNγ production but ICOS-L correlated with IL-17. Whether the same is true for γδ T cells is not currently known nor is their ability to proliferate in hypoxia with aAPC as a stimulus.

Normal donor PBMC were sorted for γδ T cells (TCRγ/δ isolation kit) and expanded in parallel in 1% O_2 and 20% O_2 on aAPC for 9 days with aAPC expressing differing co-stimulatory ligands: (i) none, (ii) CD70, (iii) CD86, (iv) CD137L (4-1BBL), or (v) CD275 (ICOSL). Co-cultures were either given no cytokine, IL-2, IL-21, or both IL-2 and IL-21. After stimulation, cells were counted for proliferation using trypan blue exclusion. Gene expression was profiled using the NanoString nCounter platform to identify candidate genes crucial for expansion in hypoxia. Polarization towards IL-17 or IFNγ producing lineages was evaluated following expansion by flow cytometry and intracellular cytokine staining. Cytolytic potency of cells expanded on different co-stimulatory ligands were evaluated by ^{51}Chromium release assay (CRA) when targeted to ovarian cancer cell lines in both hypoxia and normoxia. Expanded cells were either mock activated or stimulated with leukocyte activation cocktail (LAC; PMA/Ionomycin) in the presence of secretory pathway inhibitor GlogiPlug for 6 hours at 37°C in normoxia or hypoxia then stained for CD3, TCRγδ, IFNγ, and IL-17 and analyzed by flow cytometry. As anticipated, the γδ T cells did not appreciably expand in the absence of cytokine or aAPC. However, the addition of both IL-21 and IL-2/IL-21 led to γδ T-cell numeric expansion especially when aAPC expressed 4-1BBL and with a combination of CD86 and 4-1BBL (**Figure 10A and 10C**). It was also interesting that there was proliferative synergy between CD86 and 4-1BBL. Significantly, robust expansion of γδ T cells was observed in hypoxia in multiple scenarios, which corroborated the approach to expand hypoxia-sensitive γδ T cells. Culture conditions could be adapted to result in emergence of T cells that produced IL-17 and IFNγ (**Figure 10B and 10D**). The most IL-17 was observed with IL-21/4-1BBL in hypoxia and with IL-2/IL-21/4-1BBL in normoxia. The same conditions led to IFNγ production with the additional condition of IL-2/IL-21/CD86/4-1BBL in normoxia. It is also interesting that the absence of oxygen or lack of IL-2 abrogated the functionality of cells stimulated with CD86/4-1BBL. Moreover, IL-17 production in normoxia with IL-2/IL-21 was halted with the addition of CD86 but had no effect on IFNγ (**Figure 10D, left side, top and bottom panels**). It appears that 4-1BBL is the crucial molecule on aAPC to drive γδ T-cell proliferation and to yield IL-17 producing lineages, especially in normoxia. It was also unexpected that ICOS-L neither induced considerable growth nor led to IL-17 production. Nonetheless, the culture system can be adapted to generate γδ T cells that can produce IFNγ, IL-17, or both.

The long-term objective of this study was to create novel T cell-based treatments of disease-resistant ovarian cancer that can function in the hostile tumor environment with minimal toxicity to normal tissues. Our ROR1 chimeric antigen receptor (CAR) T-cells kill OvCa cells in both hypoxia and normoxia. Our expanded human γδ T cells killed OvCa tumor cells in vitro and in a mouse model.

KEY RESEARCH ACCOMPLISHMENTS

Major advances have been made on this study. There has been significant headway in targeting OvCa with both CAR^+ T cells and with polyclonal γδ T cells.

- ROR1 CAR T-cells kill ROR1+ cancer cells.
- γδ T cells under hypoxia can proliferate with similar kinetics as in normoxia.
- γδ T cells produce both IFNγ and IL-17.
- We are now able to routinely massively expand three γδ T cells subsets in culture with our aAPC.
- Our expanded human γδ T cells killed OvCa tumor cells in vitro and in a mouse model.

CONCLUSION

We provide two T cell-based approaches for OvCa treatment that are both directly applicable to the clinic. First, ROR1 was shown to be expressed on OvCa in both hypoxia and normoxia, and CAR^+ T cells re-directed to ROR1 could specifically and efficiently lyse OvCa targets. Second, polyclonal γδ T cells were expanded to clinically-relevant numbers on aAPC, could lyse many OvCa cell lines, and eliminated OvCa xenografts *in vivo*. Thus, translation of these T cell therapies will give women with advanced OvCa novel options in their treatment. γδ T cells are HLA-unrestricted and rapid expansion with our novel aAPCs may also have utility as off the shelf therapy for Ebola and other virus and bacteria mediated outbreaks.

PUBLICATIONS, ABSTRACTS, AND PRESENTATIONS

Publications

Deniger, DC 2013 T-cell treatments for solid and hematological tumors. Ph.D. Dissertation, *UT GSBS Dissertations and Theses (Open Access).* Paper 377.
http://digitalcommons.library.tmc.edu/utgsbs_dissertations/377

Deniger DC, Maiti S, Switzer KC, Mi T, Ramachandran V, Hurton LV, Ang S, Olivares S, Rabinovich B, Huls H, Lee DA, Bast RC, Jr., Champlin RE, Cooper LJN. Artificial antigen presenting cells propagate polyclonal gamma delta T cells with broad anti-tumor activity. *Clinical Cancer Res*, (publication online May 15, 2014) http://www.ncbi.nlm.nih.gov/pubmed/24833662.

Deniger DC, Switzer K, Mi T, Hurton L, Singh H, Huls H *et al.* Bi-specific T cells expressing polyclonal repertoire of endogenous gamma delta T-cell receptors and introduced CD19-specific chimeric antigen receptor. *Molecular Therapy* 2012; 21(3):638-47. http://www.ncbi.nlm.nih.gov/pubmed/23295945. doi: 10.1038/mt.2012.267.

Zhang M, Maiti S, Bernatchez C, Huls H, Rabinovich B, Champlin RE, Vence LM, Hwu P, Radvanyi L, Cooper LJ. A new approach to simultaneously quantify both TCR α- and β-chain diversity after adoptive immunotherapy. *Clin Cancer Res* 2012. 18: 4733-42. doi: 10.1158/1078-0432.CCR-11-3234. PMID: 22761473; PMCID: PMC3823368. (**DTEA** NanoString assay project was partially funded by Department of Defense).

Presentations

Deniger DC, Maiti S, Switzer K, Mi T, Hurton L, Singh H, Huls H, Olivares S, Cooper LJN. Gamma Delta T-Cells: Natural Tumor Killers Amplified by Chimeric Antigen Receptors. Society of Immunotherapy for Cancer 27th Annual Meeting, Bethesda, MD, October 2012.

INVENTIONS, PATENTS AND LICENSES

Nothing to report.

REPORTABLE OUTCOMES

We have accomplished the following:

- ROR1 CAR specific T-cells massive expansion in on our ROR1+ artificial antigen presenting cells (aAPC) culture.
- ROR1 CAR specific T-cells kill ovarian cancer cells (OvCa) in culture and in mouse models.
- γδ T cells Vδ1, Vδ2, and Vδ3 subsets were massively expanded in culture for the first time on our novel aAPCs.
- Comprehensive γδ T cells subset quantitation, for the first time, using specific mRNA counting on our direct T cell expression array (DTEA)[46] (Figure 6d).
- We published the utility of our massively expanded γδ T cells for leukemia in Deniger *et al* (2014)[42] (see also similar work published together by another lab [47], and commentary[48]).

OTHER ACHIEVEMENTS

Drew C. Deniger successfully defended his Ph.D. dissertation41, briefly continued as a postdoctoral fellow with us briefly, before transitioning to NIH/NCI to join the laboratory of Dr. Steven Rosenberg, a key researcher in cellular immunotherapies. Deniger et al, “Clinical implications of ROR1-specific T cells that target B-cell leukemia”, is in preparation43. Dr. Deniger and Cooper are coauthors on manuscripts on pancreatic cancer[44], and CD123 specific CAR T-cells to treat acute myelogenous leukemia (AML)[45].

REFERENCES

1. Rauh-Hain JA, Krivak TC, Del Carmen MG, Olawaiye AB. Ovarian cancer screening and early detection in the general population. *Rev Obstet Gynecol* 2011; **4**(1)**:** 15-21.

2. Pignata S, Cannella L, Leopardo D, Pisano C, Bruni GS, Facchini G. Chemotherapy in epithelial ovarian cancer. *Cancer Lett* 2011; **303**(2)**:** 73-83.

3. Milane L, Duan Z, Amiji M. Role of hypoxia and glycolysis in the development of multi-drug resistance in human tumor cells and the establishment of an orthotopic multi-drug resistant tumor model in nude mice using hypoxic pre-conditioning. *Cancer Cell Int* 2011; **11:** 3.

4. Zhu P, Ning Y, Yao L, Chen M, Xu C. The proliferation, apoptosis, invasion of endothelial-like epithelial ovarian cancer cells induced by hypoxia. *J Exp Clin Cancer Res* 2010; **29:** 124.

5. Galanis A, Pappa A, Giannakakis A, Lanitis E, Dangaj D, Sandaltzopoulos R. Reactive oxygen species and HIF-1 signalling in cancer. *Cancer Lett* 2008; **266**(1)**:** 12-20.

6. Aune G, Lian AM, Tingulstad S, Torp SH, Forsmo S, Reseland JE *et al.* Increased circulating hepatocyte growth factor (HGF): A marker of epithelial ovarian cancer and an indicator of poor prognosis. *Gynecol Oncol* 2011; **121**(2)**:** 402-6.

7. Anglesio MS, George J, Kulbe H, Friedlander M, Rischin D, Lemech C *et al.* IL6-STAT3-HIF signaling and therapeutic response to the angiogenesis inhibitor sunitinib in ovarian clear cell cancer. *Clin Cancer Res* 2011; **17**(8)**:** 2538-48.

8. Huntsman D, Resau JH, Klineberg E, Auersperg N. Comparison of c-met expression in ovarian epithelial tumors and normal epithelia of the female reproductive tract by quantitative laser scan microscopy. *Am J Pathol* 1999; **155**(2)**:** 343-8.

9. Yap TA, Sandhu SK, Alam SM, de Bono JS. HGF/c-MET targeted therapeutics: novel strategies for cancer medicine. *Curr Drug Targets* 2011; **12**(14)**:** 2045-58.

10. Bicocca VT, Chang BH, Kharabi Masouleh B, Muschen M, Loriaux MM, Druker BJ *et al.* Crosstalk between ROR1 and the Pre-B Cell Receptor Promotes Survival of t(1;19) Acute Lymphoblastic Leukemia. *Cancer Cell* 2012; **22**(5)**:** 656-67.

11. Zhang S, Chen L, Cui B, Chuang HY, Yu J, Wang-Rodriguez J *et al.* ROR1 is expressed in human breast cancer and associated with enhanced tumor-cell growth. *PLoS One* 2012; **7**(3)**:** e31127.

12. Zhang S, Chen L, Wang-Rodriguez J, Zhang L, Cui B, Frankel W *et al.* The Onco-Embryonic Antigen ROR1 Is Expressed by a Variety of Human Cancers. *Am J Pathol* 2012; **181**(6)**:** 1903-10.

13. Jena B, Dotti G, Cooper LJ. Redirecting T-cell specificity by introducing a tumor-specific chimeric antigen receptor. *Blood* 2010; **116**(7)**:** 1035-44.

14. Kalos M, Levine BL, Porter DL, Katz S, Grupp SA, Bagg A *et al.* T cells with chimeric antigen receptors have potent antitumor effects and can establish memory in patients with advanced leukemia. *Sci Transl Med* 2011; **3**(95)**:** 95ra73.

15. Porter DL, Levine BL, Kalos M, Bagg A, June CH. Chimeric antigen receptor-modified T cells in chronic lymphoid leukemia. *N Engl J Med* 2011; **365**(8)**:** 725-33.

16. Ringden O, Karlsson H, Olsson R, Omazic B, Uhlin M. The allogeneic graft-versus-cancer effect. *Br J Haematol* 2009; **147**(5)**:** 614-33.

17. Kapp M, Rasche L, Einsele H, Grigoleit GU. Cellular therapy to control tumor progression. *Curr Opin Hematol* 2009; **16**(6)**:** 437-43.

18. Blazar BR, Korngold R, Vallera DA. Recent advances in graft-versus-host disease (GVHD) prevention. *Immunol Rev* 1997; **157:** 79-109.

19. Lamb LS, Jr., Musk P, Ye Z, van Rhee F, Geier SS, Tong JJ *et al.* Human gammadelta(+) T lymphocytes have in vitro graft vs leukemia activity in the absence of an allogeneic response. *Bone Marrow Transplant* 2001; **27**(6)**:** 601-6.

20. Stresing V, Daubine F, Benzaid I, Monkkonen H, Clezardin P. Bisphosphonates in cancer therapy. *Cancer Lett* 2007; **257**(1)**:** 16-35.

21. Bonneville M, O'Brien RL, Born WK. Gammadelta T cell effector functions: a blend of innate programming and acquired plasticity. *Nat Rev Immunol* 2010; **10**(7)**:** 467-78.

22. Gomes AQ, Martins DS, Silva-Santos B. Targeting gammadelta T lymphocytes for cancer immunotherapy: from novel mechanistic insight to clinical application. *Cancer Res* 2010; **70**(24)**:** 10024-7.

23. Chiplunkar S, Dhar S, Wesch D, Kabelitz D. gammadelta T cells in cancer immunotherapy: current status and future prospects. *Immunotherapy* 2009; **1**(4)**:** 663-78.

24. Lamb LS, Jr., Henslee-Downey PJ, Parrish RS, Godder K, Thompson J, Lee C *et al.* Increased frequency of TCR gamma delta + T cells in disease-free survivors following T cell-depleted, partially mismatched, related donor bone marrow transplantation for leukemia. *J Hematother* 1996; **5**(5)**:** 503-9.

25. Lamb LS, Jr., Gee AP, Hazlett LJ, Musk P, Parrish RS, O'Hanlon TP *et al.* Influence of T cell depletion method on circulating gammadelta T cell reconstitution and potential role in the graft-versus-leukemia effect. *Cytotherapy* 1999; **1**(1)**:** 7-19.

26. Godder KT, Henslee-Downey PJ, Mehta J, Park BS, Chiang KY, Abhyankar S *et al.* Long term disease-free survival in acute leukemia patients recovering with increased gammadelta T cells after partially mismatched related donor bone marrow transplantation. *Bone Marrow Transplant* 2007; **39**(12)**:** 751-7.

27. Hackett PB, Largaespada DA, Cooper LJ. A transposon and transposase system for human application. *Mol Ther* 2010; **18**(4)**:** 674-83. PMID 20104209

28. Singh H, Figliola MJ, Dawson MJ, Huls H, Olivares S, Switzer K *et al.* Reprogramming CD19-specific T cells with IL-21 signaling can improve adoptive immunotherapy of B-Lineage malignancies. *Cancer Res* 2011; **71**(10)**:** 3516-27. PMID 21558388

29. Kryczek I, Banerjee M, Cheng P, Vatan L, Szeliga W, Wei S *et al.* Phenotype, distribution, generation, and functional and clinical relevance of Th17 cells in the human tumor environments. *Blood* 2009; **114**(6)**:** 1141-9.

30. Zou W, Restifo NP. T(H)17 cells in tumour immunity and immunotherapy. *Nat Rev Immunol* 2010; **10**(4)**:** 248-56.

31. Xu S, Cao X. Interleukin-17 and its expanding biological functions. *Cell Mol Immunol* 2010; **7**(3)**:** 164-74.

32. Hao J, Wu X, Xia S, Li Z, Wen T, Zhao N *et al.* Current progress in gammadelta T-cell biology. *Cell Mol Immunol* 2010; **7**(6)**:** 409-13.

33. Kryczek I, Wei S, Zou L, Altuwaijri S, Szeliga W, Kolls J *et al.* Cutting edge: Th17 and regulatory T cell dynamics and the regulation by IL-2 in the tumor microenvironment. *J Immunol* 2007; **178**(11)**:** 6730-3.

34. Miyahara Y, Odunsi K, Chen W, Peng G, Matsuzaki J, Wang RF. Generation and regulation of human CD4+ IL-17-producing T cells in ovarian cancer. *Proc Natl Acad Sci U S A* 2008; **105**(40)**:** 15505-10.

35. Paulos CM, Carpenito C, Plesa G, Suhoski MM, Varela-Rohena A, Golovina TN *et al.* The inducible costimulator (ICOS) is critical for the development of human T(H)17 cells. *Sci Transl Med* 2010; **2**(55)**:** 55ra78.

36. Cua DJ, Tato CM. Innate IL-17-producing cells: the sentinels of the immune system. *Nat Rev Immunol* 2010; **10**(7)**:** 479-89.

37. **Deniger** DC, Switzer K, Mi T, Hurton L, Singh H, Huls H *et al.* Bi-specific T cells expressing polyclonal repertoire of endogenous gamma delta T-cell receptors and introduced CD19-specific chimeric antigen receptor. *Molecular Therapy* 2012; 21(3):638-47. http://www.ncbi.nlm.nih.gov/pubmed/23295945. doi: 10.1038/mt.2012.267.

38. Chatila T, Silverman L, Miller R, Geha R. Mechanisms of T cell activation by the calcium ionophore ionomycin. *Journal of immunology* 1989; **143**(4)**:** 1283-9.

39. Iwata M, Ohoka Y, Kuwata T, Asada A. Regulation of T cell apoptosis via T cell receptors and steroid receptors. *Stem cells* 1996; **14**(6)**:** 632-41.

40. Lai D, Wang F, Chen Y, Wang C, Liu S, Lu B *et al.* Human ovarian cancer stem-like cells can be efficiently killed by gammadelta T lymphocytes. *Cancer Immunol Immunother* 2011.

41. **Deniger**, DC 2013 T-cell treatments for solid and hematological tumors. Ph.D. Dissertation, *UT GSBS Dissertations and Theses (Open Access).* Paper 377. http://digitalcommons.library.tmc.edu/utgsbs_dissertations/377

42. **Deniger DC**, Maiti S, Switzer KC, Mi T, Ramachandran V, Hurton LV, Ang S, Olivares S, Rabinovich B, Huls H, Lee DA, Bast RC, Jr., Champlin RE, Cooper LJN. Artificial antigen presenting cells propagate polyclonal gamma delta T cells with broad anti-tumor activity. *Clinical Cancer Res*, (publication online May 15, 2014) http://www.ncbi.nlm.nih.gov/pubmed/24833662.

43. **Deniger DC**, Kipps TJ, Olivares S, Singh H, Maiti S, Hurton LV, Switzer KC, Mi T, Thokala R, Huls H, Wierda WG, Champlin RE, Cooper LJN. Clinical implications of **ROR1**-specific T cells that target B-cell leukemia. Manuscript in preparation.

44. Ramachandran V, Arumugam T, Deng D, Huang H, Srinivas S, **Deniger DC**, Dharmarajan LA, Manickavasagam V, Chatterjee D, Cooper LJN, Lee DA, and Logsdon CD. Molecular and immune mechanism of metastasis regulation in pancreatic cancer. Manuscript in preparation.

45. Thokala R, Olivares S, Switzer KC, Mi T, **Deniger DC**, Singh H, Huls H, Champlin RE, Cooper LJN. CD123-specific T cells target leukemia stem cells and eliminate AML. Manuscript in preparation.

46. Zhang M, Maiti S, Bernatchez C, Huls H, Rabinovich B, Champlin RE, Vence LM, Hwu P, Radvanyi L, Cooper LJ. A new approach to simultaneously quantify both TCR α- and β-chain diversity after adoptive immunotherapy. *Clin Cancer Res* 2012. 18: 4733-42. doi: 10.1158/1078-0432.CCR-11-3234. PMID: 22761473; PMCID: PMC3823368.

47. Fisher J, Yan M, Heuijerjans J, Carter L, Abolhassani A, Frosch J, Wallace R, Flutter B, Hubank M, Klein N, Callard R, Gustafsson K, Anderson J. Neuroblastoma killing properties of V-delta 2 and V-delta2 negative gamma delta T cells following expansion by artificial antigen presenting cells. *Clin Cancer Res* 2014. PMID 24893631.

48. Dechanet-Merville J. Promising cell-based immunotherapy using gamma-delta T Cells: Together is better. *Clin Cancer Res* 2014. PMID 25278452.

APPENDICES

Appendix 1. Schematics of CARs used in studies. Chimeric antigen receptors (CAR) are fusion proteins of (i) antigen-specific binding regions of monoclonal antibodies constructed into single chain variable fragments (scFv), (ii) a hinge region, (iii) an IgG4 constant region (Fc) stalk, (iv) CD28 transmembrane (TM) domain, (v) co-stimulation domain (either CD28 (yellow) or CD137 (blue)), and CD3-zeta T cell signaling domains. ROR1-specific CARs signaling through CD28 (ROR1RCD28; Left) and CD137 (ROR1RCD137; Right).

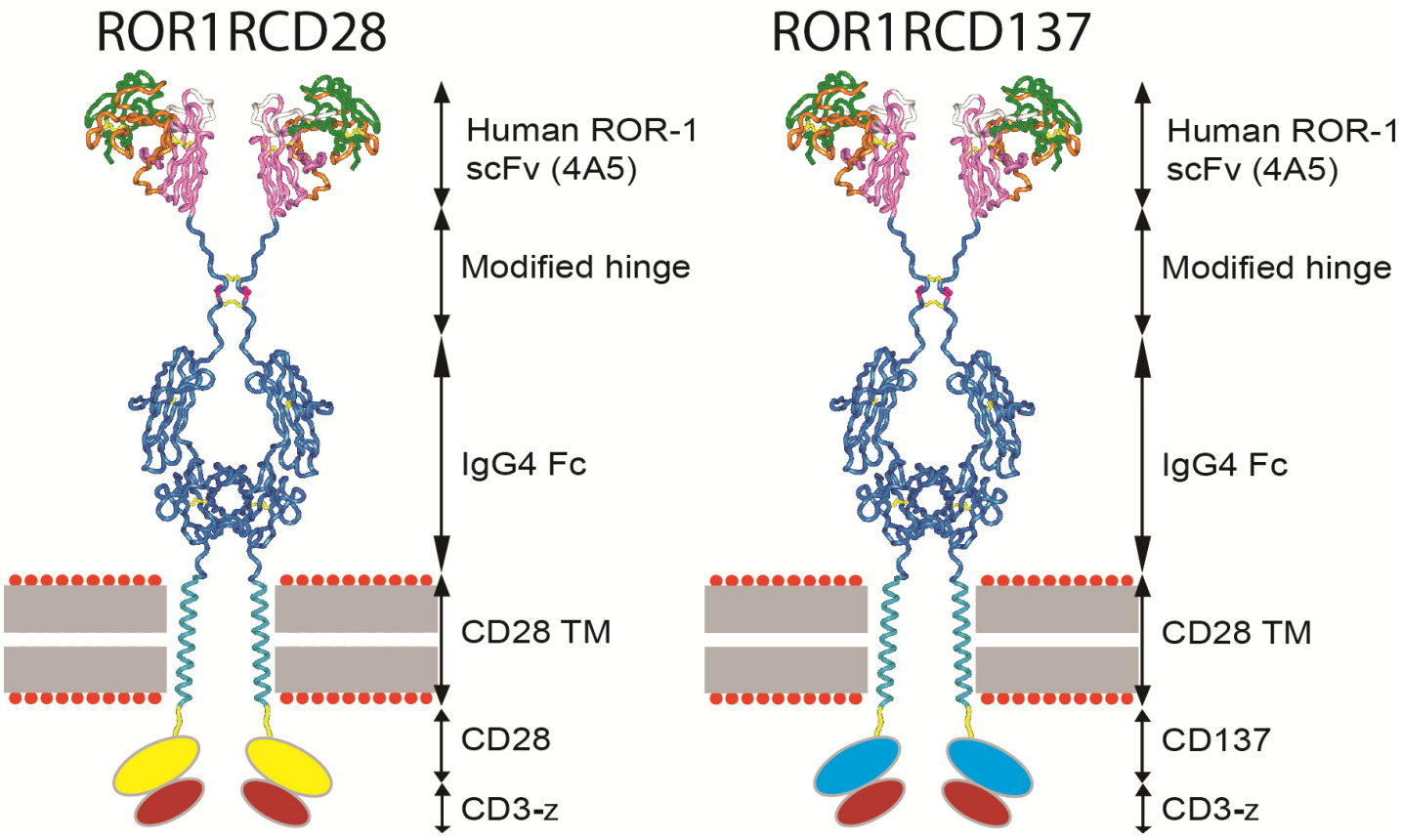

Appendix 2. Schematic for propagation of CAR⁺ T cells. Peripheral blood mononuclear cells (PBMC) were electroporated with *Sleeping Beauty* (SB) plasmids expressing SB transposon (CAR) and SB transposase by Lonza Amaxa nucleofection. Co-culture of CAR⁺ T cells with artificial antigen presenting cells (aAPC; "Clone1") led to numeric expansion of CAR⁺ T cells and enforced CAR expression through ROR1.

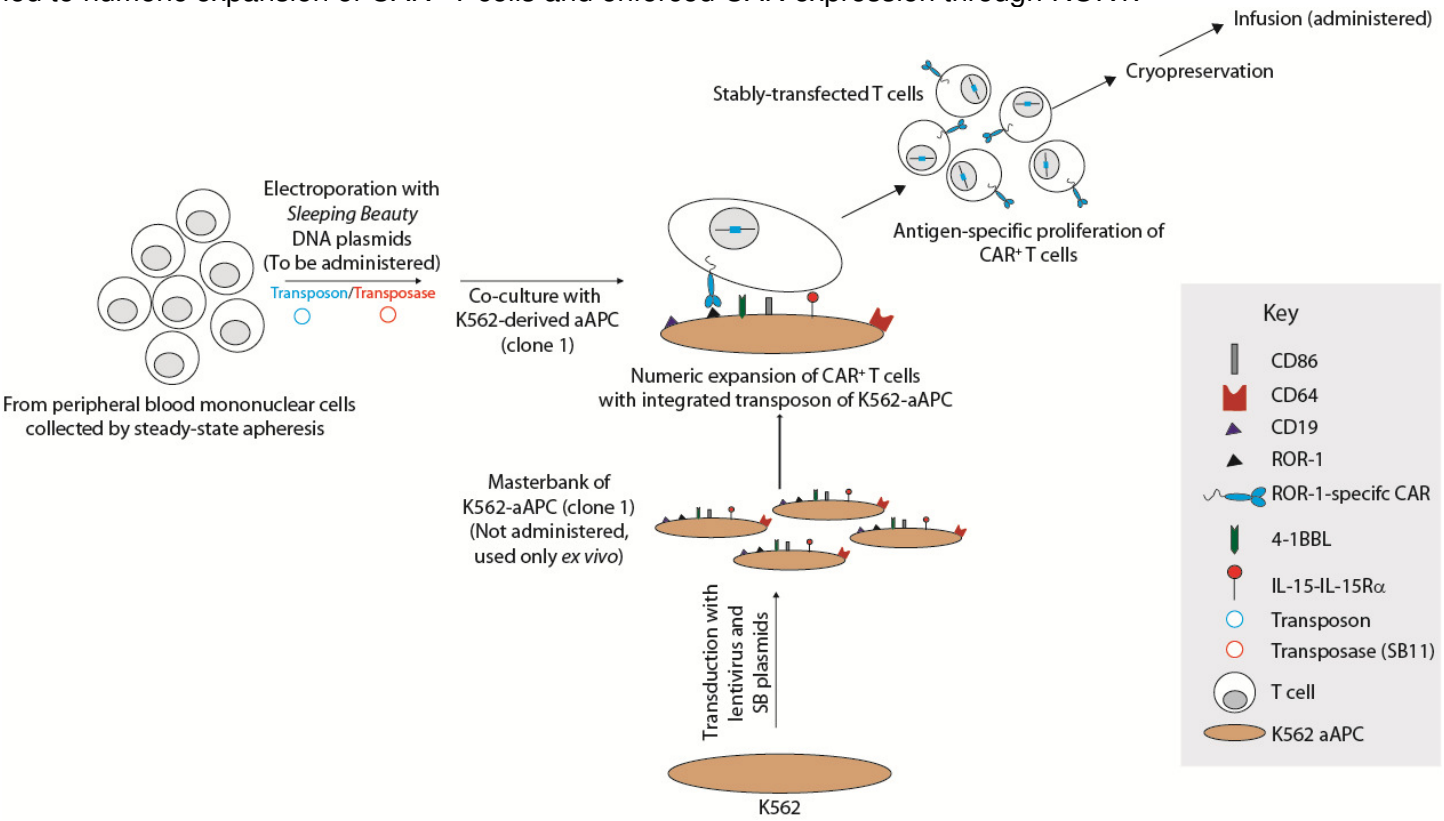

Appendix 3. Phenotype of Clone1 aAPC used for propagation of ROR1-specific CAR$^+$ T cells. Flow cytometry was used to assess recombinant expression of antigens (CD19 and ROR1), membrane-bound cytokines (IL-15 fused to IL-15Rα), co-stimulatory molecules (CD86 and CD137L), and Fc receptors (CD32 and CD64) on Clone1 aAPC. Isotype staining represented in open plots and filled plots represent antigen-specific staining.

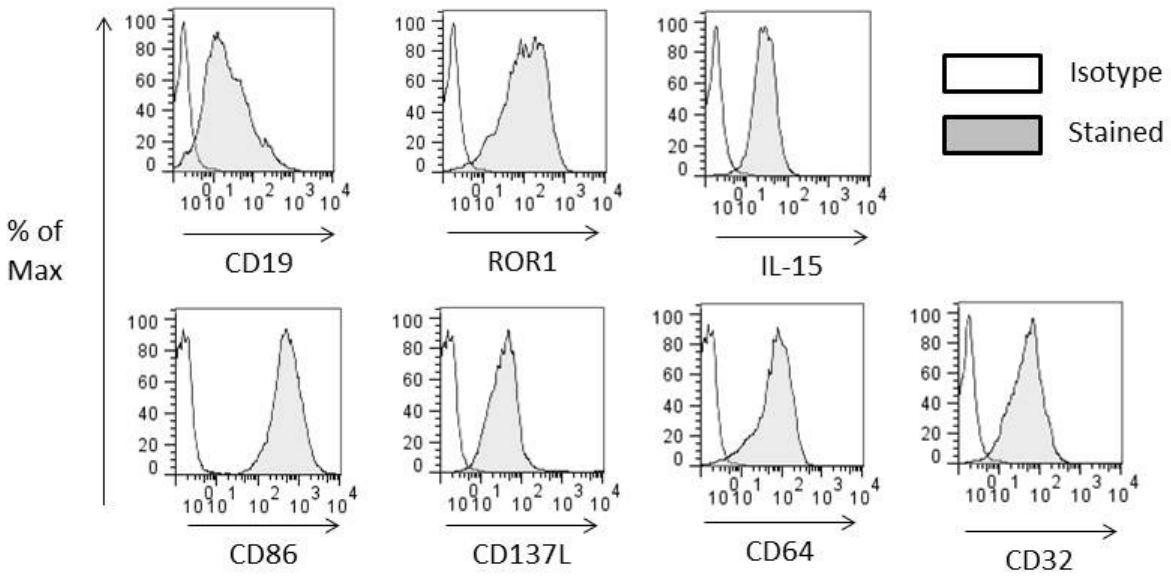

SUPPORTING DATA

Figure 1. ROR1 expression on OvCa in hypoxia and normoxia. OvCa cell lines were grown in normoxia (20% O_2) or hypoxia (1% O_2) for three days at 37°C and were then stained for ROR1 expression with 4A5 monoclonal antibody specific for ROR1.[12] (A) Representative flow plots from A2780, EFO27, and OC314 cell lines where black lines are normoxia, red lines are hypoxia, dashes are isotype controls, and solid lines are ROR1 staining. (B) Normalized ROR1 ($ROR1_{normal}$) mean fluorescence intensity (MFI) in OvCa cell lines in normoxia (open bars) and hypoxia (closed bars). MFI was calculated by: $MFI_{ROR1} - MFI_{isotype}$.

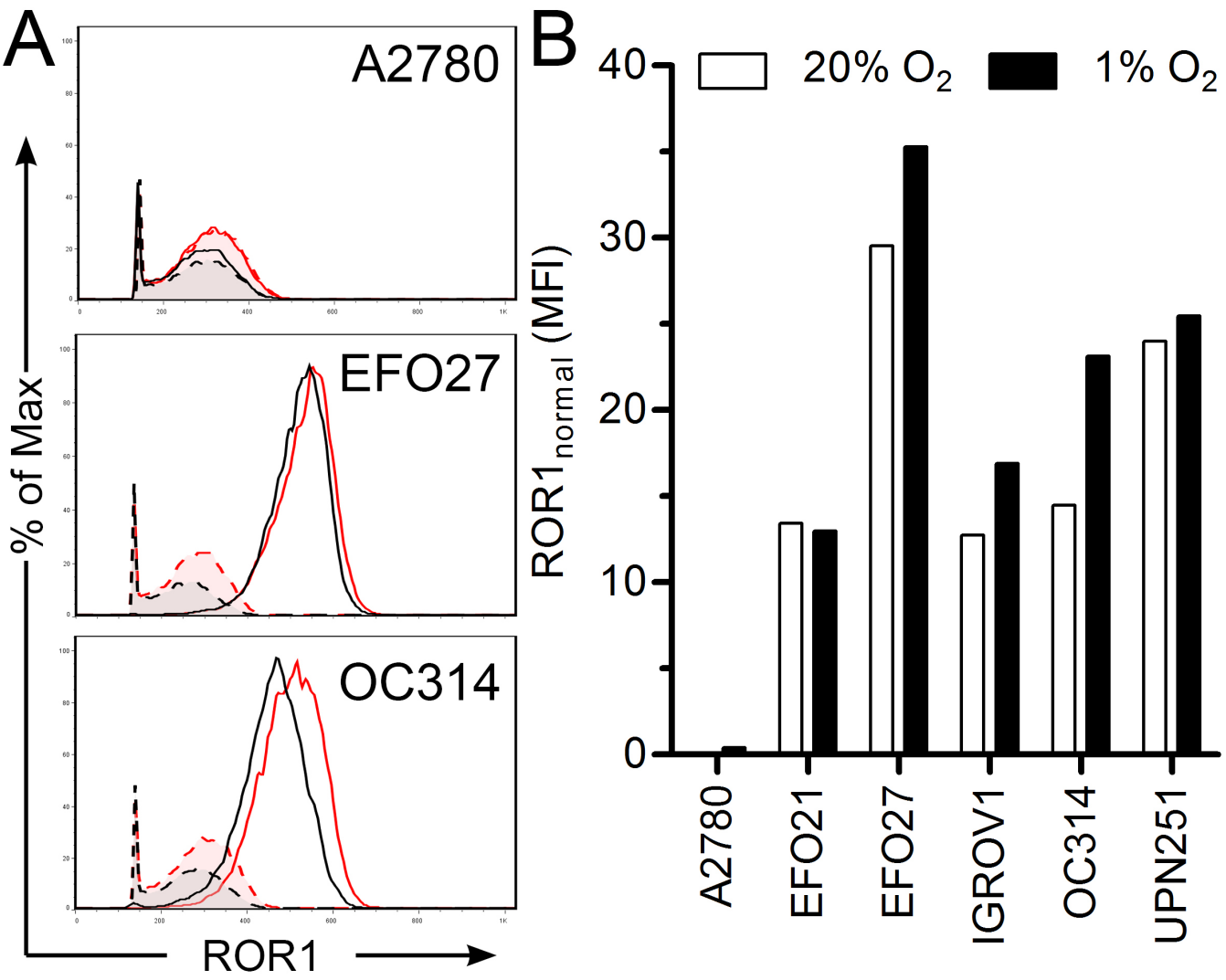

Figure 2. Expansion of CAR$^+$ T cells on ROR1$^+$ aAPC. PBMC were electroporated with ROR1-specific CARs signaling through CD28 (ROR1RCD28; closed squares) or CD137 (ROR1RCD137; open squares) and stimulated five times (each point on graphs) with ROR1$^+$ aAPC along with IL-2 and IL-21. (A) Total cell counts during culture period. (B) CAR$^+$ T cell counts during culture period.

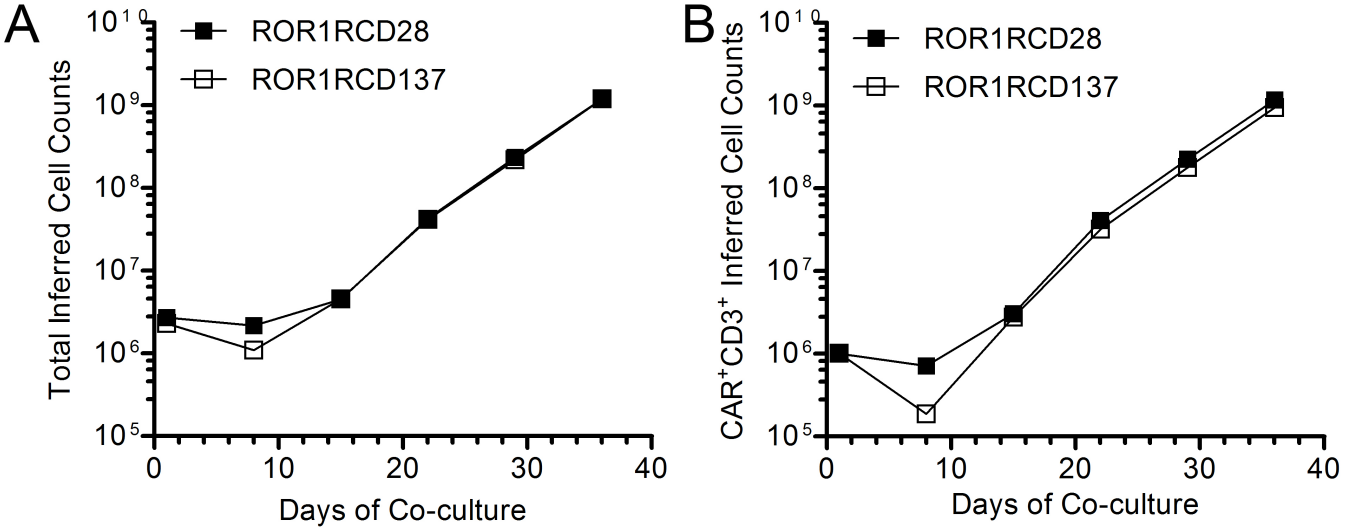

F**igure 3. CAR expression after expansion on ROR1^{+} aAPC.** Stable CAR expression after 29 days of co-culture on ROR1^{+} aAPC. Sham electroporated “No DNA” cells were stimulated with OKT3-loaded aAPC for negative controls. Gate frequencies are displayed in upper right corners.

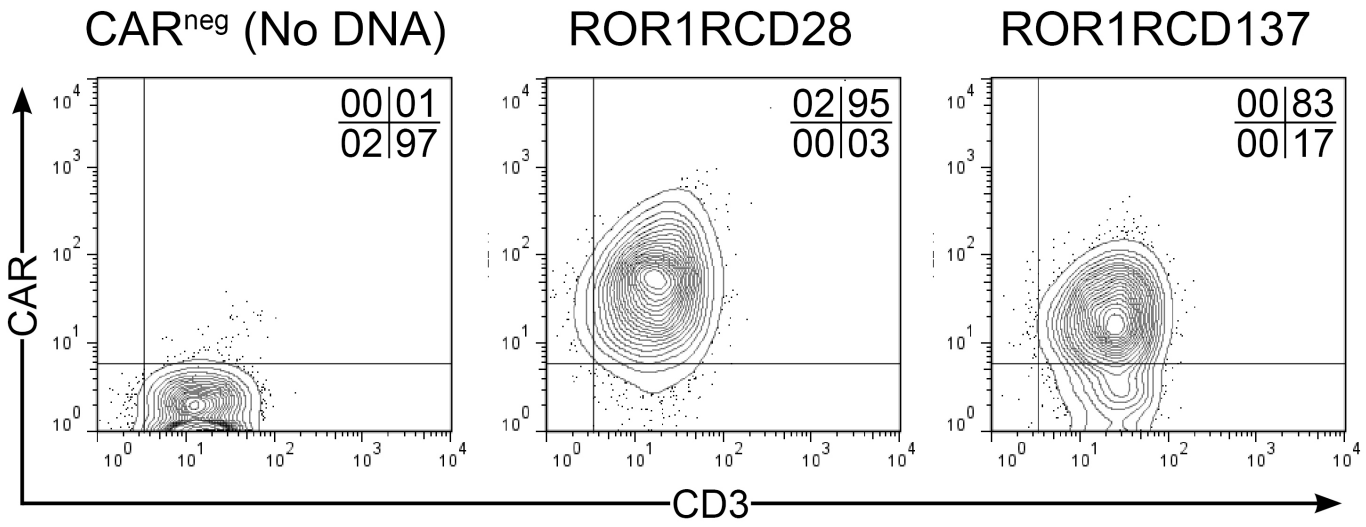

Figure 4. Specific killing of ROR1^{+} tumor cells by CAR^{+} T cells. Standard 4-hour chromium release assays were performed after 35 days of expansion on aAPC with CAR^{neg} (triangles), ROR1RCD28 (circles), or ROR1RCD137 (squares) T cells against (A) EL4-ROR1^{neg}, (B) EL4-ROR1^{+}, (C) A2780 (ROR1^{neg} OvCa), and (D) EFO27 (ROR1^{+} OvCa) cell lines. Two-way ANOVA with Bonferroni's post-tests used for statistical analyses on triplicate measurements where *p<0.05 and ***p<0.001.

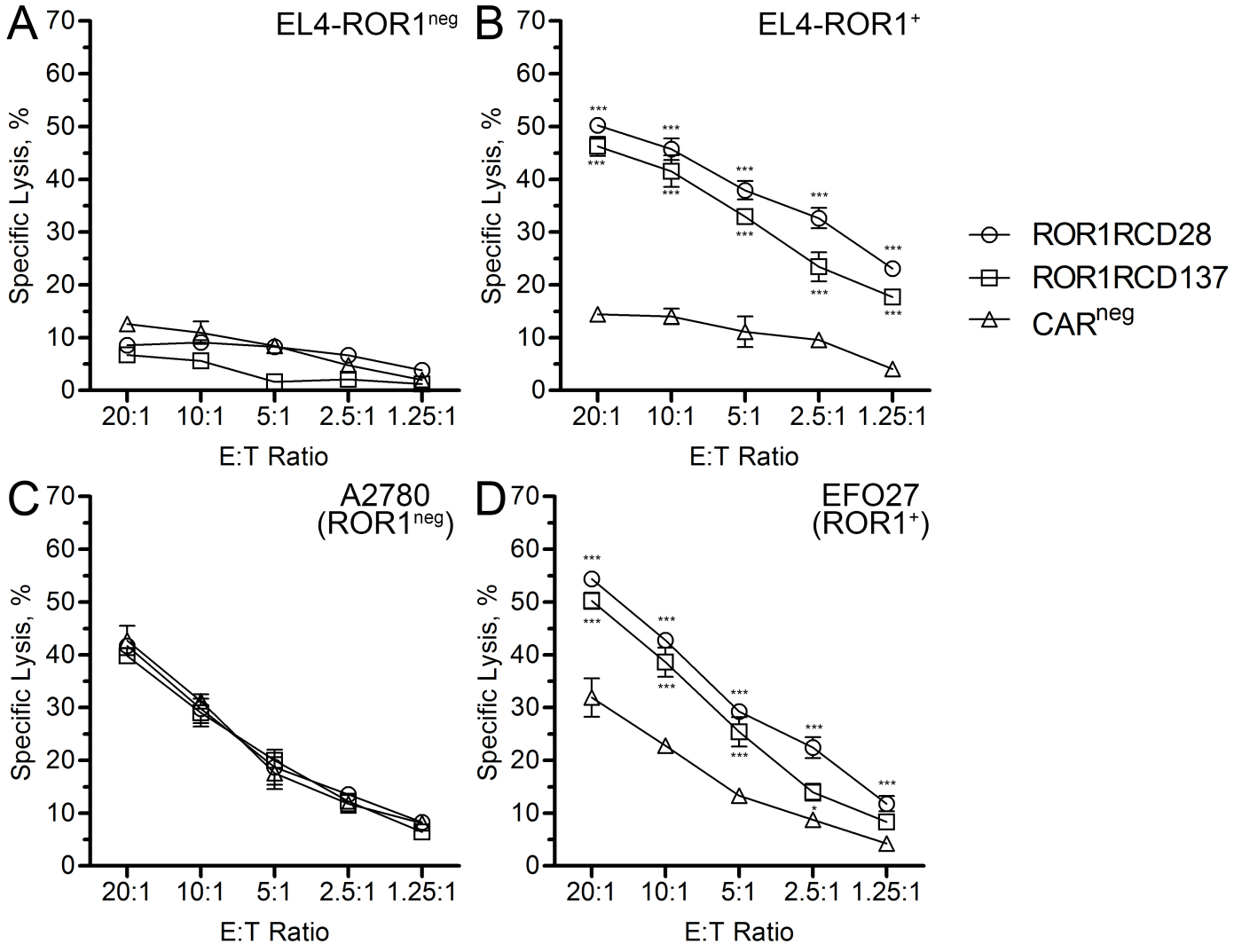

Figure 5. Expansion of γδ T cells on aAPC. (A) Flow cytometry of CD3 (y-axis) and TCRγδ (x-axis) expression in PBMC prior to paramagnetic bead sorting at Day 0 and of T cell cultures after 22 days of co-culture on aAPC. One representative donor of four healthy donors is shown and quadrant gate frequencies are displayed in the upper right corners of flow plots. (B) Total inferred cell counts of viable cells during co-culture period. (C) Fold expansion of cells in co-culture during co-culture period. Black lines are mean ± SD from 4 healthy donors, gray lines are individual donors, arrows represent stimulations with aAPC, and data are pooled from two independent experiments.

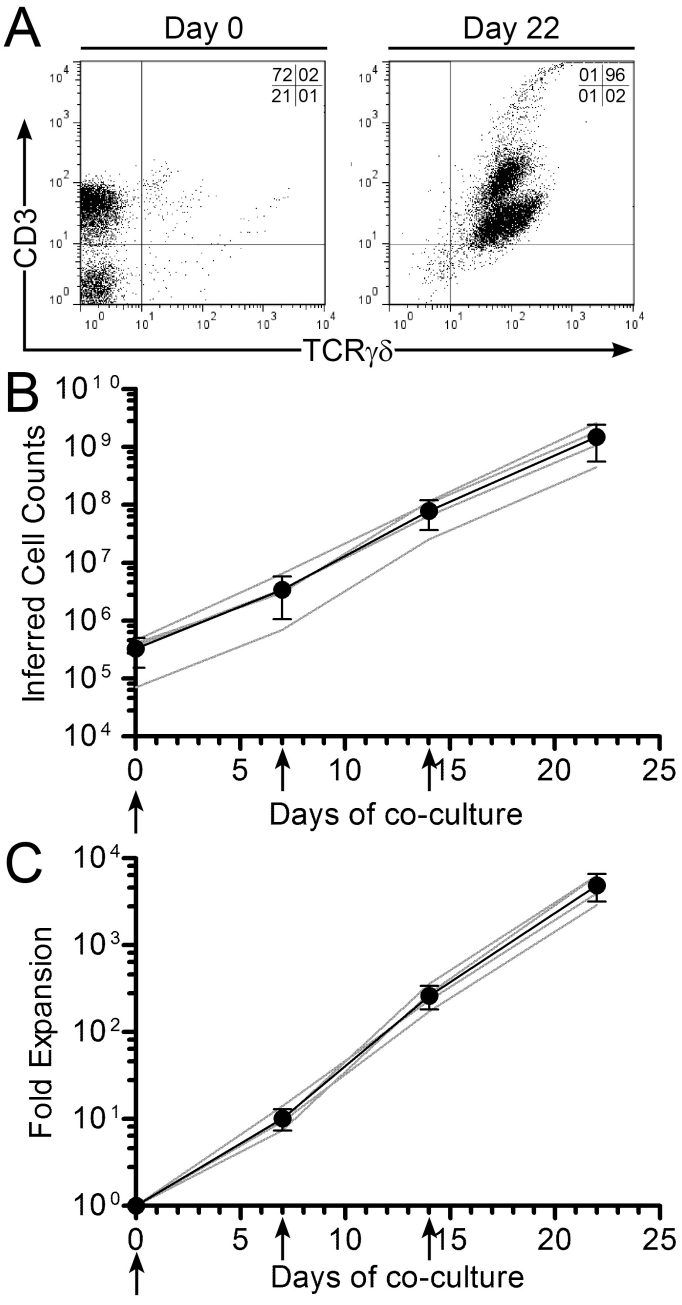

Figure 6. TCRγδ expression on aAPC-expanded γδ T cells. (A) Flow cytometry of TCRδ2 and TCRδ1 expression in γδ T cells at day 22 of co-culture. (B) Flow cytometry of TCRδ2 and TCRγ9 expression in γδ T cells at day 22 of co-culture. Numbers in lower right corners correlate with donor numbers in (A) and (B) where quadrant frequencies are displayed in upper right corners. (C) Direct TCR expression array "DTEA" detection of Vδ mRNA alleles in γδ T cells at day 22 of co-culture where Vδ1*01, Vδ2*02, and Vδ3*01 alleles are in graphs from left to right, respectively, and each of the four donors are numbered on x-axes. (D) DTEA detection of Vγ allele mRNA expression in γδ T cells at day 22. Lines are mean ± SD where each circle represents an individual healthy donor grown in two independent experiments.

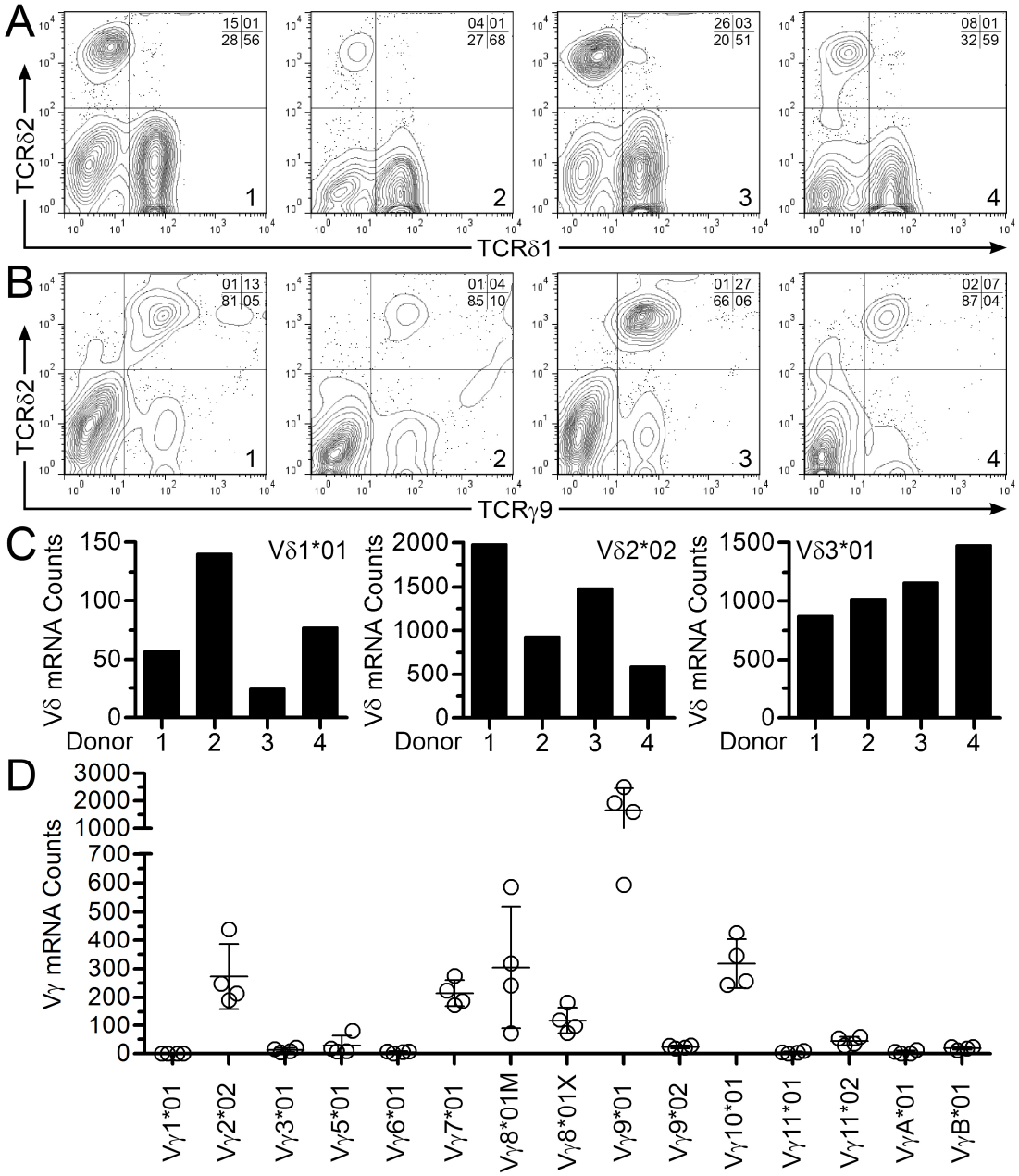

Figure 7. Cytokines and chemokines secreted by γδ T cells expanded on aAPC. Cells at day 22 were co-cultured with a mock activation cocktail (complete media) or leukocyte activation cocktail (LAC; PMA/Ionomycin) for 6 hours at 37°C. Conditioned media was interrogated on 27-Plex Luminex array to detect cytokines and chemokines. A, Th2 cytokines. B, Th17 cytokines. C, Th1 cytokines. D, Chemokines. Data are mean ± SD from 4 healthy donors. Student's t-test performed for statistical analysis between mock and LAC groups for each molecule. *p<0.05, **p<0.01, and ***p<0.001

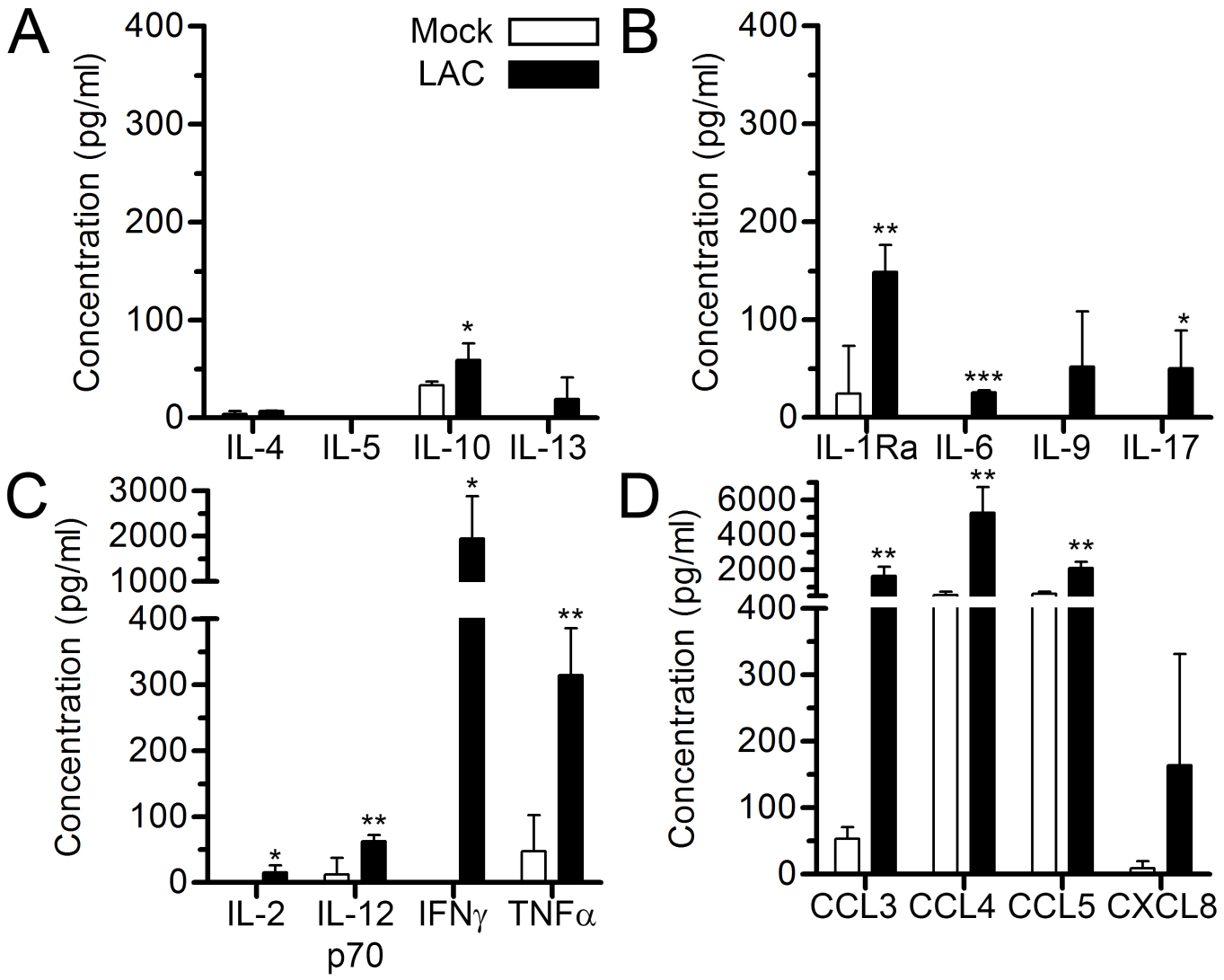

Figure 8. *In vitro* cytolysis of tumor cells by γδ T cells. Standard 4-hour chromium release assays were performed with increasing effector (γδ T cells) to target (E:T) ratios against healthy B cells from an allogeneic donor (top left; one of four representative donors) and OvCa cell lines A2780, EFO21, EFO27, IGROV1, OC314, UPN251, and CAOV3. Each line represents an individual effector where data is mean ± SD (n = 3 wells per assay) from two independent experiments.

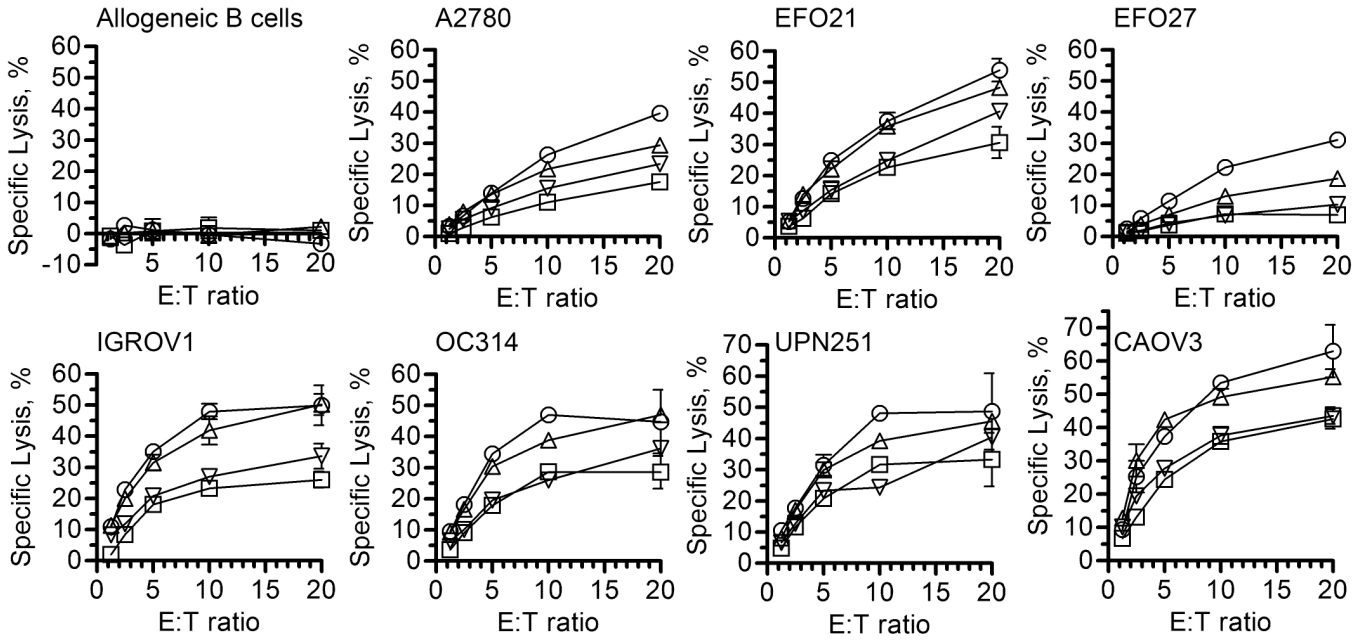

Figure 9. OvCa tumor clearance by polyclonal γδ T cells *in vivo*. (A) Schematic of experiment with legend to right. (B) Kinetics of bioluminescent flux of CAOV3-*ffLuc* xenografts from mock treated (closed squares) and γδ T cell treated (open squares) mice during experiment. Two-way ANOVA with Bonferroni's post-tests was used for statistical analysis where n = 10, *p<0.05, and ***p<0.001. (C) Representative images 43 days after engraftment and treated with PBS (top panels) or γδ T cells (bottom panels). (D) Long-term BLI flux comparison between day prior to treatment (Day 7; squares) and 79 days (circles) post-engraftment. Student's t-test performed between time points for each group with p-values above comparisons.

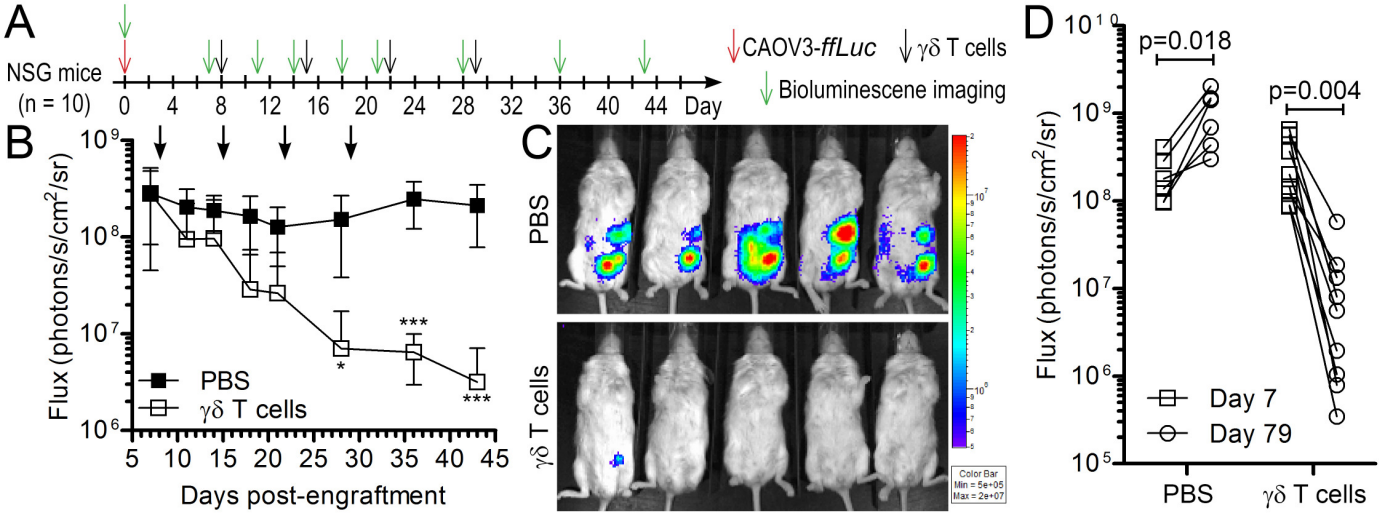

Figure 10. γδ T cells expanded on aAPC in normoxia and hypoxia and polarized towards IFNγ and IL-17 production. PBMC were sorted on TCRγ/δ+ isolation kit and 10^4 purified γδ T cells were then given a single stimulation with either IL-21 (A and B) or IL-2 and IL-21 (C and D) along with no aAPC or $2x10^4$ aAPC with one of the following co-stimulatory molecules: (i) none, (ii) CD70, (iii) CD86, (iv) 4-1BBL, (v) ICOS-L, or (vi) CD86 and 4-1BBL. Duplicate cultures were then placed in 20% O_2 or 1% O_2 for nine days at 37°C with humidified conditions. (A and C) After the 9 day incubation, cells were counted using trypan blue exclusion. Numbers above hatched bars represent fold changes of cytokine-treated cells compared to cultures without cytokines (bars not hatched). (B and D) Remaining cells were then mock activated (black line) or activated with leukocyte activation cocktail (LAC, PMA/Ionomycin, red line) for 6 hours in the presence of secretory inhibitor GolgiPlug at the same oxygen concentration as the 9 day culture. Cells were then stained for CD3, TCRγδ, IFNγ, and IL-17 and analyzed by flow cytometry. Data shown are histograms gated on $CD3^+TCR\gamma\delta^+$ cells where cytokine detected (x-axis) is in upper right corner and y-axis is % of maximum value. Top panels are 4-1BBL cultures and bottom panels are CD86/4-1BBL cultures. Left panels are 20% O_2 and right panels are 1% O_2.

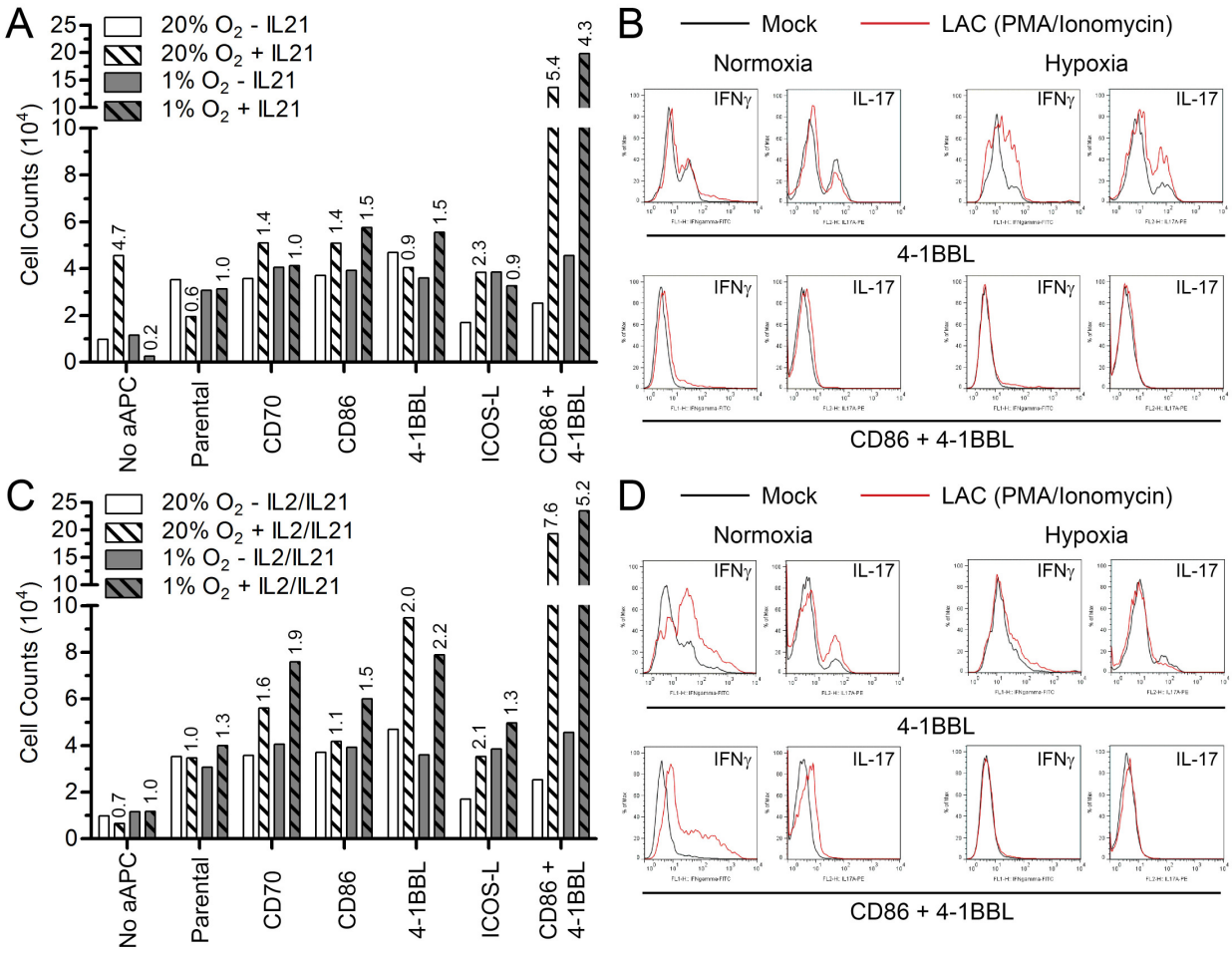

ATTACHMENT

Deniger DC, Maiti S, Switzer KC, Mi T, Ramachandran V, Hurton LV, Ang S, Olivares S, Rabinovich B, Huls H, Lee DA, Bast RC, Jr., Champlin RE, Cooper LJN. Artificial antigen presenting cells propagate polyclonal gamma delta T cells with broad anti-tumor activity. *Clinical Cancer Res*, (publication online May 15, 2014) http://www.ncbi.nlm.nih.gov/pubmed/24833662.

Activating and propagating polyclonal gamma delta T cells with broad specificity for malignancies

Drew C. Deniger[1,2], Sourindra N. Maiti[1], Tiejuan Mi[1], Kirsten C. Switzer[1], Vijaya Ramachandran[3], Lenka V. Hurton[1,2], Sonny Ang[1], Simon Olivares[1], Brian A. Rabinovich[1], Helen Huls[1], Dean A. Lee[1,2], Robert C. Bast, Jr[4], Richard E. Champlin[5], Laurence J.N. Cooper[1,2]

[1]Pediatrics, University of Texas MD Anderson Cancer Center; Houston, TX
[2]University of Texas Graduate School of Biomedical Sciences at Houston; Houston, TX
[3]Cancer Biology, University of Texas MD Anderson Cancer Center; Houston TX
[4]Experimental Therapeutics, University of Texas MD Anderson Cancer Center; Houston TX
[5]Stem Cell Transplantation and Cellular Therapy, University of Texas MD Anderson Cancer Center; Houston, TX

Running title: Polyclonal gamma delta therapy for cancer

CORRESPONDING AUTHOR
Laurence J.N. Cooper, M.D., Ph.D.
University of Texas MD Anderson Cancer Center
Pediatrics, Unit 907, 1515 Holcombe Blvd., Houston, TX 77030
Phone: (713) 563-3208; Fax: (713) 792-9832; E-mail: ljncooper@mdanderson.org

COUNTS
Statement of translational relevance: 149 words (limit 150 words)
Abstract = 250 words (limit 250)
Text = 4,998 words (Limit 5,000)
Tables and figures: 6 Figures (1 color; limit 6),
Supplemental Data: 1 Supplemental Table, 13 Supplemental Figures (4 color)
References: 50 (Limit 50)

Conflict of interest statement: The authors (D.C.D. and L.J.N.C.) have a patent application associated with methods and data described and arising from this publication. L.J.N.C. founded and owns InCellerate Inc. He has patents with Sangamo BioSciences with artificial nucleases. He consults with American Stem cells, Inc., GE Healthcare, Bristol-Myers Squibb, and Ferring Pharmaceuticals. He receives honoraria from Miltenyi Biotec. The authors declare no other competing financial interests.

TRANSLATIONAL RELEVANCE

γδ T cells have anti-cancer activity, but only one subset, Vγ9Vδ2, has been harnessed for immunotherapy. Our study establishes that artificial antigen presenting cells (aAPC), IL-2, and IL-21 can activate and propagate γδ T cells with polyclonal TCR repertoire to clinical scale. The heterogeneous population of γδ T cells produced from *ex vivo* culture secreted pro-inflammatory cytokines, lysed a broad range of malignancies, and improved survival in an ovarian cancer xenograft model. Given that γδ T cells are not thought to recognize ligands in the context of MHC, there is limited risk of graft-versus host disease in an allogeneic setting. Thus, 3rd party γδ T cells from an unrelated (healthy) donor could be produced in bulk and be administered as an off-the-shelf investigational therapy for hematologic and solid tumors. The aAPC are already available as a clinical reagent, which will facilitate the human application of polyclonal γδ T cells.

ABSTRACT

Purpose: To activate and propagate populations of γδ T cells expressing polyclonal repertoire of γ and δ TCR chains for adoptive immunotherapy for cancer, which has yet to be achieved.

Experimental Design: Clinical-grade artificial antigen presenting cells (aAPC) derived from K562 tumor cells were used as irradiated feeders to activate and expand human γδ T cells to clinical scale. These cells were tested for proliferation, TCR expression, memory phenotype, cytokine secretion, and tumor killing.

Results: γδ T cell proliferation was dependent upon CD137L expression on aAPC and addition of exogenous IL-2 and IL-21. Propagated γδ T cells were polyclonal as they expressed Vδ1, Vδ2, Vδ3, Vδ5, Vδ7, and Vδ8 with Vγ2, Vγ3, Vγ7, Vγ8, Vγ9, Vγ10, and Vγ11 TCR chains. Interferon-γ production by Vδ1, Vδ2, and $V\delta1^{neg}V\delta2^{neg}$ subsets was inhibited by pan-TCRγδ antibody when added to co-cultures of polyclonal γδ T cells and tumor cell lines. Polyclonal γδ T cells killed acute and chronic leukemia, colon, pancreatic, and ovarian cancer cell lines, but not healthy autologous or allogeneic normal B cells. Blocking antibodies demonstrated that polyclonal γδ T cells mediated tumor cell lysis through combination of DNAM1, NKG2D, and TCRγδ. The adoptive transfer of activated and propagated γδ T cells expressing polyclonal versus defined Vδ TCR chains imparted a hierarchy (polyclonal>Vδ1>$V\delta1^{neg}V\delta2^{neg}$>Vδ2) of survival of mice with ovarian cancer xenografts.

Conclusions: Polyclonal γδ T cells can be activated and propagated with clinical-grade aAPC and demonstrate broad anti-tumor activities, which will facilitate the implementation of γδ T cell cancer immunotherapies in humans.

INTRODUCTION

Human γδ T cells exhibit an endogenous ability to specifically kill tumors and hold promise for adoptive immunotherapy. They have innate and adaptive qualities exhibiting a range of effector functions, including cytolysis upon cell contact (1, 2). Recognition and subsequent killing of tumor is achieved upon ligation of antigens to heterodimers of γ and δ T-cell receptor (TCR) chains. The human TCR variable (V) region defines 14 unique Vγ alleles, 3 unique Vδ alleles (Vδ1, Vδ2, and Vδ3), and 5 Vδ alleles that share a common nomenclature with Vα alleles (Vδ4/Vα14, Vδ5/Vα29, Vδ6/Vα23, Vδ7/Vα36, and Vδ8/Vα38-2) (3). T cells expressing TCRα/TCRβ heterodimers compose approximately 95% of peripheral blood (PB) T cells and recognize peptides in the context of major histocompatibility complex (MHC) (4). In contrast, TCRγδ ligands are recognized independent of MHC and these cells are infrequent (1-5% of T cells) in PB (1, 5, 6). Many conserved ligands for TCRγδ are present on cancer cells, thus an approach to propagating these T cells from small starting numbers while maintaining a polyclonal repertoire of γδ TCRs has appeal for human application.

Clinical trials highlight the therapeutic potential of γδ T cells, but numeric expansion is needed for adoptive immunotherapy because they circulate at low frequencies in PB. Methods to propagate αβ T cells, *e.g.*, using interleukin-2 (IL-2) and/or antibody cross-linking CD3, cannot sustain proliferation of γδ T cells (7, 8). Aminobisphosphonates, *e.g.*, Zoledronic acid (Zol), have been used to initiate a proliferative signal in γδ T cells (5, 9), but only one lineage of γδ T cells, expressing Vγ9Vδ2 TCR, can be reliably expanded by Zol. The adoptive transfer of Vγ9Vδ2 T cells has yielded clinical responses for investigational treatment of solid and hematological cancers (10-14). Furthermore, long-term remission of leukemia among recipients of

haploidentical αβ T cell-depleted hematopoietic stem-cell transplantation (HSCT) correlated with increased engraftment frequency of donor-derived Vδ1 cells (8, 15-17). However, direct administration of Vδ1 cells or other non-Vγ9Vδ2 cell lineages has yet to be performed. In addition, no reports to date have described the therapeutic impact of $V\delta1^{neg}V\delta2^{neg}$ cells in cancer immunotherapy and this subset has not been directly compared to T cells expressing Vδ1 and Vδ2 TCRs. Thus, there are significant gaps in the knowledge and human application of non-Vγ9Vδ2 lineages.

Given that γδ T cells have endogenous anti-cancer activity, such as against K562 cells (8, 18), we hypothesized that malignant cells would serve as a cellular substrate to propagate polyclonal γδ T cells. K562 cells have been genetically modified to function as artificial antigen presenting cells (aAPC) to *ex vivo* activate and numerically expand αβ T cells and NK cells (19-23). We determined that interleukin-2 (IL-2), IL-21, and γ-irradiated K562-derived aAPC (designated clone #4, genetically modified to co-express CD19, CD64, CD86, CD137L, and a membrane-bound mutein of IL-15 (mIL15); used in selected clinical trials at MD Anderson Cancer Center) can sustain the proliferation of γδ T cells with polyclonal TCR repertoire. Polyclonal γδ T cells exhibited broad tumor reactivity and displayed a multivalent response to tumors as evidenced by the ability of separated Vδ sub-populations to kill and secrete cytokine against the same tumor target. Further, killing by polyclonal populations was multifactorial being mediated through DNAM1, NKG2D, and TCRγδ. Tumor xenografts were eliminated by both polyclonal and distinct γδ T-cell subsets, and mice treated with polyclonal γδ T cells had superior survival. Given the availability of aAPC as a clinical reagent, trials can for the first time, evaluate polyclonal populations of γδ T cells as a cancer immunotherapy.

MATERIALS AND METHODS

Cell lines

HCT-116, Kasumi-3, and K562 were acquired from American Type Culture Collection (ATCC; Manassas, VA). Jurkat was purchased from Deutsche Sammlung von Mikroorganismen und Zellkulturen (DSMZ; Germany). cALL-2 and RCH-ACV were gifts from Dr. Jeff Tyner (Oregon Health & Science University). BxPC-3, MiaPaCa-2, and Su8686 (pancreatic cancer) were donated by Dr. Vijaya Ramachandran (MD Anderson Cancer Center). A2780, CAOV3, EFO21, EFO27, Hey, IGROV1, OAW42, OC314, OVCAR3, and UPN251 (ovarian cancer) were provided by Dr. Robert C. Bast, Jr. (MD Anderson Cancer Center). Identities of all cell lines were confirmed by STR DNA Fingerprinting at MD Anderson Cancer Center's "Characterized Cell Line Core" and cells were used within 6 months of authentication.

Propagation of γδ T cells

Peripheral blood mononuclear cells (PBMC) and umbilical cord blood (UCB) were isolated from healthy volunteers by Ficoll-Hypaque (GE Healthcare) after informed consent (24). Thawed PBMC (10^8) were initially treated with CD56 microbeads (cat# 130-050-401, Miltenyi Biotec, Auburn, CA) and separated on LS columns (cat# 130-042-401, Miltenyi Biotec) to deplete NK cells from cultures because they proliferate on aAPC (23) and would contaminate the purity of the γδ T-cell product. Unlabeled cells from CD56 depletion sorting were then labeled with TCRγ/δ+ T-cell isolation kit (cat# 130-092-892, Miltenyi Biotec) and placed on LS columns to separate γδ T cells in the unlabeled fraction from other cells attached to magnet. γδ T cells were

co-cultured at a ratio of one T cell to two γ-irradiated (100 Gy) aAPC (clone #4) in presence of exogenous IL-2 (Aldesleukin; Novartis, Switzerland; 50 IU/mL), and IL-21 (cat# AF20021; Peprotech, Rocky Hill, NJ; 30 ng/mL) in complete media (CM; RPMI, 10% FBS, 1% Glutamax). Cells were serially re-stimulated with addition of γ-irradiated aAPC every 7 days for 2 to 5 weeks in presence of soluble cytokines, which were added three times per week beginning the day of aAPC addition. K562 were genetically modified to function as aAPC (clone #4) as previously described (25, 26). Validation of co-expression of CD19, CD64, CD86, CD137L, and eGFP (IL-15 peptide fused in frame to IgG4 Fc stalk and co-expressed with eGFP) on aAPC clone #4 was performed before addition to T-cell cultures (25). Fluorescence activated cell sorting (FACS) was used to isolate Vδ1 ($TCR\delta1^{+}TCR\delta2^{neg}$), Vδ2 ($TCR\delta1^{neg}TCR\delta2^{+}$), and $V\delta1^{neg}V\delta2^{neg}$ ($TCR\delta1^{neg}TCR\delta2^{neg}$) populations, which were stimulated twice as above with aAPC clone #4, phenotyped, and used for functional assays. γδ T cells from UCB were isolated by FACS from thawed mononuclear cells using anti-TCRγδ and anti-CD3 monoclonal antibodies (mAbs) and were stimulated for five weeks on aAPC/cytokines as per PBMC.

Abundance and identity of mRNA molecules by DTEA

At designated times after co-culture on aAPC, T cells were lysed at a ratio of 160 µL RLT Buffer (Qiagen) per 10^6 cells and frozen at -80°C. RNA lysates were thawed and immediately analyzed using nCounter Analysis System (NanoString Technologies, Seattle, WA) with "designer TCR expression array" (DTEA), as previously described (27, 28). DTEA data was normalized to both spike positive control RNA and housekeeping genes (ACTB, G6PD, OAZ1, POLR1B, POLR2A, RPL27, Rps13, and TBP). Spiked positive control normalization factor was calculated from the

average of sums for all samples divided by the sum of counts for an individual sample. Spiked positive control normalization factor was calculated from the average of geometric means for all samples divided by the geometric mean for an individual sample. Normalized counts were reported.

Flow cytometry

Cells were phenotyped with antibodies detailed in **Supplemental Table 1**. Gating strategy is displayed in **Supplemental Figure 1**. Samples were acquired on FACS Calibur (BD Biosciences, San Jose, CA) and analyzed with FlowJo software (version 7.6.3).

Cytokine production and cytolysis assays

Expression of cytokines was assessed by intracellular staining and secretion of cytokines into tissue culture supernatants was evaluated by Luminex multiplex analysis. *In vitro* specific lysis was assessed using a standard 4-hour CRA, as previously described (25). Additional information can be found in the supplemental materials and methods.

Mouse experiments

In vivo anti-tumor efficacy was assessed in NSG mice (NOD.Cg-Prkdc^{scid}Il2rγ^{tm1Wjl}/SzJ; Jackson Laboratories). CAOV3 ovarian cancer cell line was transduced with recombinant lentivirus (**Supplemental Figure 2**) encoding mKate red fluorescence protein (29) to identify transduced

cells and enhanced *firefly luciferase* (*effLuc*) for non-invasive bioluminescence imaging (30). CAOV3-e*ffLuc*-mKate (clone 1C2; $3x10^6$ cells/mouse) tumors were established by intraperitoneal (i.p.) injection and mice were randomly distributed into treatment groups. Eight days later (designated Day 0), a dose escalation regimen was initiated with γδ T cells administered i.p. and PBS administered i.p. as a negative control. T-cell doses were $3x10^6$, $6x10^6$, 10^7, and $1.5x10^7$ on days 0, 7, 14, and 21, respectively. Non-invasive BLI was performed during the course of the experiments to serially measure tumor burden of CAOV3-e*ffLuc*-mKate following subcutaneous administration of D-Luciferin (cat#122796, Caliper, Hopkinton, MA) as detected with IVIS-100 Imager (Caliper). BLI was analyzed using Living Image software (version 2.50, Xenogen, Caliper).

RESULTS

Ex vivo numeric expansion of γδ T cells on aAPC depends on co-stimulation and cytokines

The adoptive transfer of γδ T cells requires *ex vivo* propagation as starting numbers from PBMC are limiting (gating on lymphocyte pool: 3.2% ± 1.2%; mean ± standard deviation (SD); n=4; **Figure 1A**). γδ T cells from PBMC were isolated by "negative" paramagnetic bead selection and co-cultured for 22 days with weekly addition of γ-irradiated K562-derived aAPC (clone #4) in the presence of soluble recombinant IL-2 and IL-21 in alignment with protocols at MD Anderson for propagation of clinical-grade αβ T cells. This resulted in the outgrowth of a population of T cells homogeneously co-expressing CD3 and TCRγδ (97.9% ± 0.6%). NK cells ($CD3^{neg}CD56^{+}$) and αβ T cells ($TCR\alpha\beta^{+}$) were absent from these cultures supporting the purity of the γδ T-cell product. Populations of $TCR\delta1^{+}TCR\delta2^{neg}$, $TCR\delta1^{neg}TCR\delta2^{+}$, and $TCR\delta1^{neg}TCR\delta2^{neg}$ were detected indicating that aAPC, IL-2, and IL-21 supported polyclonal γδ T cell proliferation (**Figure 1A far right**). Cells were activated as marked by expression of CD38 (93.5% ± 3.5%) and CD95 (99.7% ± 0.1%) (**Supplemental Figure 3**). This approach to propagation yielded $>10^9$ γδ T cells from $<10^6$ total initiating cells (**Figure 1B**), which represented a $4.9x10^3 \pm 1.7x10^3$ (mean ± SD; n=4) fold increase. Thus, aAPC with recombinant human cytokines supported the robust numeric expansion of polyclonal γδ T cells from small starting numbers of γδ T cells derived from PBMC.

The addition of exogenous cytokines and presence of mIL15, CD86, and CD137L on clinical-grade aAPC were assessed for their ability to support the outgrowth of γδ T cells. Parental K562 cells were stably transfected with *Sleeping Beauty* (SB) transposons to introduce individual stimulatory molecules, cloned to achieve homogeneous expression (**Supplemental**

Figure 4), and then used to assess their impact on γδ T-cell proliferation. Co-cultures with exogenous IL-2 and IL-21 were initiated with paramagnetic bead-purified γδ T cells and five sets of γ-irradiated K562: (i) parental, (ii) mIL15^{+}, (iii) mIL15^{+}CD86^{+}, (iv) mIL15^{+}CD137L^{+}, and (v) mIL15^{+}CD86^{+}CD137L^{+} (clone #4). γδ T cells cultured in parallel without APC demonstrated that soluble IL-2 and IL-21 sustained only limited numeric expansion of γδ T cells (**Figure 1C**). Propagation improved upon addition of parental K562 cells, indicating that endogenous molecules on these cells can activate γδ T cells for proliferation. The expression of mIL15 with or without CD86 did not further improve the ability of γδ T cells to propagate compared with parental K562. In contrast, improved rates of propagation of γδ T cells were observed upon co-culture with mIL15^{+}CD137L^{+} and mIL15^{+}CD86^{+}CD137L^{+} aAPC. Thus, it appears that CD137L on aAPC clone#4 provides a dominant co-stimulatory proliferative signal for γδ T cells. In the absence of IL-2 and IL-21 the proliferation of γδ T cells ceased on aAPC clone#4, and together these cytokines exhibited an additive benefit to the rate of γδ T-cell propagation (**Figure 1D**). This validated our approach to combining aAPC clone #4 with cytokines to sustain the proliferation of polyclonal γδ T cells *ex vivo*, and demonstrated that CD137L on aAPC, IL-2, and IL-21 were driving factors for proliferation of polyclonal γδ T cells to clinical scale.

Ex vivo numeric expansion of neonatal γδ T cells on aAPC in presence of IL-2 and IL-21

Allogeneic UCB is an important source of γδ T cells for adoptive transfer, because it contains younger cells and a more diverse TCRγδ repertoire relative to PBMC, which could increase the number of ligands targeted by the engrafted cells and result in long-term engraftment in the

recipient (31). However, the limited number of mononuclear cells within a banked UCB unit curtails the number of neonatal γδ T cells directly available for adoptive transfer. Thus, we evaluated whether aAPC could sustain proliferation from small starting numbers of neonatal γδ T cells. Fluorescence activated cell sorting (FACS) was used to isolate 10^4 UCB-derived γδ T cells (~0.01% of a typical UCB unit) which were co-cultured on aAPC clone #4 with IL-2 and IL-21. After 35 days, there was a 10^7-fold increase in cell number, as an average of 10^{11} UCB-derived γδ T cells (Range: $6x10^9$ – $3x10^{11}$; n=5) were propagated from the 10^4 initiating γδ T cells (**Supplemental Figure 5A**). Two additional stimulations were performed for γδ T cells derived from UCB compared to PBMC highlighting their potential for proliferating to clinically-appealing numbers. The propagated γδ T-cell populations exhibited uniform co-expression of CD3 and TCRγδ and lacked TCRαβ$^+$ T cells or presence of CD3^{neg}CD56$^+$ NK cells (**Supplemental Figure 5B-D**). Collectively, these data demonstrate that aAPC clone #4 with IL-2 and IL-21 could sustain the *ex vivo* proliferation of γδ T cells from a small starting population of neonatal UCB.

Ex vivo activated and propagated γδ T cells express polyclonal and defined TCRγδ repertoire

Upon establishing that γδ T cells could numerically expand on aAPC and selected cytokines, we sought to determine the TCR repertoire of the propagated cells. Prior to numeric expansion, resting γδ T cell repertoire followed TCRδ2>TCRδ1^{neg}TCRδ2^{neg}>TCRδ1 by flow cytometry (**Supplemental Figure 6**). However, the γδ T-cell repertoire followed TCRδ1>TCRδ1^{neg}TCRδ2^{neg}>TCRδ2 following expansion, suggesting that there was a

proliferative advantage for Vδ1 cells within polyclonal γδ T-cell cultures. To look more in-depth at TCRγδ diversity in aAPC-expanded γδ T cells, we adapted a non-enzymatic digital multiplex assay used to quantify the TCR diversity in γδ T cells expressing a CD19-specific chimeric antigen receptor (CAR) (27) termed "direct TCR expression array" (DTEA). Following expansion (Day 22), four of eight Vδ alleles (Vδ1, Vδ2, Vδ3, and Vδ8) were detected in PBMC-derived γδ T cells (**Figure 2A**) and were co-expressed with Vγ2, Vγ7, Vγ8 (two alleles), Vγ9, Vγ10, and Vγ11 (**Figure 2B**). Similarly, a polyclonal assembly of Vδ and Vγ chains was observed in γδ T cells from UCB following expansion (Day 34-35), albeit with reduced abundance of Vδ2 cells, more Vγ2, and presence of Vγ3, Vδ5, and Vδ7 cells not seen from PBMC (**Figure 2C-D**). Similar patterns of Vδ and Vγ mRNA usage were detected in PBMC and UCB before and after expansion (**Supplemental Figure 7**) although overall mRNA counts were fewer in the resting cells (Day 0) relative to the activated γδ T cells. Thus, aAPC-expanded γδ T cells maintain a polyclonal TCR repertoire from both PBMC and UCB.

We sought to validate these mRNA data by sorting polyclonal populations with TCRδ-specific antibodies and repeating DTEA on isolated cultures. There are only two TCRδ-specific mAbs commercially available and they identified 3 discrete Vδ populations (Vδ1: $TCR\delta1^{+}TCR\delta2^{neg}$, Vδ2: $TCR\delta1^{neg}TCR\delta2^{+}$, and $V\delta1^{neg}V\delta2^{neg}$: $TCR\delta1^{neg}TCR\delta2^{neg}$) within aAPC-expanded γδ T cells from PBMC (**Figure 1A**) and UCB (**Supplemental Figure 8**) with abundance following Vδ1>$V\delta1^{neg}V\delta2^{neg}$>Vδ2. FACS isolated subsets from PBMC-derived γδ T-cell pools were propagated with clone #4 as discrete populations and maintained their identity as assessed by expression of TCRδ isotypes (**Figure 3A**). Each of the separated subsets could be identified by a pan-specific TCRγδ antibody confirming that these cells were indeed γδ T cells

(**Figure 3B**). Furthermore, each population could be differentiated based on pan-TCRγδ antibody mean fluorescence intensity (MFI) where Vδ2, Vδ1^{neg}Vδ2^{neg}, and Vδ1 T cells corresponded to the TCRγδ^{low} (43 ± 9; mean ± SD; n=4), TCRγδ^{intermediate} (168 ± 40), and TCRγδ^{hi} (236 ± 56) groupings, respectively. No differences in proliferation kinetics on aAPC were observed between isolated Vδ-sorted subsets (**Figure 3C**) indicating that the observed inversion of Vδ1 and Vδ2 frequencies in polyclonal cultures before versus after expansion was not due to a proliferative defect in one of the subsets. DTEA demonstrated that isolated and propagated Vδ1, Vδ2, and Vδ1^{neg}Vδ2^{neg} sub-populations were homogeneous populations as they predominantly expressed Vδ1*01, Vδ2*02, and Vδ3*01 mRNA species at 261 ± 35, 3910 ± 611, and 5559 ± 1119 absolute counts, respectively (**Figure 3D**). Therefore, there were fewer Vδ1*01 mRNA species expressed by Vδ1 cells relative to the Vδ2*02 expressed by Vδ2 cells and Vδ3*01 expressed by Vδ1^{neg}Vδ2^{neg} cells. Moreover, these data indicated that the relatively low counts observed for Vδ1*01 in polyclonal populations with a preponderance of TCRδ1^{+} cells was not a defect in DTEA detection but rather a product of fewer total mRNA transcripts relative to other Vδ species. Given the wide range of mRNA transcript quantities for each allele, DTEA was not useful for calculation of relative frequencies of Vδ subsets in polyclonal populations but rather was indicative of presence or absence of a particular γδ T cell subset. Expression of other Vδ2 alleles (Vδ1*01_07 and Vδ1*01_75) was absent from polyclonal γδ T cells (**Figure 2A**) and each of the sorted subsets (data not shown). Small amounts of Vδ4, Vδ5, Vδ6, and Vδ7 mRNA species were detected in the three subsets of T cells sorted for Vδ expression (**Supplemental Figure 9**). Vδ8 mRNA was exclusively present in sorted Vδ1^{neg}Vδ2^{neg} cells and these T cells are likely the main contributors of Vδ8 in bulk γδ T cells. The same Vγ mRNA present in polyclonal

cultures was detected in Vδ-sorted cultures (**Supplemental Figure 10**). Furthermore, Vδ1 and $V\delta1^{neg}V\delta2^{neg}$ were not different ($p=0.419$; Two-way ANOVA) but Vδ2 was different to both Vδ1 ($p<0.0001$) and $V\delta1^{neg}V\delta2^{neg}$ ($p<0.0001$) in Vγ usage. Collectively, these results confirmed DTEA from unsorted cultures and strongly supported the polyclonal TCRγδ expression on γδ T cells activated to proliferate by aAPC and cytokines.

Interferon-γ produced in response to tumors is dependent on TCRγδ

A multiplex analysis of cytokines and chemokines was performed to determine whether aAPC-propagated γδ T cells might foster a pro-inflammatory response in a tumor micro-environment (**Figure 4A**). The T_H1-associated cytokines interferon-γ (IFNγ) and tumor necrosis factor-α (TNFα) were secreted in abundance by γδ T cells upon exposure to leukocyte activated cocktail (LAC; PMA and Ionomycin for non-specific mitogenic stimulation), in addition to small amounts of IL-2 and IL-12 p70. In contrast, no significant production of the T_H2-associated cytokines IL-4, IL-5, and IL-13 was observed from LAC-treated γδ T cells, but there was a small increase in IL-10 production over baseline. Similarly, Th17-associated cytokines IL-1RA, IL-6, and IL-17 were secreted at low levels by LAC-treated γδ T cells. The chemokines CCL3, CCL4, and CCL5 were detected in abundance. Minor contributions of non-γδ T cells in the culture that could have been activated by LAC to secrete cytokines could not be ruled out, but given that the cells tested were 97.9% ± 0.6% $CD3^+TCR\gamma\delta^+$ these data indicate that it was activation of γδ T cells that led to a largely pro-inflammatory response. IFNγ was the most responsive of all the assessed cytokines and was chosen to measure responses of Vδ subsets to tumor cells (**Figure**

4B). Co-culture of polyclonal aAPC-propagated/activated γδ T cells with cancer cells resulted in a hierarchy of IFNγ production following Vδ2>Vδ1>Vδ1^{neg}Vδ2^{neg} as shown by MFI of 855 ± 475, 242 ± 178, and 194 ± 182 (mean ± SD; n=4), respectively. IFNγ production by Vδ1, Vδ2, and Vδ1^{neg}Vδ2^{neg} subsets was inhibited by pan-TCRγδ antibody when added to of γδ T cell/tumor co-cultures indicating that response to the tumor in each subset was dependent upon activation through TCRγδ (**Figure 4C**). This observation supported the premise that a single cancer cell could be targeted by discrete γδ TCRs. Thus, a multivalent pro-inflammatory response to the tumor cell was achieved by polyclonal γδ T cells.

Polyclonal γδ T cells lyse a broad range of tumor cells through combination of DNAM1, NKG2D, and TCRγδ

After establishing that propagated γδ T cells could be activated to produce pro-inflammatory cytokines, we examined their ability to specifically lyse a panel of tumor cell lines. Polyclonal γδ T cells demonstrated a range of cytolysis against solid and hematological cancer-cell lines without a clear preference towards a particular tumor histology or grade (**Figure 5 and Supplemental Figure 11**). We previously established that B-cell acute lymphoblastic leukemia (ALL) cell line NALM-6 was largely resistant to lysis by γδ T cells, which required a CD19-specific CAR to acquire significant killing capability (27). In this study it was also observed that autologous and allogeneic normal B cells were spared from cytolysis (**Figure 5A**), and that B-ALL cell line cALL-2 and murine T cell lymphoma cell line EL4 were lysed poorly by polyclonal γδ T cells, which indicated that some cells were resistant and/or not recognized by polyclonal γδ T cells. In contrast, T-ALL cell line Jurkat and B-ALL cell lines RCH-ACV were

both killed efficiently by polyclonal γδ T cells (**Figure 5B**), indicating that γδ T cells could be used to target some B-cell and T-cell malignancies. Kasumi-3 is a $CD33^{+}CD34^{+}$ undifferentiated leukemia cell line that was lysed at intermediate levels by γδ T cells. Chronic myelogenous leukemia (CML) cell line K562 and K562-derived clone#4 aAPC were killed by polyclonal γδ T cells, which corroborated the notion that these cells could serve as a proliferative substrate. Pancreatic cancer cell lines BxPc-3, MiaPaCa-2, and Su8686, were lysed by γδ T cells, as was the colon carcinoma cell line HCT-116 (**Figure 5C**). Ovarian cell lines were killed by polyclonal γδ T cells in the following order of decreasing sensitivity: CAOV3 > EFO21 > UPN251 > IGROV1 > OC314 > Hey > A2780 > OVCAR3 > OAW42 > EFO27. Each of the separated Vδ subsets lysed hematological (Jurkat and K562) and solid (OC314 and CAOV3) tumor cell lines, which showed that polyclonal γδ T cells could direct a multivalent response against common targets (**Supplemental Figure 12**). The strength of cytolysis followed the hierarchy of TCR usage (Vδ2>$Vδ1^{neg}Vδ2^{neg}$>Vδ1) that was consistent with the premise that a propensity to be triggered for effector function would increase with T-cell differentiation (**Supplemental Figure 13**). Lysis by polyclonal populations was apparently not due to one specific Vδ subtype but rather from contributions of multiple γδ T-cell subsets, because it was observed that (1) a number of tumor cell lines were equivalently killed by polyclonal γδ T cells containing different frequencies of Vδ1, Vδ2, and $Vδ1^{neg}Vδ2^{neg}$ cells and (2) a polyclonal population was not identified with dominant cytolysis. We also sought to determine which surface molecules were responsible for cytolysis by blocking immunoreceptors with antibodies (**Figure 5D**). Our experimental approach also took into account that γδ T cells co-express DNAM1 (97.7% ± 0.9%; mean ± SD; n=4) and NKG2D (40.1% ± 16.5%) which can activate both T cells and NK cells for killing (32, 33). Addition of individual antibodies did not reduce lysis, except for TCRγδ in 2 of

3 cell lines tested. In contrast, a pool of antibodies binding NKG2D, DNAM1, TCRγδ resulted in significant inhibition, in a dose-dependent manner, of γδ T-cell mediated cytolysis against all 3 targets. Collectively, these data established that *ex vivo*-propagated γδ T cells have broad anti-tumor capabilities likely mediated by activation though DNAM1, NKG2D, and TCRγδ.

Established ovarian cancer xenografts are eliminated by adoptive transfer of γδ T cells

To test whether polyclonal γδ T cells were effective in targeting and killing tumors *in vivo*, we created a xenograft model for ovarian cancer in immunocompromised mice. NSG mice were injected intraperitoneally with CAOV3-e*ffLuc*-mKate ovarian cancer cells and then randomized into five treatment groups. Following eight days of tumor engraftment, either PBS (vehicle/mock), Vδ1, Vδ2, $V\delta1^{neg}V\delta2^{neg}$, or polyclonal γδ T cells were administered in escalating doses (**Figure 6**). Tumor burden and biodistribution were serially measured by non-invasive bioluminescence imaging. Established tumors continued to grow in vehicle-treated mice, but tumor bioburden was significantly reduced ($p \leq 0.001$) in mice receiving γδ T-cell treatments at day 72, relative to their initial tumor burden (**Figure 6A-B**). Adoptive transfer of polyclonal γδ T cells, Vδ1, and $V\delta1^{neg}V\delta2^{neg}$ T cells significantly ($p \leq 0.01$), and Vδ2 almost significantly ($p=0.055$), increased long-term survival compared to mock-treated mice. This corresponded to overall survival following polyclonal>Vδ1>$V\delta1^{neg}V\delta2^{neg}$>Vδ2 (**Figure 6C**). This is the first time that three Vδ subsets have been compared for their ability to target tumor *in vivo* and is the first display of *in vivo* anti-tumor activity by $V\delta1^{neg}V\delta2^{neg}$ cells. In sum, activated and propagated γδ T cells were effective in treating cancer *in vivo* and thus represent an attractive approach to adoptive immunotherapy.

DISCUSSION

This study establishes our aAPC clone #4 as a cellular platform for the sustained proliferation of multiple γδ T cell populations that demonstrate extensive reactivity against hematologic and solid malignancies. T cells expressing defined Vδ TCRs have been associated with clinical responses against cancer. For example, the Vδ1 subset correlated with complete responses observed in patients with ALL and acute myelogenous leukemia (AML) after αβ T cell-depleted haploidentical HSCT (15-17). Vδ1 cells were also shown to kill glioblastoma independent of cytomegalovirus (CMV) status (34). However, Vδ1 cells have not been directly administered. Our data establish that such cells could mediate anti-tumor immunity and supports the adoptive transfer Vδ1 T cells for cancer therapy. In contrast to Vδ1 and $V\delta1^{neg}V\delta2^{neg}$ cells, T cells expressing Vδ2 TCR have been directly infused and elicited responses against solid and hematological tumors (9, 35). Little is known about $V\delta1^{neg}V\delta2^{neg}$ T cells, but these lymphocytes have displayed recognition of the non-classical MHC molecule CD1d with corresponding NKT-like functions and have also been correlated with immunity to human immunodeficiency virus (HIV) and CMV (36-39). Our results are the first to directly show that $V\delta1^{neg}V\delta2^{neg}$ cells exhibit anti-tumor activities, and given their propensity to engage both viruses and cancer the add-back of this subset could especially benefit immunocompromised cancer patients. Because aAPC with IL-2 and IL-21 can propagate polyclonal γδ T cells, mAbs can now be raised against Vδ3, Vδ5, Vδ7, and Vδ8 isotypes to help elucidate their potential roles in clearance of pathogens and cancer. In aggregate, our data support the adoptive transfer of γδ T cells that maintain expression of multiple Vδ TCR types as investigational treatment for cancer.

The molecules on aAPC that activate γδ T cells for numeric expansion are not well known. K562-derived aAPC express endogenous MHC Class-I chain-related protein A and B (MICA/B) which are ligands for both Vδ1 and NKG2D (6, 40). Indeed, NKG2D was observed on polyclonal γδ T cells that also predominantly expressed Vδ1 TCR (**Figure 1A**). Polyclonal γδ T cells also demonstrate expression for activating receptors typically found on NK cells (NKp30, NKp44, and NKp46; collectively expressed at 26% ± 7%), and future studies will examine their contribution to γδ T-cell effector function. Some malignant cells were recognized poorly by γδ T cells, *e.g.*, EL4, EFO27, OAW42, cALL-2, and NALM-6, which provides an opportunity to further interrogate the mechanism by which γδ T cells recognize and kill tumor cells. Given that inhibition of cytolysis was maximized by neutralizing DNAM1, NKG2D, and TCRγδ receptors simultaneously, it may be that sensitivity of a tumor cell resides on the expression of ligand combinations that can bind these receptors. Two ligands recognized by Vδ2 TCR are surface mitochondrial F_1-ATPase and phospho-antigens, both of which are found in K562 cells (41, 42). Enhanced responses of T cells expressing Vγ9Vδ2 were observed when K562 cells were treated with aminobisphosphonates (41) and a similar strategy could be employed upon co-culture with aAPC clone #4 to increase the abundance of T cells bearing Vδ2 TCR (18). Future studies will evaluate additional TCRγδ ligands that naturally occur in these aAPC.

We enforced expression of co-stimulatory molecules to ascertain and improve the capability of K562-derived aAPC to propagate γδ T cells expressing a diversity of TCR. Indeed, CD137L was the dominant co-stimulatory proliferative signal on aAPC for expansion of γδ T cells with broad tumor-reactivity (**Figure 1C**), and its receptor, CD137, has been used to enrich tumor-reactive αβ T cells following antigen exposure and presumably TCR stimulation (43-45).

CD137 was not expressed on resting γδ T cells prior to expansion, suggesting that the importance of CD137L co-stimulation by aAPC followed TCR stimulation by the aAPC and expression of CD137 on the γδ T cell surface. $CD27^{+}$ and $CD27^{neg}$ γδ T cells have been shown to produce IFNγ and IL-17 (46), respectively; therefore, CD27 could be used as a marker for isolating γδ T cells with a preferred cytokine output. ICOS-ligand in absence of CD86 was shown to polarize $CD4^{+}$ αβ T cells to produce IL-17 instead of IFNγ (47), and current studies are investigating whether combinations of co-stimulatory molecules can selectively propagate cytokine-producing sub-populations of γδ T cells. Thus, the aAPC co-culture system in the context of desired cytokines provides a clinically-relevant methodology to tailor the type of therapeutic γδ T cell produced for adoptive immunotherapy.

Our data have implications for the design and interpretation of clinical trials. Expression of IL-15 was important for the maintenance of transferred γδ T cells *in vivo* (48), supporting the use of IL-15 on aAPC, and future studies could inform on other molecules that could be introduced to maximize the cell therapy product. Correlative studies are enhanced by our observation that TCRγδ mAb can be used to readily distinguish the three (Vδ1, Vδ2, and $Vδ1^{neg}Vδ2^{neg}$) T-cell subsets based on MFI of TCRγδ expression (**Figure 3B**). Given that γδ T cells are not thought to recognize ligands in the context of MHC (17), there is potential to infuse allogeneic, including 3^{rd} party, γδ T cells in lymphodepleted hosts to achieve an anti-tumor effect while mitigating the risk of graft-versus-host disease. Restoration of lymphopoiesis may result in graft rejection, but a therapeutic window could be established whereby tumors are directly killed by infused γδ T cells, which may result in desired bystander effects as conserved or neo-antigens are presented to other lymphocytes. Indeed, γδ T cells have been shown to lyse cancer cells,

cross-present tumor-specific antigens to αβ T cells, and license them to kill tumors (49, 50). The aAPC clone #4 has been produced as a master cell bank in compliance with current good manufacturing practice and provides a clear path to generating clinical-grade γδ T cells for human application. Human trials can now, for the first time, test the efficacy of adoptive transfer of T cells with polyclonal TCRγδ repertoire for treatment of solid and hematological tumors.

ACKNOWLEDGEMENTS

We thank Dr. Carl June and colleagues (University of Pennsylvania) for help generating K562-derived aAPC clone #4 and Dr. Perry Hackett (University of Minnesota) for his assistance with the SB system. Our thanks to Drs. George McNamara (MD Anderson Cancer Center) and Eric Tran (National Cancer Institute) who edited the text. The Immune Monitoring Core Lab (IMCL; MD Anderson Cancer Center) performed Luminex assays and the flow cytometry core lab (MD Anderson Cancer Center) assisted with FACS facility. Cancer Center Support Grant (CCGS) supported STR DNA fingerprinting at MD Anderson Cancer center. D.C.D. is an American Legion Auxiliary Fellow in Cancer Research (UT-GSBS-Houston), Andrew Sowell-Wade Huggins Scholar in Cancer Research (Cancer Answers Foundation), and a Teal Pre-doctoral Scholar (Department of Defense Ovarian Cancer Research Program). This work was supported by funding from: Cancer Center Core Grant (CA16672); RO1 (CA124782, CA120956, CA141303); R33 (CA116127); P01 (CA148600); S10RR026916; Albert J. Ward Foundation; Burroughs Wellcome Fund; Cancer Prevention and Research Institute of Texas; CLL Global Research Foundation; Department of Defense; Estate of Noelan L. Bibler; Gillson Longenbaugh Foundation; Harry T. Mangurian, Jr., Fund for Leukemia Immunotherapy.; Fund for Leukemia Immunotherapy; Institute of Personalized Cancer Therapy; Leukemia and Lymphoma Society; Lymphoma Research Foundation; Miller Foundation; Mr. Herb Simons; Mr. and Mrs. Joe H. Scales; Mr. Thomas Scott; MD Anderson Cancer Center Moon Shot; National Foundation for Cancer Research; Pediatric Cancer Research Foundation; Production Assistance for Cellular Therapies (PACT); TeamConnor; Thomas Scott; William Lawrence and Blanche Hughes Children's Foundation.

REFERENCES

1. Bonneville M, O'Brien RL, Born WK. Gammadelta T cell effector functions: a blend of innate programming and acquired plasticity. Nat Rev Immunol. 2010;10:467-78.
2. Vantourout P, Hayday A. Six-of-the-best: unique contributions of gammadelta T cells to immunology. Nat Rev Immunol. 2013;13:88-100.
3. Lefranc MP. Nomenclature of the human T cell receptor genes. Curr Protoc Immunol. 2001;Appendix 1:Appendix 1O.
4. Turchinovich G, Pennington DJ. T cell receptor signalling in gammadelta cell development: strength isn't everything. Trends Immunol. 2011;32:567-73.
5. Kabelitz D, Wesch D, He W. Perspectives of gammadelta T cells in tumor immunology. Cancer Res. 2007;67:5-8.
6. Xu B, Pizarro JC, Holmes MA, McBeth C, Groh V, Spies T, et al. Crystal structure of a gammadelta T-cell receptor specific for the human MHC class I homolog MICA. Proc Natl Acad Sci U S A. 2011;108:2414-9.
7. Lopez RD, Xu S, Guo B, Negrin RS, Waller EK. CD2-mediated IL-12-dependent signals render human gamma delta-T cells resistant to mitogen-induced apoptosis, permitting the large-scale ex vivo expansion of functionally distinct lymphocytes: implications for the development of adoptive immunotherapy strategies. Blood. 2000;96:3827-37.
8. Lamb LS, Jr., Gee AP, Hazlett LJ, Musk P, Parrish RS, O'Hanlon TP, et al. Influence of T cell depletion method on circulating gammadelta T cell reconstitution and potential role in the graft-versus-leukemia effect. Cytotherapy. 1999;1:7-19.
9. Stresing V, Daubine F, Benzaid I, Monkkonen H, Clezardin P. Bisphosphonates in cancer therapy. Cancer Lett. 2007;257:16-35.
10. Kondo M, Sakuta K, Noguchi A, Ariyoshi N, Sato K, Sato S, et al. Zoledronate facilitates large-scale ex vivo expansion of functional gammadelta T cells from cancer patients for use in adoptive immunotherapy. Cytotherapy. 2008;10:842-56.
11. Lang JM, Kaikobad MR, Wallace M, Staab MJ, Horvath DL, Wilding G, et al. Pilot trial of interleukin-2 and zoledronic acid to augment gammadelta T cells as treatment for patients with refractory renal cell carcinoma. Cancer Immunol Immunother. 2011;60:1447-60.
12. Wilhelm M, Kunzmann V, Eckstein S, Reimer P, Weissinger F, Ruediger T, et al. Gammadelta T cells for immune therapy of patients with lymphoid malignancies. Blood. 2003;102:200-6.
13. Nagamine I, Yamaguchi Y, Ohara M, Ikeda T, Okada M. Induction of gamma delta T cells using zoledronate plus interleukin-2 in patients with metastatic cancer. Hiroshima J Med Sci. 2009;58:37-44.
14. Nicol AJ, Tokuyama H, Mattarollo SR, Hagi T, Suzuki K, Yokokawa K, et al. Clinical evaluation of autologous gamma delta T cell-based immunotherapy for metastatic solid tumours. Br J Cancer. 2011;105:778-86.
15. Godder KT, Henslee-Downey PJ, Mehta J, Park BS, Chiang KY, Abhyankar S, et al. Long term disease-free survival in acute leukemia patients recovering with increased gammadelta T cells after partially mismatched related donor bone marrow transplantation. Bone Marrow Transplant. 2007;39:751-7.
16. Lamb LS, Jr., Henslee-Downey PJ, Parrish RS, Godder K, Thompson J, Lee C, et al. Increased frequency of TCR gamma delta + T cells in disease-free survivors following T cell-

depleted, partially mismatched, related donor bone marrow transplantation for leukemia. J Hematother. 1996;5:503-9.
17. Lamb LS, Jr., Musk P, Ye Z, van Rhee F, Geier SS, Tong JJ, et al. Human gammadelta(+) T lymphocytes have in vitro graft vs leukemia activity in the absence of an allogeneic response. Bone Marrow Transplant. 2001;27:601-6.
18. D'Asaro M, La Mendola C, Di Liberto D, Orlando V, Todaro M, Spina M, et al. V gamma 9V delta 2 T lymphocytes efficiently recognize and kill zoledronate-sensitized, imatinib-sensitive, and imatinib-resistant chronic myelogenous leukemia cells. J Immunol. 2010;184:3260-8.
19. Singh H, Figliola MJ, Dawson MJ, Olivares S, Zhang L, Yang G, et al. Manufacture of Clinical-Grade CD19-Specific T Cells Stably Expressing Chimeric Antigen Receptor Using Sleeping Beauty System and Artificial Antigen Presenting Cells. PLoS One. 2013;8:e64138.
20. Maus MV, Thomas AK, Leonard DG, Allman D, Addya K, Schlienger K, et al. Ex vivo expansion of polyclonal and antigen-specific cytotoxic T lymphocytes by artificial APCs expressing ligands for the T-cell receptor, CD28 and 4-1BB. Nat Biotechnol. 2002;20:143-8.
21. Suhoski MM, Golovina TN, Aqui NA, Tai VC, Varela-Rohena A, Milone MC, et al. Engineering artificial antigen-presenting cells to express a diverse array of co-stimulatory molecules. Mol Ther. 2007;15:981-8.
22. Numbenjapon T, Serrano LM, Singh H, Kowolik CM, Olivares S, Gonzalez N, et al. Characterization of an artificial antigen-presenting cell to propagate cytolytic CD19-specific T cells. Leukemia. 2006;20:1889-92.
23. Denman CJ, Senyukov VV, Somanchi SS, Phatarpekar PV, Kopp LM, Johnson JL, et al. Membrane-bound IL-21 promotes sustained ex vivo proliferation of human natural killer cells. PLoS One. 2012;7:e30264.
24. Singh H, Manuri PR, Olivares S, Dara N, Dawson MJ, Huls H, et al. Redirecting specificity of T-cell populations for CD19 using the Sleeping Beauty system. Cancer Res. 2008;68:2961-71.
25. Singh H, Figliola MJ, Dawson MJ, Huls H, Olivares S, Switzer K, et al. Reprogramming CD19-Specific T Cells with IL-21 Signaling Can Improve Adoptive Immunotherapy of B-Lineage Malignancies. Cancer Res. 2011;71:3516-27.
26. Manuri PV, Wilson MH, Maiti SN, Mi T, Singh H, Olivares S, et al. piggyBac transposon/transposase system to generate CD19-specific T cells for the treatment of B-lineage malignancies. Hum Gene Ther. 2010;21:427-37.
27. Deniger DC, Switzer K, Mi T, Maiti S, Hurton L, Singh H, et al. Bispecific T-cells expressing polyclonal repertoire of endogenous gammadelta T-cell receptors and introduced CD19-specific chimeric antigen receptor. Mol Ther. 2013;21:638-47.
28. Zhang M, Maiti S, Bernatchez C, Huls H, Rabinovich B, Champlin RE, et al. A new approach to simultaneously quantify both TCR alpha- and beta-chain diversity after adoptive immunotherapy. Clin Cancer Res. 2012;18:4733-42.
29. Turkman N, Shavrin A, Ivanov RA, Rabinovich B, Volgin A, Gelovani JG, et al. Fluorinated cannabinoid CB2 receptor ligands: synthesis and in vitro binding characteristics of 2-oxoquinoline derivatives. Bioorg Med Chem. 2011;19:5698-707.
30. Rabinovich BA, Ye Y, Etto T, Chen JQ, Levitsky HI, Overwijk WW, et al. Visualizing fewer than 10 mouse T cells with an enhanced firefly luciferase in immunocompetent mouse models of cancer. Proc Natl Acad Sci U S A. 2008;105:14342-6.

31. Morita CT, Parker CM, Brenner MB, Band H. TCR usage and functional capabilities of human gamma delta T cells at birth. J Immunol. 1994;153:3979-88.
32. Gilfillan S, Chan CJ, Cella M, Haynes NM, Rapaport AS, Boles KS, et al. DNAM-1 promotes activation of cytotoxic lymphocytes by nonprofessional antigen-presenting cells and tumors. J Exp Med. 2008;205:2965-73.
33. Bauer S, Groh V, Wu J, Steinle A, Phillips JH, Lanier LL, et al. Activation of NK cells and T cells by NKG2D, a receptor for stress-inducible MICA. Science. 1999;285:727-9.
34. Knight A, Arnouk H, Britt W, Gillespie GY, Cloud GA, Harkins L, et al. CMV-Independent Lysis of Glioblastoma by Ex Vivo Expanded/Activated Vdelta1+ gammadelta T Cells. PLoS One. 2013;8:e68729.
35. Chiplunkar S, Dhar S, Wesch D, Kabelitz D. gammadelta T cells in cancer immunotherapy: current status and future prospects. Immunotherapy. 2009;1:663-78.
36. Knight A, Madrigal AJ, Grace S, Sivakumaran J, Kottaridis P, Mackinnon S, et al. The role of Vdelta2-negative gammadelta T cells during cytomegalovirus reactivation in recipients of allogeneic stem cell transplantation. Blood. 2010;116:2164-72.
37. Kabelitz D, Hinz T, Dobmeyer T, Mentzel U, Marx S, Bohme A, et al. Clonal expansion of Vgamma3/Vdelta3-expressing gammadelta T cells in an HIV-1/2-negative patient with CD4 T-cell deficiency. Br J Haematol. 1997;96:266-71.
38. Mangan BA, Dunne MR, O'Reilly VP, Dunne PJ, Exley MA, O'Shea D, et al. Cutting edge: CD1d restriction and th1/th2/th17 cytokine secretion by human vdelta3 T cells. J Immunol. 2013;191:30-4.
39. Willcox CR, Pitard V, Netzer S, Couzi L, Salim M, Silberzahn T, et al. Cytomegalovirus and tumor stress surveillance by binding of a human gammadelta T cell antigen receptor to endothelial protein C receptor. Nat Immunol. 2012;13:872-9.
40. Numbenjapon T, Serrano LM, Chang WC, Forman SJ, Jensen MC, Cooper LJ. Antigen-independent and antigen-dependent methods to numerically expand CD19-specific CD8+ T cells. Exp Hematol. 2007;35:1083-90.
41. Vantourout P, Mookerjee-Basu J, Rolland C, Pont F, Martin H, Davrinche C, et al. Specific requirements for Vgamma9Vdelta2 T cell stimulation by a natural adenylated phosphoantigen. J Immunol. 2009;183:3848-57.
42. Scotet E, Martinez LO, Grant E, Barbaras R, Jeno P, Guiraud M, et al. Tumor recognition following Vgamma9Vdelta2 T cell receptor interactions with a surface F1-ATPase-related structure and apolipoprotein A-I. Immunity. 2005;22:71-80.
43. Turcotte S, Gros A, Hogan K, Tran E, Hinrichs CS, Wunderlich JR, et al. Phenotype and function of T cells infiltrating visceral metastases from gastrointestinal cancers and melanoma: implications for adoptive cell transfer therapy. J Immunol. 2013;191:2217-25.
44. Chacon JA, Wu RC, Sukhumalchandra P, Molldrem JJ, Sarnaik A, Pilon-Thomas S, et al. Co-stimulation through 4-1BB/CD137 improves the expansion and function of CD8(+) melanoma tumor-infiltrating lymphocytes for adoptive T-cell therapy. PLoS One. 2013;8:e60031.
45. Gros A, Robbins PF, Yao X, Li YF, Turcotte S, Tran E, et al. PD-1 identifies the patient-specific CD8+ tumor-reactive repertoire infiltrating human tumors. J Clin Invest. 2014.
46. Caccamo N, La Mendola C, Orlando V, Meraviglia S, Todaro M, Stassi G, et al. Differentiation, phenotype, and function of interleukin-17-producing human Vgamma9Vdelta2 T cells. Blood. 2011;118:129-38.

47. Paulos CM, Carpenito C, Plesa G, Suhoski MM, Varela-Rohena A, Golovina TN, et al. The inducible costimulator (ICOS) is critical for the development of human T(H)17 cells. Sci Transl Med. 2010;2:55ra78.
48. Izumi T, Kondo M, Takahashi T, Fujieda N, Kondo A, Tamura N, et al. Ex vivo characterization of gammadelta T-cell repertoire in patients after adoptive transfer of Vgamma9Vdelta2 T cells expressing the interleukin-2 receptor beta-chain and the common gamma-chain. Cytotherapy. 2013;15:481-91.
49. Anderson J, Gustafsson K, Himoudi N, Yan M, Heuijerjans J. Licensing of gammadeltaT cells for professional antigen presentation: A new role for antibodies in regulation of antitumor immune responses. Oncoimmunology. 2012;1:1652-4.
50. Himoudi N, Morgenstern DA, Yan M, Vernay B, Saraiva L, Wu Y, et al. Human gammadelta T lymphocytes are licensed for professional antigen presentation by interaction with opsonized target cells. J Immunol. 2012;188:1708-16.

FIGURES LEGENDS

Figure 1. Sustained proliferation of polyclonal PBMC-derived γδ T cells on γ-irradiated aAPC in presence of soluble IL-2 and IL-21. (**A**) Frequency of γδ T cells before (Day 0) and after (Day 22) co-culture on γ-irradiated aAPC, IL-2, and IL-21 where expression of CD3, CD56, TCRαβ, TCRγδ, TCRδ1, and TCRδ2 is shown at Day 22 of co-culture. One of 7 representative donors is shown. Quadrant frequencies (percentage) within flow plots are displayed in upper right corners. (**B**) Inferred cell counts of polyclonal γδ T cells are displayed calculated based on weekly yields and relative fold changes, where three arrows represent addition of aAPC. Black line is mean ± SD (n=4) pooled from 2 independent experiments and each gray line is an individual donor. (**C**) Fold increase over 9 days of γδ T cells co-cultured with IL-2 and IL-21 along with aAPC expressing membrane-bound IL-15 (mIL15), CD86, and/or CD137L. Data are mean ± SD (n=3) pooled from 2 independent experiments and each shape represents an individual donor. Two-way ANOVA with Bonferroni's post-tests was used for statistical analysis. *$p<0.05$ and **$p<0.01$ (**D**) Fold increase over 9 days of γδ T cells co-cultured with aAPC (clone #4) in the presence of either soluble recombinant IL-2 and/or IL-21. Data are mean ± SD (n=3) pooled from 2 independent experiments where each shape represents an individual donor. Two-way ANOVA with Bonferroni's post-tests was used for statistical analysis. *$p<0.05$

Figure 2. Abundance of Vδ and Vγ mRNA species in γδ T cells propagated and activated *ex vivo*. Quantification of mRNA species coding for (**A**) Vδ and (**B**) Vγ alleles in PBMC-derived γδ T cells by DTEA at day 22 of co-culture on aAPC/IL-2/IL-21. Quantification of mRNA species

coding for (**C**) Vδ and (**D**) Vγ alleles in UCB-derived γδ T cells by DTEA at day 34-35 of co-culture on aAPC/IL-2/IL-21. Box-and-whiskers plots display 25% and 75% percentiles where lines represent maximum, mean, and minimum from top to bottom (n=4). Solid lines at bottom of graphs represent limit-of-detection (LOD) calculated from mean ± 2xSD of DTEA negative controls. Student's paired one-tailed t-tests were performed for each allele relative to the sample LOD. *$p<0.05$ and **$p<0.01$

Figure 3. Sustained proliferation of PBMC-derived Vδ T-cell subsets expanded on γ-irradiated aAPC/IL-2/IL-21. After two 7-day stimulations with aAPC (clone #4) and IL-2/IL-21 the bulk population of γδ T cells were separated into Vδ1, Vδ2, and $Vδ1^{neg}Vδ2^{neg}$ subsets by FACS based on staining of T cells defined as $TCRδ1^{+}TCRδ2^{neg}$, $TCRδ1^{neg}TCRδ2^{+}$, and $TCRδ1^{neg}TCRδ2^{neg}$, respectively. (**A**) Expression of TCRδ1 and TCRδ2 chains on Vδ1, Vδ2, and $Vδ1^{neg}Vδ2^{neg}$ subsets of γδ T cells (from left to right) after 15 days of numeric expansion on aAPC and cytokines as isolated groups. One of 4 representative donors is shown pooled from 2 independent experiments. Quadrant frequencies (percentage) within flow plots are displayed in upper right corners. Frequency of $TCRδ1^{+}TCRδ2^{neg}$ (open bars), $TCRδ1^{neg}TCRδ2^{+}$ (black bars), and $TCRδ1^{neg}TCRδ2^{neg}$ (gray bars) cell surface protein expression in subsets of γδ T cells after 15 days numeric expansion on aAPC and cytokines as isolated groups. Data are mean ± SD (n=4) pooled from 2 independent experiments. (**B**) Flow cytometry plots of CD3 and TCRγδ expression in Vδ1, Vδ2, and $Vδ1^{neg}Vδ2^{neg}$ subsets (from left to right). Mean fluorescence intensity (MFI) of TCRγδ staining in Vδ1, Vδ2, and $Vδ1^{neg}Vδ2^{neg}$ T-cell subsets where each shape represents a different donor and data are mean ± SD (n=4) pooled from 2 independent

experiments. (**C**) Proliferation of each isolated Vδ subset stimulated twice with aAPC clone #4 (arrows) in presence of cytokines and total cell counts are displayed. Data are mean ± SD (n=4) pooled from 2 independent experiments. (**D**) DTEA was used to identify and measure abundance of mRNA species coding for Vδ1*01, Vδ2*02, and Vδ3*01 (from left to right) in γδ T-cell sub-populations after 15 days of proliferation on aAPC and cytokines as separated subsets. Box-and-whiskers plots display 25% and 75% percentiles where lines represent maximum, mean, and minimum from top to bottom (n=4). Student's paired, two-tailed t-tests were undertaken for statistical analyses between groups. **p<0.01 and ***p<0.001

Figure 4. Dependence on TCRγδ for IFNγ secretion in response to tumor cells. At Day 22 of co-culture on γ-irradiated aAPC (clone #4) with IL-2 and IL-21, T cells were incubated with CM (mock) or leukocyte activation cocktail (LAC; PMA/Ionomycin) for 6 hours at 37^{o}C. Tissue culture supernatants were interrogated using 27-Plex Luminex array to detect presence of (**A**) T_H1, T_H2, and T_H17 cytokines and selected chemokines (from left to right). Data are mean ± SD pooled from 4 donors in 2 independent experiments where each donor had triplicate experimental wells pooled prior to multiplex analysis. Student's one-tailed t-test performed for statistical analysis between mock and LAC groups. *p<0.05, **p<0.01, and ***p<0.001 (**B**) Polyclonal γδ T cells were incubated for 1 hour prior to and during 6 hour tumor cell co-culture with normal mouse serum or neutralizing TCRγδ antibody (clone IM). Cells were stained for TCRδ1, TCRδ2, CD3, and IFNγ to gate T-cell subsets and assess IFNγ production. Comparisons of histograms detailing Vδ1, Vδ2, and $Vδ1^{neg}Vδ2^{neg}$ gates (from left to right) co-cultured with CAOV3 ovarian cancer cells and treated with serum (open) or TCRγδ (shaded). Numbers next to

histograms are MFI. Flow plots are representative of 1 of 3 PB donors co-cultured with CAOV3 cells in 2 independent experiments. (**C**) Percent inhibition of IFNγ secretion in response to CAOV3 cells was calculated for each Vδ T-cell subset based on the following equation: Inhibition (%) = 100 – 100 x $[(MFI_{TUMOR + T\ CELL} - MFI_{T\ CELL\ ONLY})_{TCR\gamma\delta} / (MFI_{TUMOR + T\ CELL} - MFI_{T\ CELL\ ONLY})_{Serum}]$. Data are mean ± SD (n=3) pooled from 2 independent experiments.

Figure 5. Specific lysis of tumor-cell panel by polyclonal γδ T cells. (**A-C**) Standard 4-hour CRA was performed with increasing effector (polyclonal γδ T cells; each shape represents a different donor) to target (E:T) ratios against (**A**) healthy B cells from an allogeneic donor (one of four representative donors), (**B**) hematological tumor cell lines derived from B-ALL: RCH-ACV, T-ALL: Jurkat, and CML: K562, (**C**) solid tumor cell lines derived from pancreatic cancer: BxPc-3, colon cancer: HCT-116, and ovarian cancer: OC314 and CAOV3. Data are mean ± SD (n=3 wells per assay) from 2 independent experiments. (**D**) Neutralizing antibodies to NKG2D (squares), DNAM1 (triangles), TCRγδ (inverted triangles), or a pool (diamonds) of all three antibodies were used to block killing of Jurkat (left), IGROV1 (middle), or OC314 (right) tumor targets antibodies at 0.3, 1, and 3 μg/mL and an E:T ratio of 12:1 in standard 4-hour CRA. Normal mouse serum (circles) served as control for addition of antibody and wells without antibody were used for normalization purposes. Specific lysis was normalized to wells without antibody to yield relative cytolysis as defined by: Relative cytolysis (%) = $(\text{Specific Lysis})_{\text{With Antibody}}$ / $(\text{Specific Lysis})_{\text{Without Antibody}}$ x 100. Data are mean ± SD (n=4 donors) from triplicates pooled and normalized from 2 independent experiments. Repeated-measures Two-way

ANOVA was used for statistical analysis between antibody treatments. **p<0.01 and ***p<0.001

Figure 6. *In vivo* clearance of ovarian cancer upon adoptive transfer of polyclonal γδ T cells and γδ T-cell subsets propagated/activated on aAPC with IL-2 and IL-21. CAOV3-e*ffLuc*-mKate tumor cells were injected into NSG mice at Day -8 and engrafted until Day 0 when treatment was started with either PBS (vehicle/mock) or γδ T cells. Four T-cell doses were administered in weekly escalating doses. (**A**) BLI images at Day 0 (top panels) or Day 72 (bottom panels) in PBS, Vδ1, Vδ2, $Vδ1^{neg}Vδ2^{neg}$, and polyclonal γδ T-cell treatment groups. Images are representative of 6-14 mice from 2 independent experiments. (**B**) BLI measurements of mice at Day 0 (white) and Day 72 (gray) pooled from 2 independent experiments. Box-and-whiskers plots display 25% and 75% percentiles where lines represent maximum, mean, and minimum from top to bottom (n = 6-14). Student's paired, two-tailed t-tests were used for statistical analysis between time points. (**C**) Overall survival of mice treated with PBS (dashed), polyclonal (black), Vδ1 (red), Vδ2 (blue), or $Vδ1^{neg}Vδ2^{neg}$ (green) γδ T cells. Log-rank (Mantel-Cox) test was used to calculate p values. *p<0.05, **p<0.01, and ***p≤0.001

Author Manuscript Published OnlineFirst on May 15, 2014; DOI: 10.1158/1078-0432.CCR-13-3451
Author manuscripts have been peer reviewed and accepted for publication but have not yet been edited.

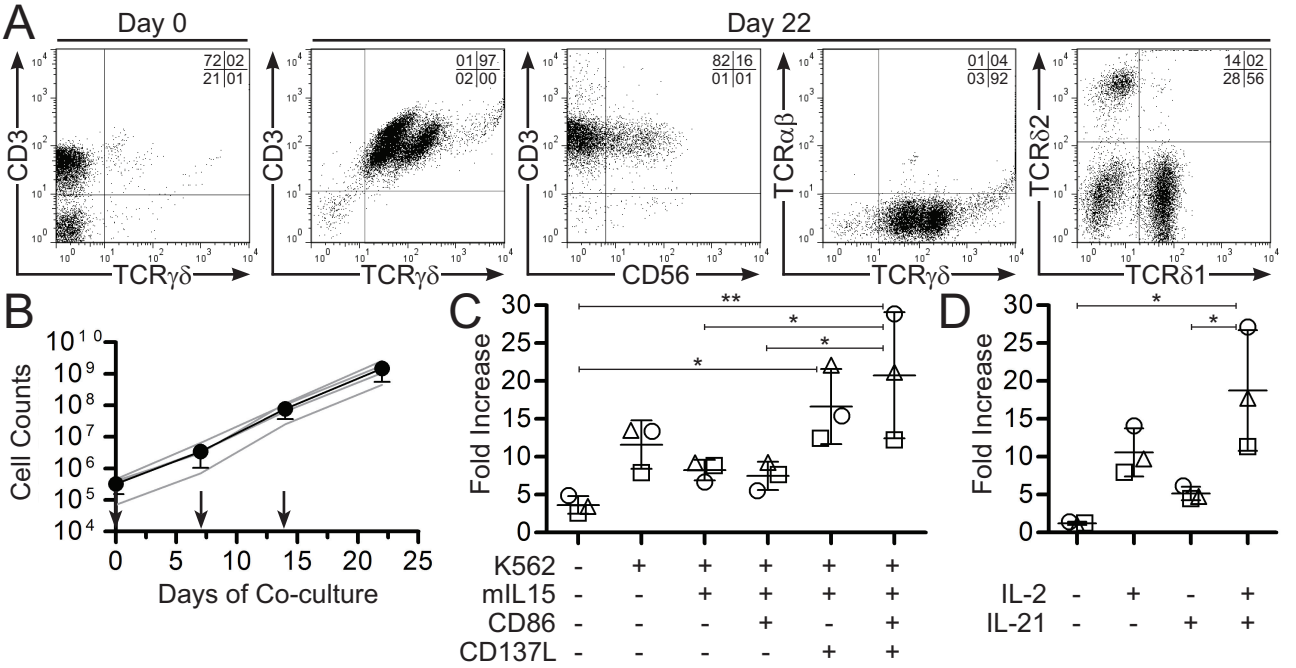

Figure 1

Author Manuscript Published OnlineFirst on May 15, 2014; DOI: 10.1158/1078-0432.CCR-13-3451
Author manuscripts have been peer reviewed and accepted for publication but have not yet been edited.

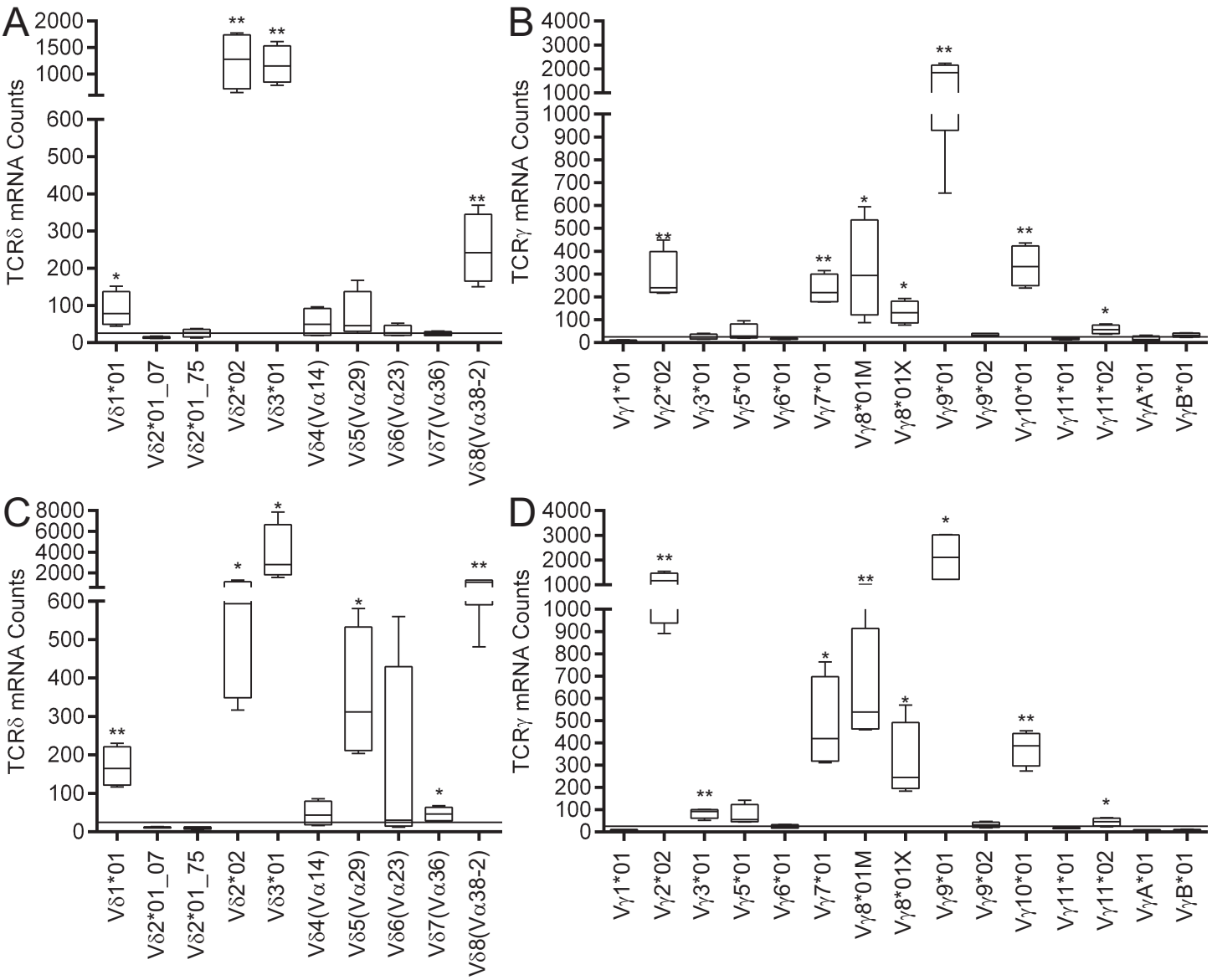

Figure 2

Author Manuscript Published OnlineFirst on May 15, 2014; DOI: 10.1158/1078-0432.CCR-13-3451
Author manuscripts have been peer reviewed and accepted for publication but have not yet been edited.

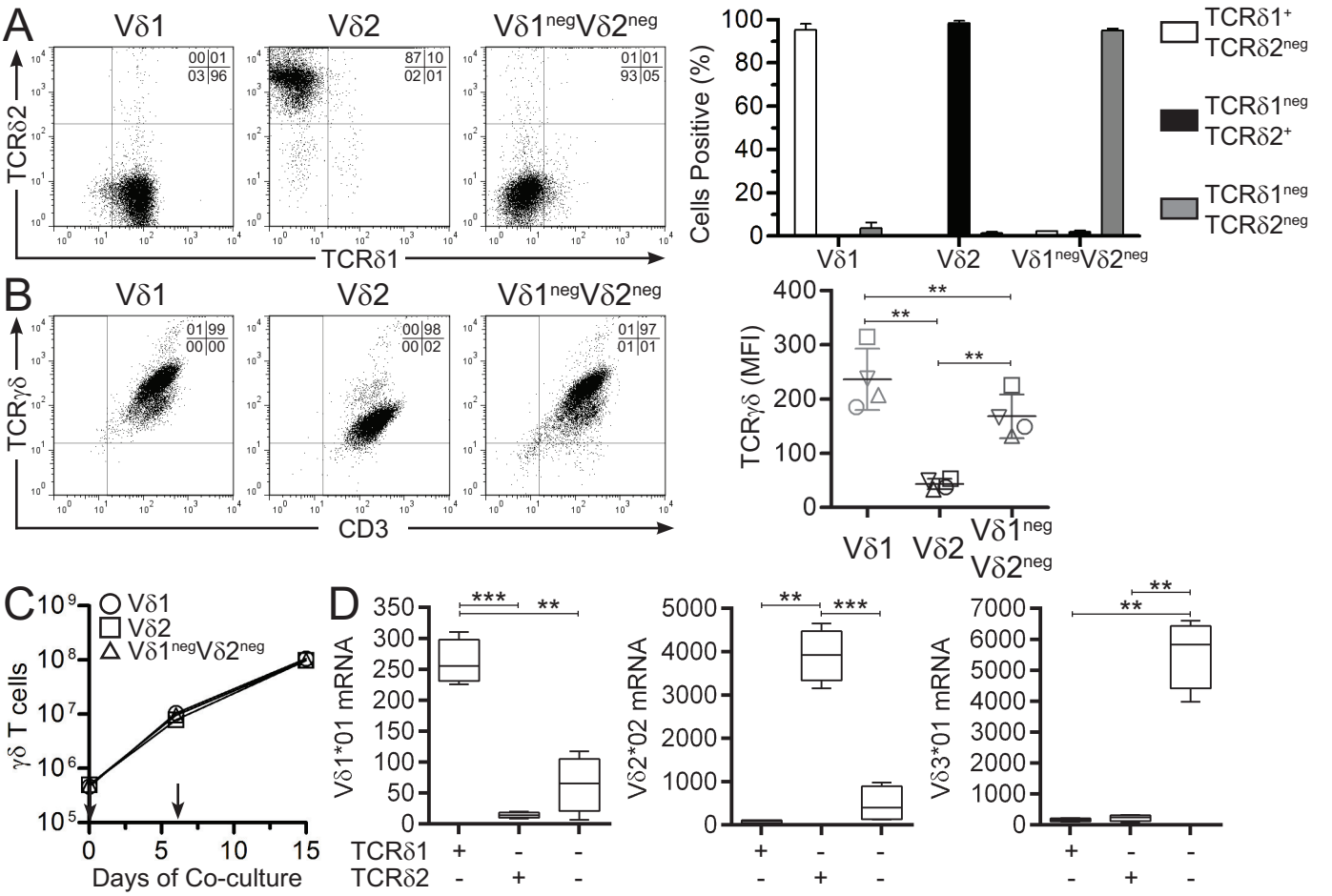

Figure 3

Author Manuscript Published OnlineFirst on May 15, 2014; DOI: 10.1158/1078-0432.CCR-13-3451
Author manuscripts have been peer reviewed and accepted for publication but have not yet been edited.

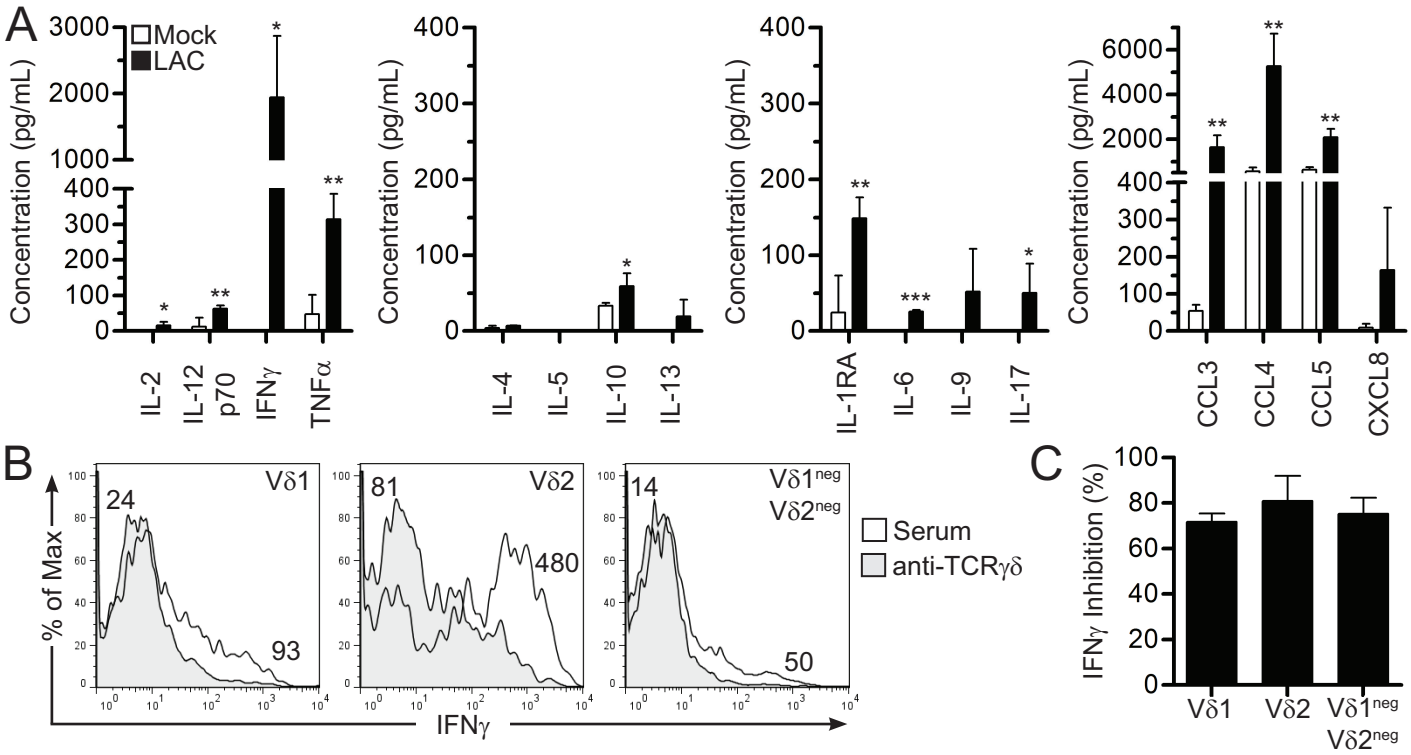

Figure 4

Author Manuscript Published OnlineFirst on May 15, 2014; DOI: 10.1158/1078-0432.CCR-13-3451
Author manuscripts have been peer reviewed and accepted for publication but have not yet been edited.

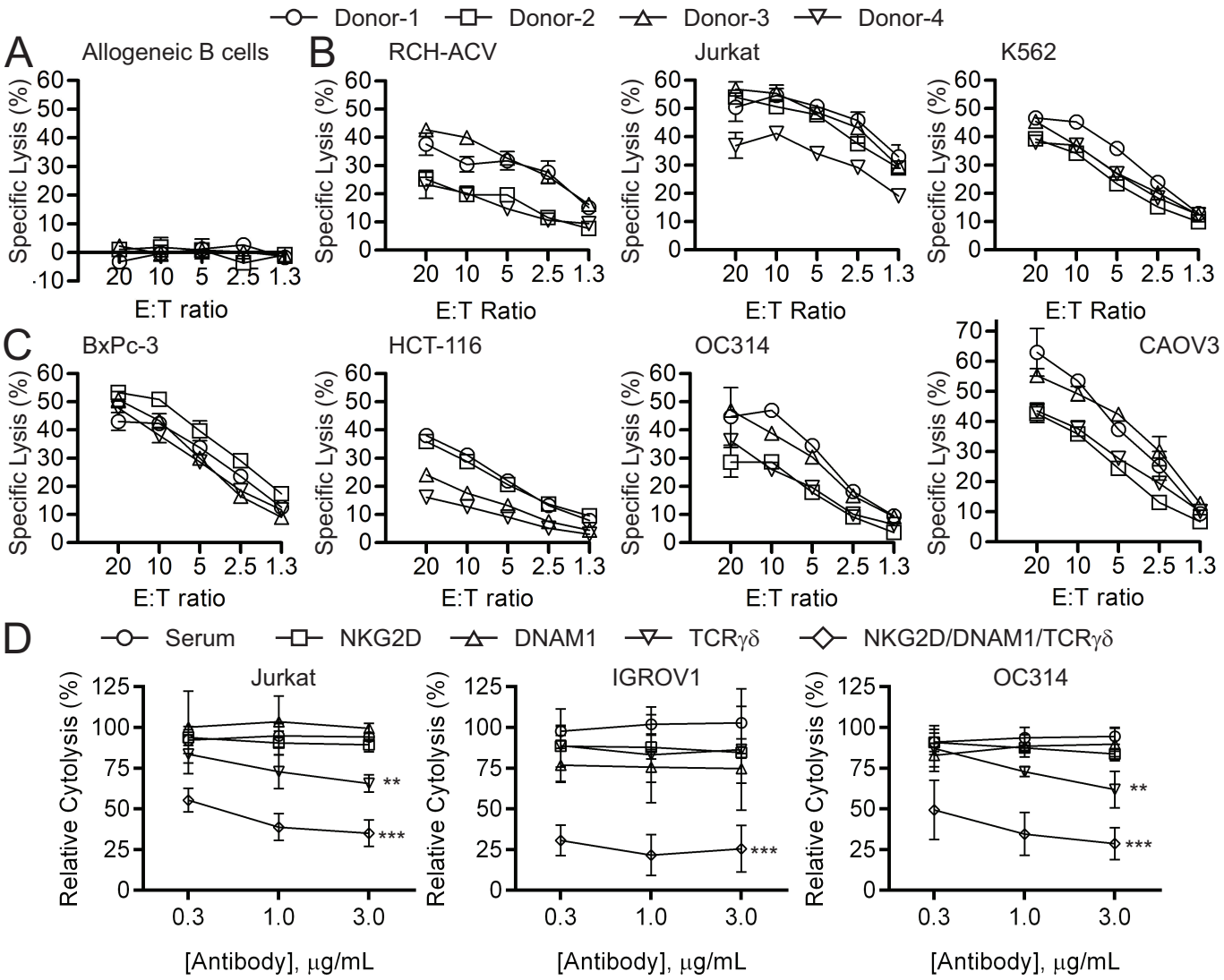

Figure 5

Author Manuscript Published OnlineFirst on May 15, 2014; DOI: 10.1158/1078-0432.CCR-13-3451
Author manuscripts have been peer reviewed and accepted for publication but have not yet been edited.

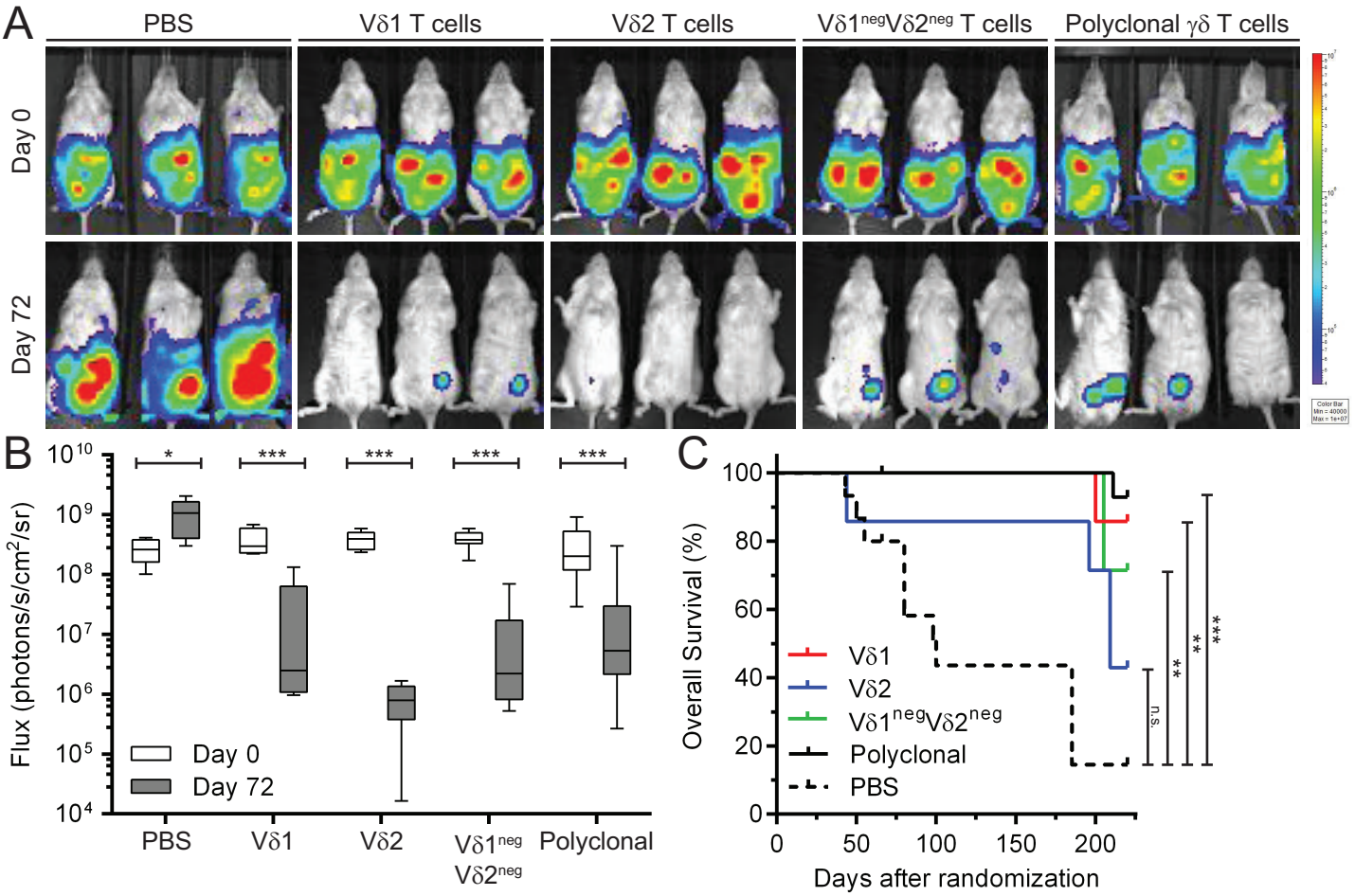

Figure 6

SUPPLEMENTAL MATERIAL:

"Activating and propagating polyclonal gamma delta T cells with broad specificity for malignancies"

ADDITIONAL MATERIALS AND METHODS

Tumor cell line culture conditions

Cell cultures were maintained in (i) RPMI (Gibco, Grand Island NY): K562 parental cells, aAPC clone#4, aAPC clone A6, aAPC clone A3, aAPC clone D4, Jurkat, cALL-2, RCH-ACV, Kasumi-3, A2780, EFO21, EFO27, Hey, IGROV1, OC314, OVCAR3, and UPN251, (ii) DMEM (Sigma, St. Louis, MO): 293-METR, CAOV3, BxPC-3, MiaPaCa-2, OAW42, and Su8686, or (iii) McCoy's 5A (Sigma): HCT-116. Each media was supplemented with 10% heat-inactivated fetal bovine serum (Hyclone, Logan, UT) and 1% Glutamax-100 (Gibco). UPN251 and OAW42 cells were supplemented with insulin-transferrin-selenium solution (Gibco). Cells were cultured under humidified conditions with 5% CO_2 at 37^{o}C.

Co-culture of γδ T cells on designer aAPC, IL-2, and/or IL-21

In order to assess the dependence of γδ T cells on cytokines for proliferation, co-cultures were initiated with 10^5 γδ T cells and $2x10^5$ aAPC (clone #4) then were added to an equal volume of (i) CM, (ii) CM and 100 U/mL IL-2, (iii) CM and 60 ng/mL IL-21, or (iv) CM, 100 U/mL IL-2, and 60 ng/mL IL-21. T cells were enumerated using Cellometer Auto T4 Cell Counter

(Nexcelom, Lawrence, MA) 9 days after initiating co-cultures to determine yields. K562 cells were genetically modified with one or more co-stimulatory molecules to generate three new aAPC (**Supplemental Figure 4**). A *Sleeping Beauty* (SB) transposon expressing IL-15 peptide fused in frame to IL-15Rα and SB11 transposase were co-electro-transferred into parental K562 cells ($CD86^{neg}$ and $CD137L^{neg}$) using by Nucleofection (Nucleofector II, Lonza, Basel, Switzerland) and Kit V (cat# VCA-1003, Lonza). FACS was used to isolate $mIL15^{+}$ cells and establish a clone (designated clone A6; $mIL15^{+}CD86^{neg}CD137L^{neg}$) which was then electroporated with SB11 and SB transposons expressing CD86 or CD137L. Cells were FACS sorted again to obtain clones A3 ($mIL15^{+}CD86^{+}CD137L^{neg}$) and D4 ($mIL15^{+}CD86^{neg}CD137L^{+}$). Co-cultures were initiated with 10^5 γδ T cells in CM supplemented with 100 U/mL IL-2 and 60 ng/mL IL-21 and were added to $2x10^5$ γ-irradiated (i) parental K562 cells, (ii) clone A6, (iii) clone A3, (iv) clone D4, (v) clone #4 aAPC, or (vi) no aAPC. T cells were enumerated 9 days after initiating as described above for cytokine experiments.

Intracellular cytokine production, Luminex, and neutralizing antibody cytolysis assays

For intracellular cytokine analyses, γδ T cells were incubated with NMS or TCRγδ blocking antibody (clone IMMU510 (IM); Thermo Fisher, Pittsburg, PA) at 37°C for 1 hour and added to an equal volume and number of target cells (CAOV3 or OC314) to yield final antibody concentration of 1.0 μg/mL. Co-cultures were incubated for 6 hours at 37°C in the presence of Brefeldin-A (GolgiPlug; BD Biosciences) to block exocytosis and secretion of cytokines. Co-cultures were then (i) stained for surface markers, *e.g.*, CD3, TCRδ1, and TCRδ2, (ii) fixed and permeabilized with BD Cytofix/Cytoperm (cat# 555028, BD Biosciences), (iii) stained for

intracellular IFNγ, and (iv) analyzed by flow cytometry. Co-cultures to assess cytokine secretion were incubated for 24 hours in CM (mock treatment) or leukocyte activation cocktail (LAC; 5 ng/mL PMA and 500 ng/mL Ionomycin) and supernatants from triplicate wells were pooled and analyzed by Bio-Plex Human Cytokine Group-I 27-plex Assay (cat# L50-0KCAF0Y, BioRad Technologies, Hercules, CA) using Luminex100 (xMap Technologies, Austin, TX). B cells from healthy donors were isolated with CD19 microbeads (cat# 130-050-301, Miltenyi Biotec) the day of each assay and used as target cells in CRA. Antibodies specific for NKG2D (clone 1D11; BD Biosciences), DNAM1 (clone DX11; BD Biosciences), and TCRγδ (clone IM) were used for neutralization experiments at 0.3, 1.0, and 3.0 μg/mL in CRA at E:T ratio of 12:1. Normal mouse serum (NMS; Jackson ImmunoResearch) was used as a negative control at the same concentrations and wells without antibodies were used for purposes of data normalization.

Lentivirus packaging and transduction of CAOV3 cells

Lentivirus particles were packaged according to a modified version of a protocol described elsewhere (29) to introduce mKate red fluorescence protein and enhanced *firefly Luciferase* (e*ffLuc*) into tumor cells for non-invasive imaging by BLI (30). Briefly, packaging cells (293-METR) were plated on T125 flasks and transfected the following day with pCMV R8.2, VSV-G, and pLVU3G-e*ffLuc*-T2A-mKateS158A (**Supplemental Figure 2**) plasmids in conjunction with Lipofectamine 2000 transfection reagent according to manufacturer's instructions (Invitrogen). Viral particles were harvested 48 and 72 hours post-transfection and concentrated through 100 kDa NMWL filters (cat# UFC810096, MilliPore, Billerica, MA). CAOV3 cells were plated in a 6-well plate and the following day virus coding for e*ffLuc*-mKate was added with 8 μg/ml

polybrene. Plate was spun at 1,800 rpm for 1.5 hours and 6 hours later the viral-conditioned supernatant was replaced with DMEM complete media, which was changed the following day. Single-cell clones of transduced CAOV3 were derived by limiting dilution that displayed the same morphology as the parental cell line and clone 1C2 was chosen as it had uniform mKate fluorescence with high ($>10^6$ signal to noise ratio) e*ffLuc* activity.

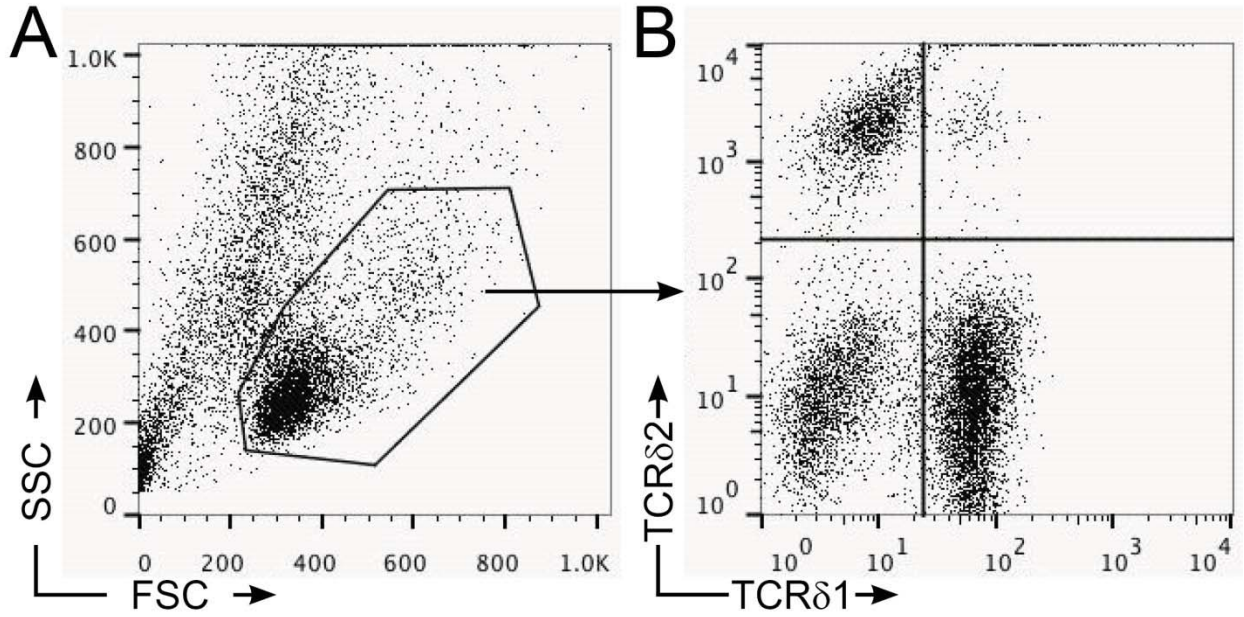

Supplemental Figure 1. An example of the gating strategy for γδ T-cell analyses. (A) Lymphocytes were gated by forward scatter (FSC) and side scatter (SSC) in the activated T-cell gate and were (B) analyzed for surface protein expression of markers of interest. A representative donor's expression of TCRδ1 and TCRδ2 are shown. Isotype controls were used to validate gating. Staining was performed as described (27).

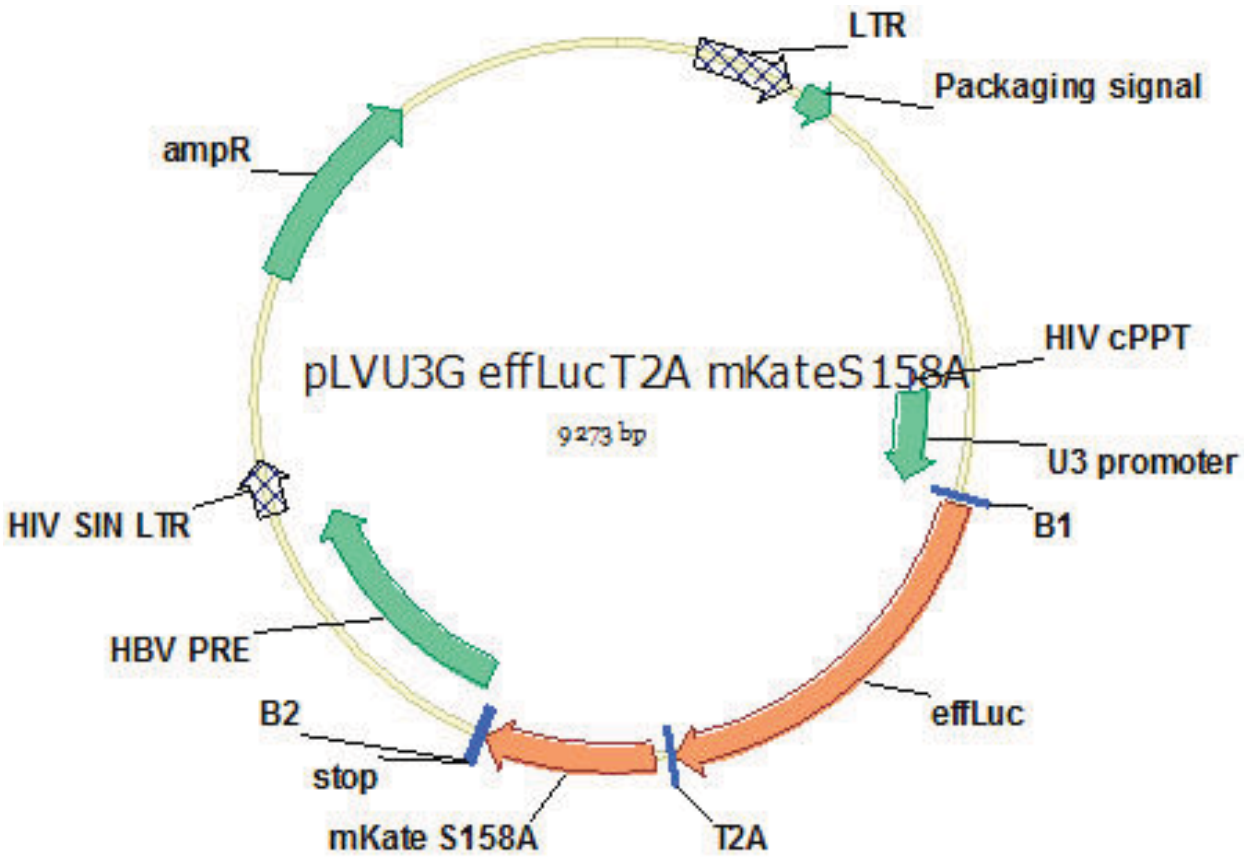

Supplemental Figure 2. Schematic of DNA plasmid pLVU3G-e*ffLuc*-T2A-mKateS158A used to co-express enhanced firefly luciferase (e*ffLuc*) and mKate. Annotations are, LTR: long terminal repeat; HIV cPPT: HIV central polypurine tract; B1: Gateway donor site B1; e*ffLuc*: enhanced *firefly Luciferase*; T2A: T2A ribosomal slip site; mKate S158A: enhanced mKate red fluorescence protein; B2: Gateway donor site B2; HBV PRE: Hepatitis B post-translational regulatory element; HIV SIN LTR: HIV self-inactivating long terminal repeat; ampR: ampicillin resistance (β-Lactamase).

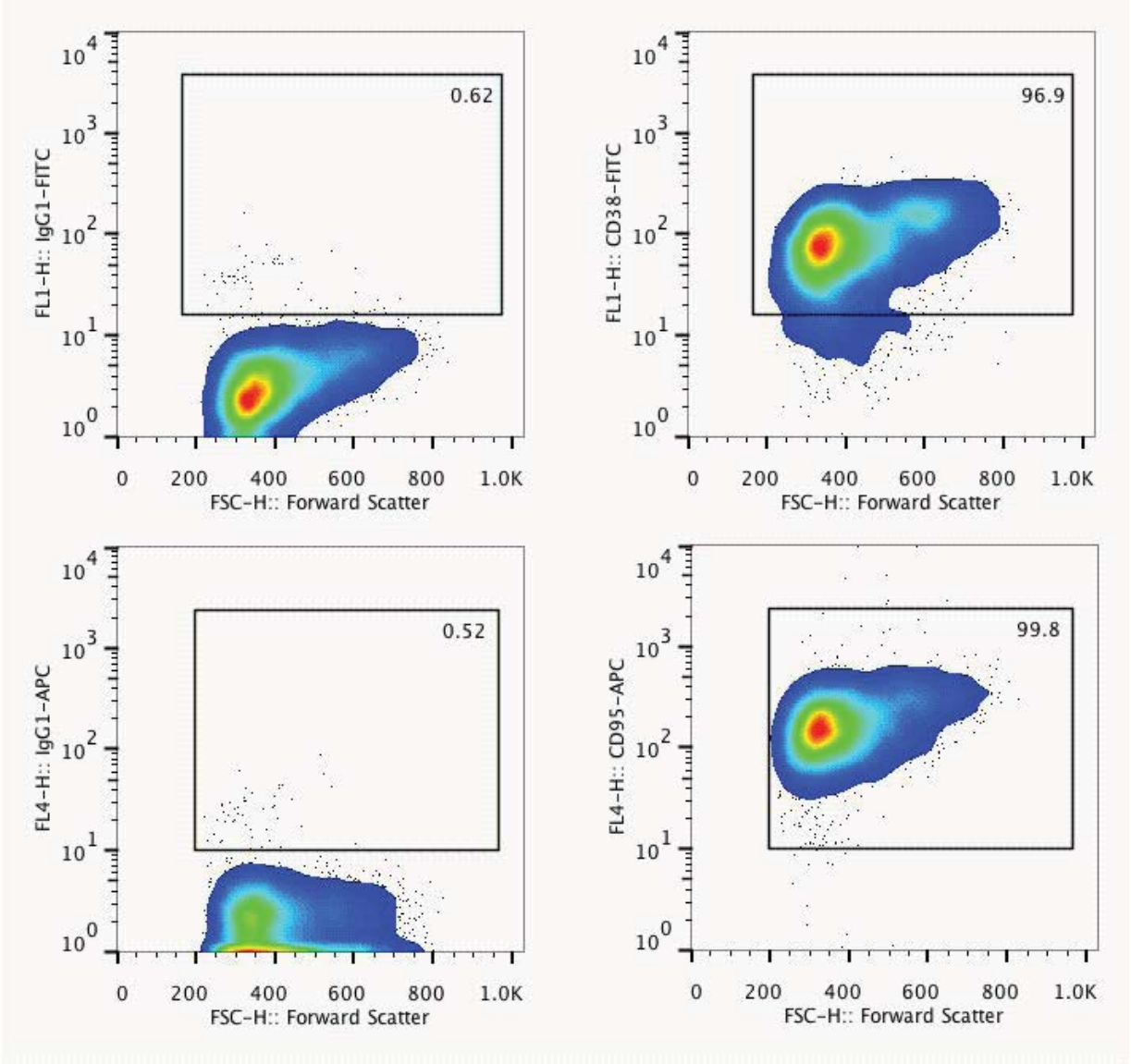

Supplemental Figure 3. Expression of activation markers CD38 and CD95 on propagated γδ T cells. Lymphocytes were gated by forward and side scatter and evaluated for expression of CD38 and CD95 (shown as a percentage). Left panels are isotype controls, upper right panel is CD38 expression, and bottom right panel is CD95 expression in one of four representative donors. Forward scatter is displayed on x-axes.

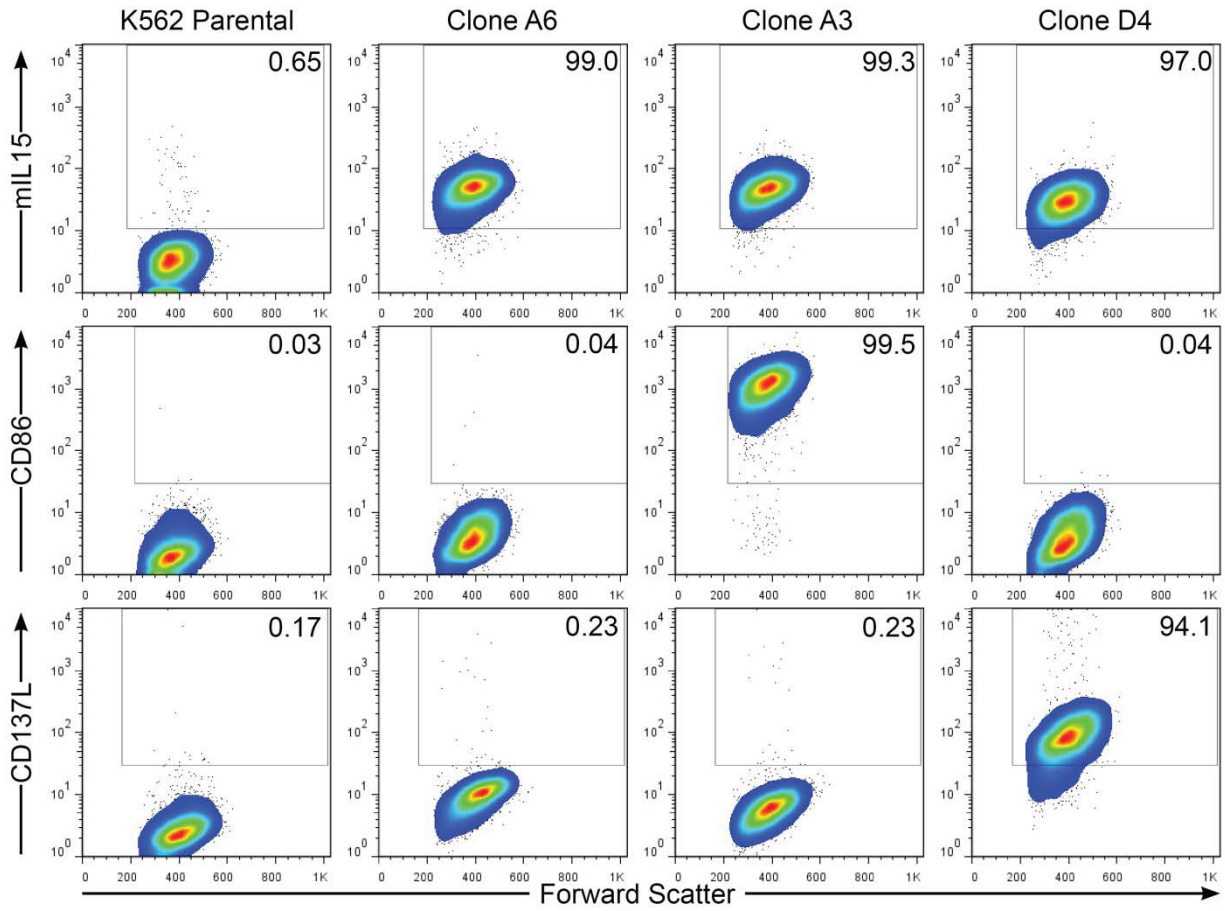

Supplemental Figure 4. aAPC developed for co-culture with γδ T cells to determine the impact of introduced co-stimulatory molecules. K562 cells were electroporated with SB transposase and transposon expressing a variant of membrane-bound IL-15 (mIL15), in which IL-15 cytokine/peptide is fused to IL-15 receptor-α. Genetically-modified cells were single-cell sorted by FACS to generate aAPC clone A6. Note that aAPC clone A6 uses a different variant of mIL15 than aAPC clone #4 (IL-15 cytokine is bound to surface of aAPC by IgG4 hinge/Fc stalk). Clone A6 was then electroporated with SB transposase and SB transposons containing either CD86 or CD137L and genetically modified cells were single cell sorted by FACS to generated aAPC clones A3 and D4. Cell surface immunophenotypes of aAPC are shown where forward scatter is displayed on x-axes and mIL15, CD86, and CD137L are displayed on top, middle, and bottom y-axes, respectively.

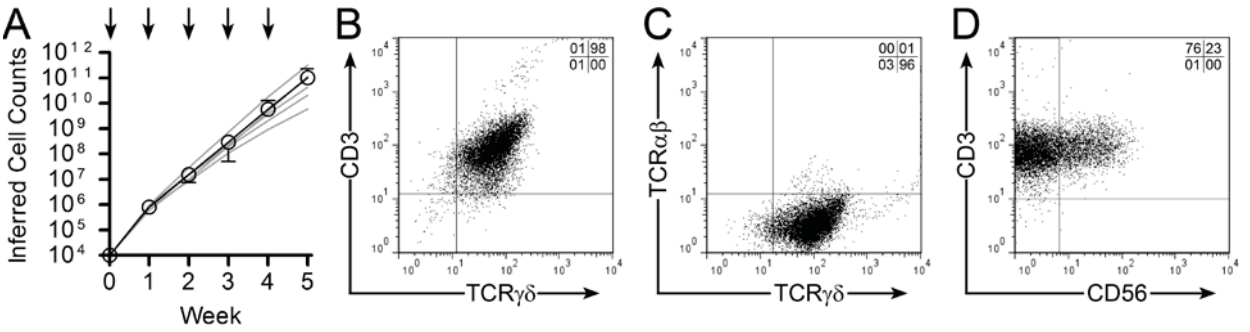

Supplemental Figure 5. Expansion of UCB-derived γδ T cells on aAPC with IL-2 and IL-21. γδ T cells from UCB units underwent FACS based on staining with CD3 and TCRγδ and were stimulated weekly with aAPC clone#4 in presence of soluble recombinant IL-2 and IL-21. (**A**) Total inferred cell numbers from co-cultures where black line represents the mean ± SD (n=5) pooled from 4 independent experiments and gray lines are the individual donors. Arrows represent the addition of γ-irradiated aAPC. Expression of (**B**) CD3 (y-axis) and TCRγδ (x-axis), (**C**) TCRαβ (y-axis) and TCRγδ (x-axis), and (**D**) CD3 (y-axis) and CD56 (x-axis) of a representative donor (1 of 5 from four independent experiments) by flow cytometry after 5 weeks of expansion on aAPC with IL-2 and IL-21. Quadrant frequencies (percentage) are displayed in upper right corners.

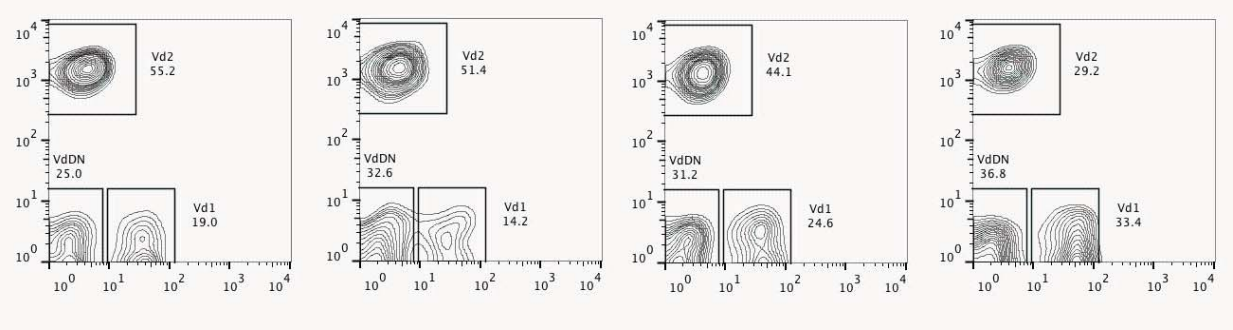

Supplemental Figure 6. Surface expression of TCRδ1 and TCRδ2 chains on γδ T cells derived from PBMC prior to propagation. Expression by flow cytometry of TCRδ2 (y-axes) and TCRδ1 (x-axes) on γδ T cells derived from PBMC prior to numeric expansion on aAPC. Each flow plot is an individual donor. Gate frequencies for each population (Vδ1, Vδ2, and $V\delta1^{neg}V\delta2^{neg}$ (VδDN)) are displayed next to gates. Gating strategy was lymphocytes, then $CD3^{+}TCR\gamma\delta^{+}$, then as shown.

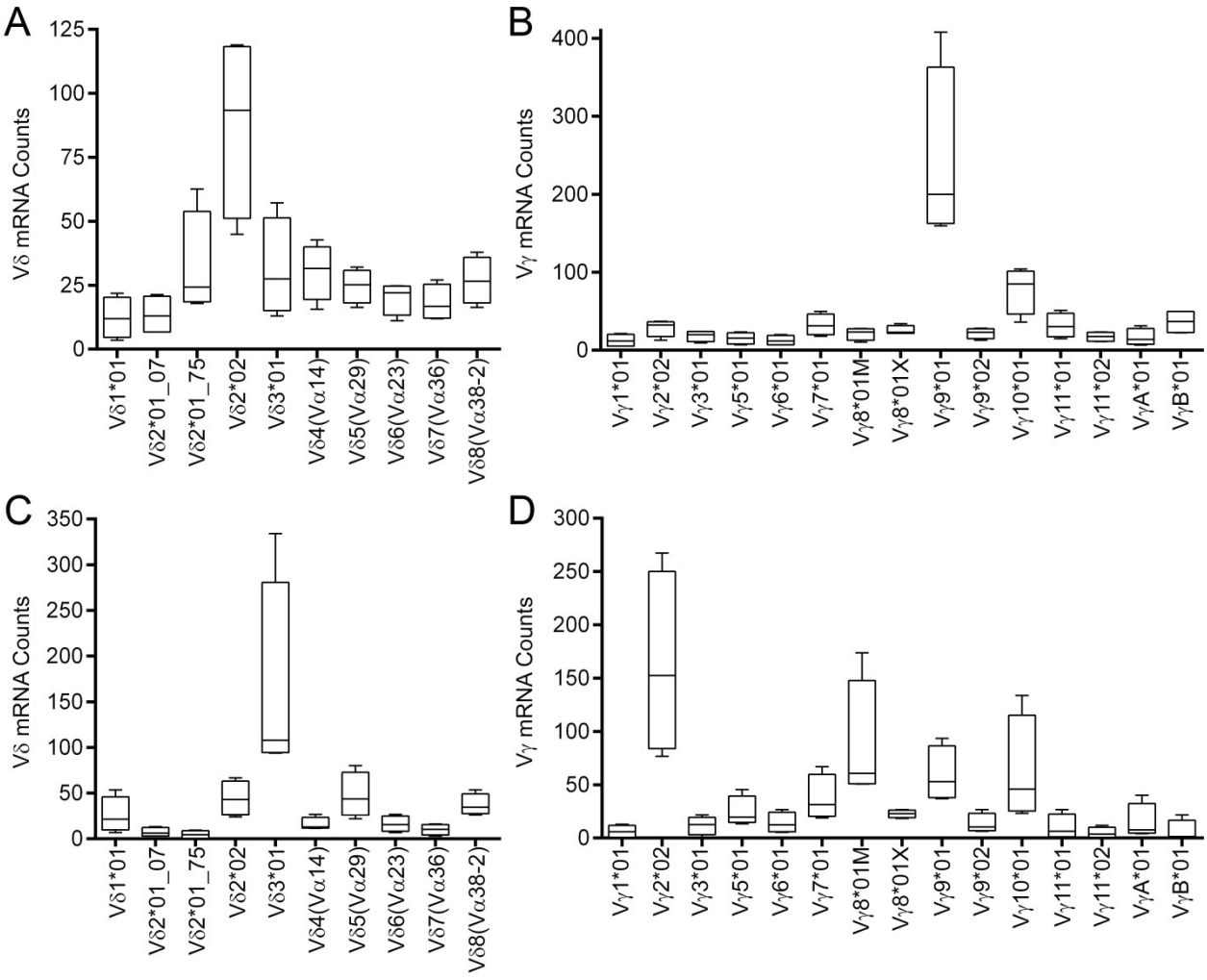

Supplemental Figure 7. Abundance of Vδ and Vγ mRNA species in γδ T cells prior to *ex vivo* numeric expansion. Quantification of mRNA species coding for (**A**) Vδ and (**B**) Vγ alleles in PBMC γδ T cells and (**C**) Vδ and (**D**) Vγ alleles in UCB γδ T cells by DTEA before co-culture (day 0) on aAPC/IL-2/IL-21. Box-and-whiskers plots display 25% and 75% percentiles where lines represent maximum, mean, and minimum from top to bottom (n=4).

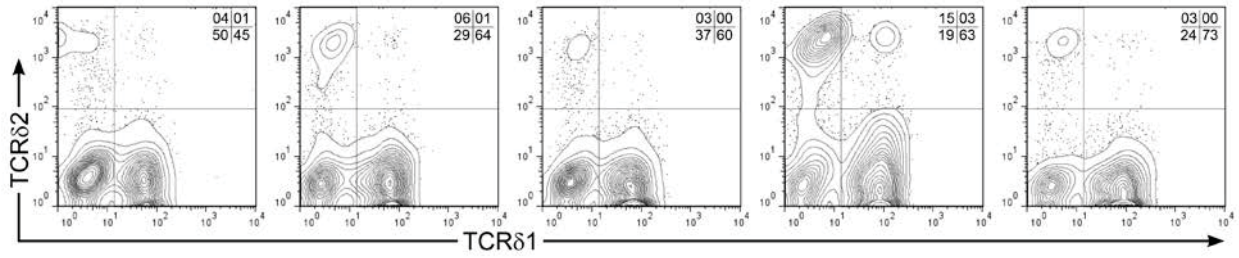

Supplemental Figure 8. Surface expression of TCRδ1 and TCRδ2 chains on γδ T cells derived from UCB and propagated on aAPC with IL-2 and IL-21. Expression by flow cytometry of TCRδ2 (y-axes) and TCRδ1 (x-axes) on γδ T cells derived from UCB following 35 days of co-culture on aAPC clone #4 in presence of IL-2 and IL-21. Quadrant frequencies (percentage) are displayed in upper right corners. T cells were propagated in 4 independent experiments.

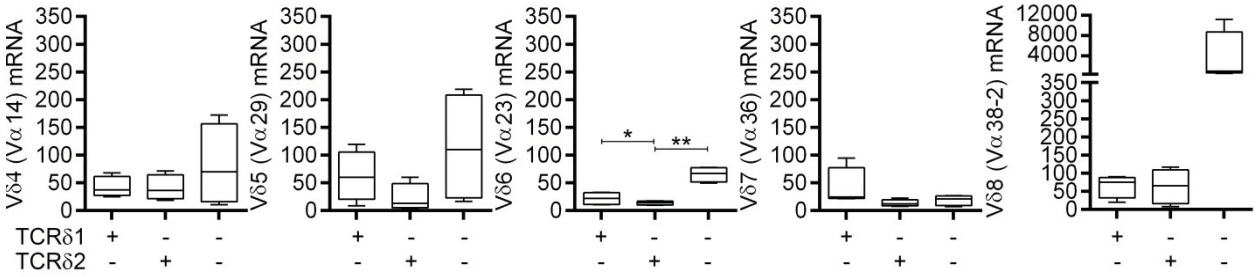

Supplemental Figure 9. mRNA expression of shared Vα/Vδ alleles in γδ T cells separated and then propagated on aAPC, IL-2, and IL-21. Expression of shared Vδ and Vα alleles by DTEA following 15 days of co-culture of Vδ1, Vδ2, and Vδ1^{neg}Vδ2^{neg} populations on aAPC clone #4 in presence of soluble IL-2 and IL-21. Detection of (from left to right) Vδ4 (Vα14), Vδ5 (Vα29), Vδ6 (Vα23), Vδ7 (Vα36), and Vδ8 (Vα38-2) in each separated subset. Student's paired two-tailed t-tests performed for statistical analysis between populations.

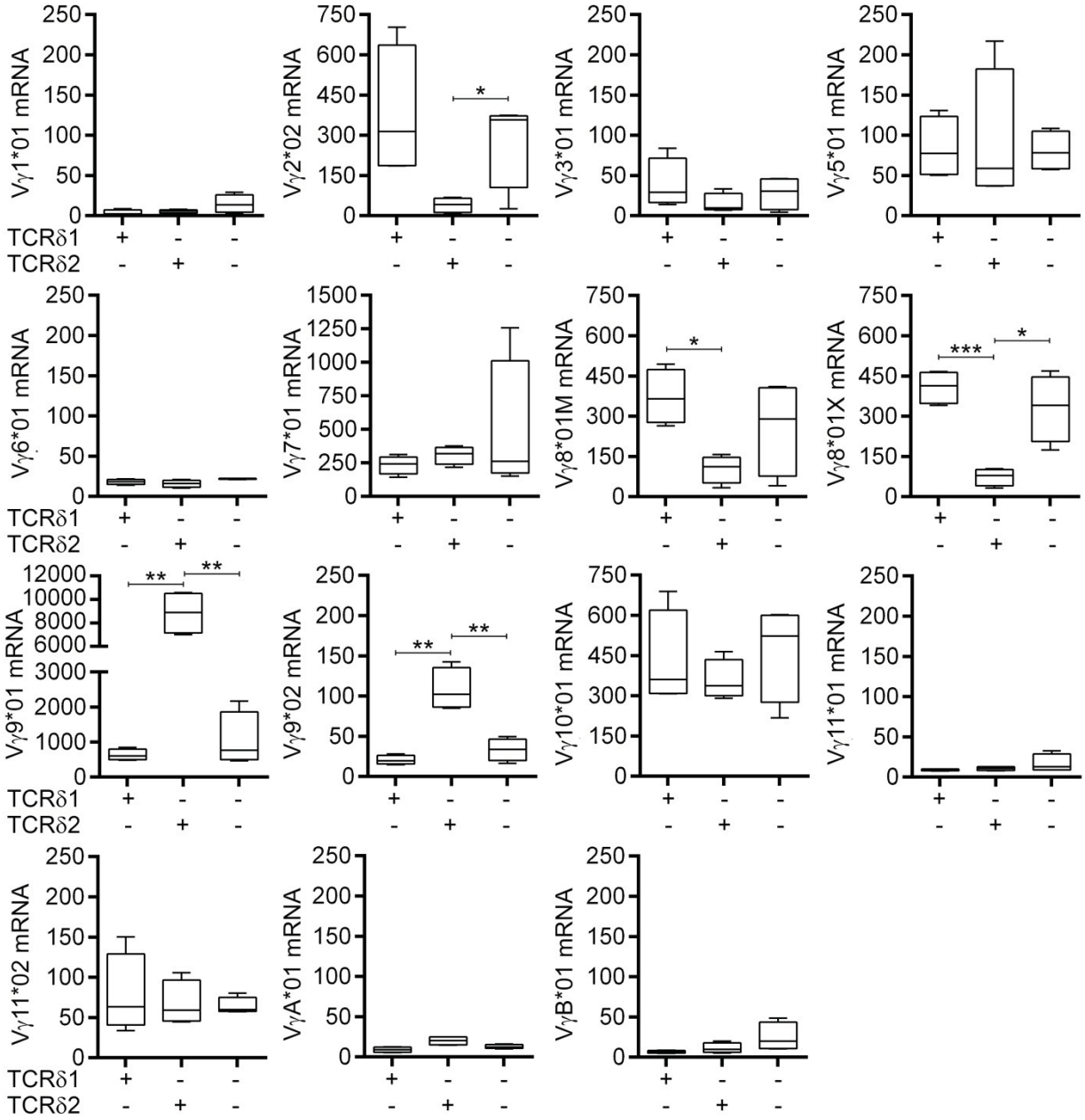

Supplemental Figure 10. Abundance of mRNA species coding for Vγ chains in γδ T-cell subsets. Polyclonal γδ T cells from PBMC were stimulated twice with aAPC clone #4 in presence of IL-2 and IL-21 and then FACS separated into TCRδ1^{+}TCRδ2^{neg}, TCRδ1^{neg}TCRδ2^{+}, and TCRδ1^{neg}TCRδ2^{neg} sub-populations. These were then stimulated as isolated subsets 2 more times with aAPC clone #4 in presence of IL-2 and IL-21. DTEA was used to identify and quantify mRNA coding for (from top left going left to right then top to bottom) Vγ1*01, Vγ2*02, Vγ3*01, Vγ5*01, Vγ6*01, Vγ7*01, Vγ8*01M, Vγ8*01X, Vγ9*01, Vγ9*02, Vγ10*01, Vγ11*01, Vγ11*02, VγA*01, and VγB*01. Box-and-whiskers plots display 25% and 75% percentiles where lines represent maximum, mean, and minimum from top to bottom (n=4). Student's paired two-tailed t-tests were performed for each allele between the Vδ-sorted populations. *p<0.05 and **p<0.01

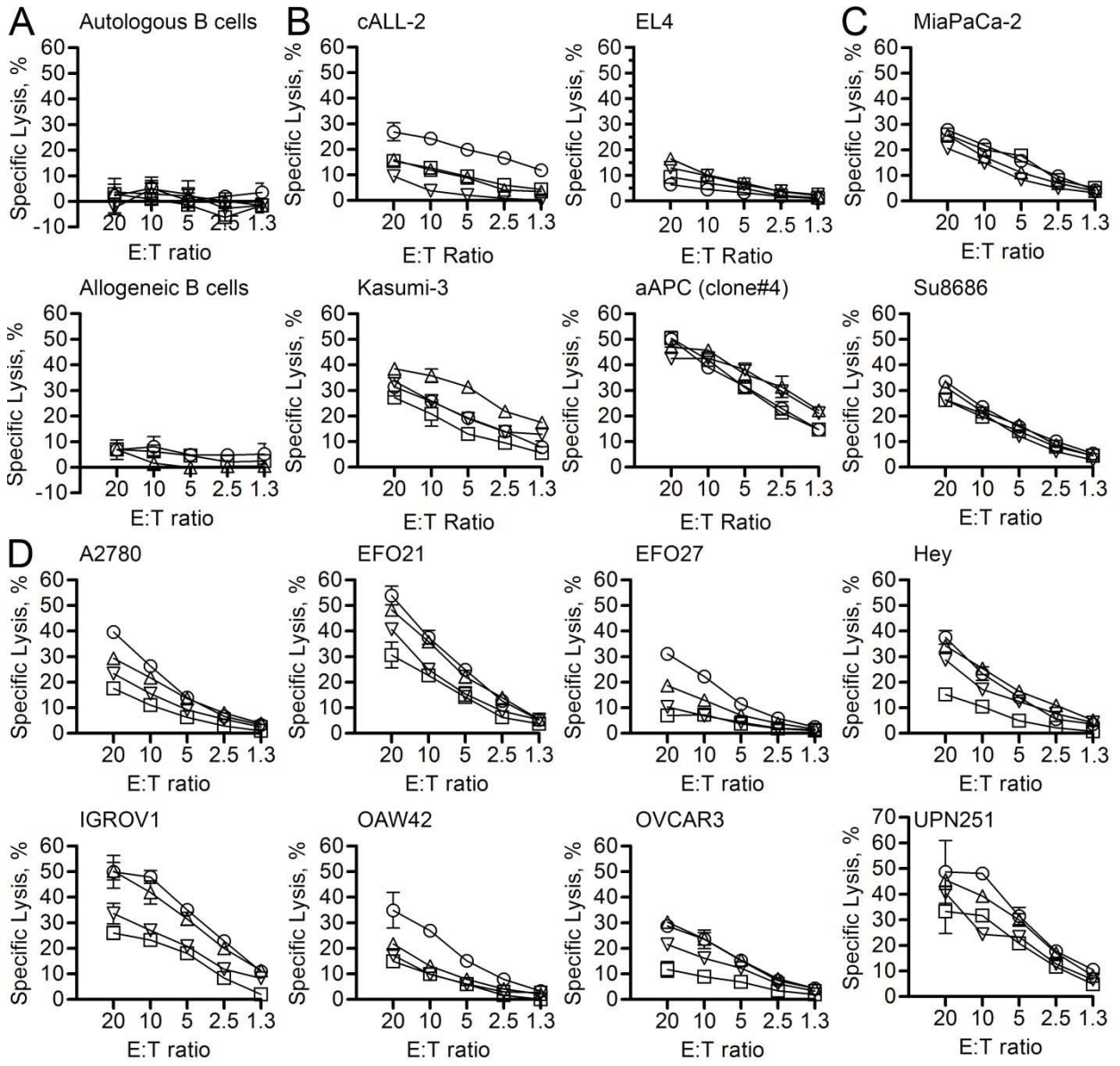

Supplemental Figure 11. *In vitro* lysis of tumor cell line panel by polyclonal γδ T cells. Standard 4-hour CRA were performed with increasing effector (polyclonal γδ T cells) to target (E:T) ratios against (**A**) healthy autologous and allogeneic (1 of 4 donors) B cells, (**B**) hematological cell lines derived from B-ALL: cALL-2, T-ALL (murine): EL4, undifferentiated leukemia: Kasumi-3, and K562-derived aAPC clone #4, (**C**) pancreatic cancer cell lines: MiaPaCa-2 and Su8686, and (**D**) ovarian cancer cell lines: A2780, EFO21, EFO27, Hey, IGROV1, OAW42, OVCAR3, and UPN251. Each line represents an individual γδ T-cell population derived from a PBMC donor and lysis data are presented as mean ± SD (n=3 wells per assay) pooled from 2 independent experiments.

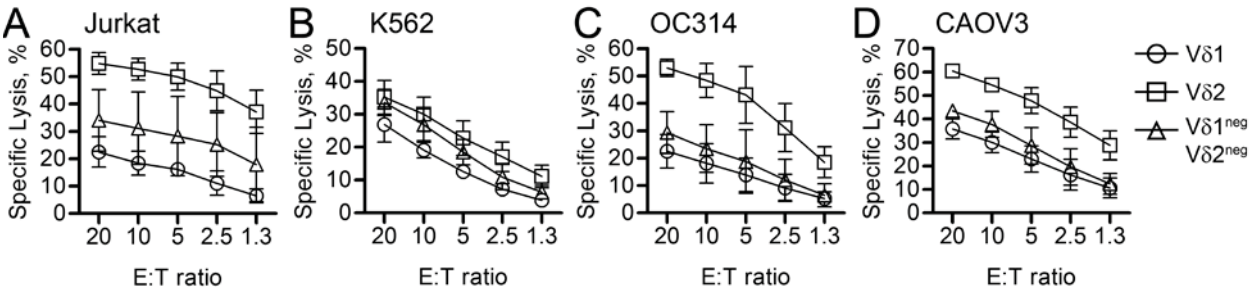

Supplemental Figure 12. Specific lysis of hematological and solid tumor cells by Vδ T-cell subsets. Standard 4-hour CRA with Vδ1 (circles), Vδ2 (squares), and $V\delta1^{neg}V\delta2^{neg}$ (triangles) γδ T-cell subsets effectors targeting (**A**) Jurkat, (**B**) K562, (**C**) OC314, and (**D**) CAOV3 cancer cell lines. Data were pooled from 2 independent experiments and are mean ± SD (n=4) of donor averages from triplicate measurements in CRA.

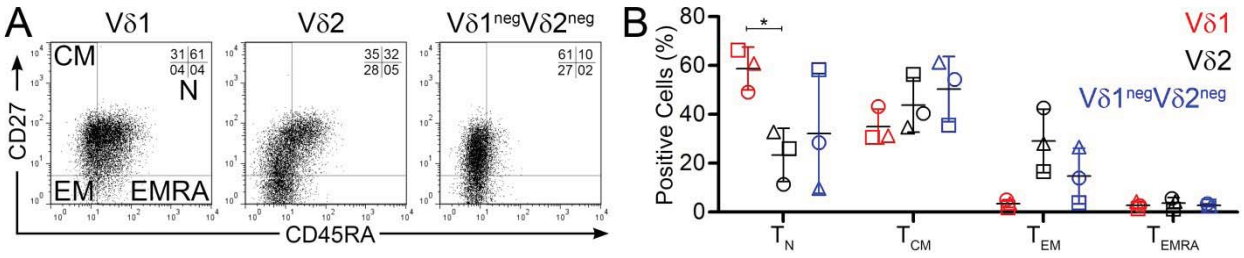

Supplemental Figure 13. Immunophenotypes associated with PBMC-derived Vδ T-cell subsets expanded on aAPC/IL-2/IL-21 (**A**) CD45RA and CD27 expression in Vδ1, Vδ2, and Vδ1^{neg}Vδ2^{neg} subsets (from left to right). (**B**) Assignment of γδ T cells to naïve (T_N), central memory (T_{CM}), effector memory (T_{EM}), and effector memory RA (T_{EMRA}) populations based on expression of CD27 and CD45RA, as indicated in part (**A**). Each shape represents a different donor and data are mean ± SD (n=3) pooled from 2 independent experiments. All flow plots are representative of 4 normal donors from 2 independent experiments. Quadrant frequencies (percentage) of flow plots are displayed in upper right corners.

Supplemental Table 1. Antibodies used.

Antibody specificity	Clone	Vendor
CD3	SK7	BD Biosciences
CD4	RPA-T4	BD Biosciences
CD8	RPA-T8	BD Biosciences
CD19	HIB19	BD Biosciences
CD25	M-A251	BD Biosciences
CD27	M-T271	BD Biosciences
CD28	L293	BD Biosciences
CD32	FLI8.26 (2003)	BD Biosciences
CD38	HB7	BD Biosciences
CD45RA	HI100	BD Biosciences
CD45RO	UCHL1	BD Biosciences
CD56	B159	BD Biosciences
CD57	NK-1	BD Biosciences
CD62L	Dreg 56	BD Biosciences
CD64	10.1	BD Biosciences
CD86	2331 FUN-1	BD Biosciences
CD95	DX2	BD Biosciences
CD122	TM-Beta 1	BD Biosciences
CD127	HIL-7R-M21	BD Biosciences
CD137L	C65-485	BD Biosciences
CCR7	TG8	eBiosciences
CXCR4	12G5	BD Biosciences
CLA	HECA-452	BD Biosciences
CCR4	1G1	BD Biosciences
ICOS	ISA-3	eBiosciences
PD-1	MIH4	BD Biosciences
TCRαβ	WT31	BD Biosciences
TCRγδ	B1	BD Biosciences
TCRγδ	IMMU510	Thermo Fisher
TCRδ1	TS-1	Thermo/Pierce
TCRδ2	B6	BD Biosciences
TCRγ9	B3	BD Biosciences
NMS	015-000-120	Jackson ImmunoResearch
DNAM1	DX11	BD Biosciences
NKG2D	1D11	BD Biosciences
IL15	34559	R&D Systems
IFNγ	4S.B3	BD Biosciences

SUPPLEMENTAL MATERIAL:

"Activating and propagating polyclonal gamma delta T cells with broad specificity for malignancies"

ADDITIONAL MATERIALS AND METHODS

Tumor cell line culture conditions

Cell cultures were maintained in (i) RPMI (Gibco, Grand Island NY): K562 parental cells, aAPC clone#4, aAPC clone A6, aAPC clone A3, aAPC clone D4, Jurkat, cALL-2, RCH-ACV, Kasumi-3, A2780, EFO21, EFO27, Hey, IGROV1, OC314, OVCAR3, and UPN251, (ii) DMEM (Sigma, St. Louis, MO): 293-METR, CAOV3, BxPC-3, MiaPaCa-2, OAW42, and Su8686, or (iii) McCoy's 5A (Sigma): HCT-116. Each media was supplemented with 10% heat-inactivated fetal bovine serum (Hyclone, Logan, UT) and 1% Glutamax-100 (Gibco). UPN251 and OAW42 cells were supplemented with insulin-transferrin-selenium solution (Gibco). Cells were cultured under humidified conditions with 5% CO_2 at 37^{o}C.

Co-culture of γδ T cells on designer aAPC, IL-2, and/or IL-21

In order to assess the dependence of γδ T cells on cytokines for proliferation, co-cultures were initiated with 10^5 γδ T cells and $2x10^5$ aAPC (clone #4) then were added to an equal volume of (i) CM, (ii) CM and 100 U/mL IL-2, (iii) CM and 60 ng/mL IL-21, or (iv) CM, 100 U/mL IL-2, and 60 ng/mL IL-21. T cells were enumerated using Cellometer Auto T4 Cell Counter

(Nexcelom, Lawrence, MA) 9 days after initiating co-cultures to determine yields. K562 cells were genetically modified with one or more co-stimulatory molecules to generate three new aAPC (**Supplemental Figure 4**). A *Sleeping Beauty* (SB) transposon expressing IL-15 peptide fused in frame to IL-15Rα and SB11 transposase were co-electro-transferred into parental K562 cells ($CD86^{neg}$ and $CD137L^{neg}$) using by Nucleofection (Nucleofector II, Lonza, Basel, Switzerland) and Kit V (cat# VCA-1003, Lonza). FACS was used to isolate $mIL15^{+}$ cells and establish a clone (designated clone A6; $mIL15^{+}CD86^{neg}CD137L^{neg}$) which was then electroporated with SB11 and SB transposons expressing CD86 or CD137L. Cells were FACS sorted again to obtain clones A3 ($mIL15^{+}CD86^{+}CD137L^{neg}$) and D4 ($mIL15^{+}CD86^{neg}CD137L^{+}$). Co-cultures were initiated with 10^5 γδ T cells in CM supplemented with 100 U/mL IL-2 and 60 ng/mL IL-21 and were added to $2x10^5$ γ-irradiated (i) parental K562 cells, (ii) clone A6, (iii) clone A3, (iv) clone D4, (v) clone #4 aAPC, or (vi) no aAPC. T cells were enumerated 9 days after initiating as described above for cytokine experiments.

Intracellular cytokine production, Luminex, and neutralizing antibody cytolysis assays

For intracellular cytokine analyses, γδ T cells were incubated with NMS or TCRγδ blocking antibody (clone IMMU510 (IM); Thermo Fisher, Pittsburg, PA) at 37°C for 1 hour and added to an equal volume and number of target cells (CAOV3 or OC314) to yield final antibody concentration of 1.0 μg/mL. Co-cultures were incubated for 6 hours at 37°C in the presence of Brefeldin-A (GolgiPlug; BD Biosciences) to block exocytosis and secretion of cytokines. Co-cultures were then (i) stained for surface markers, *e.g.*, CD3, TCRδ1, and TCRδ2, (ii) fixed and permeabilized with BD Cytofix/Cytoperm (cat# 555028, BD Biosciences), (iii) stained for

intracellular IFNγ, and (iv) analyzed by flow cytometry. Co-cultures to assess cytokine secretion were incubated for 24 hours in CM (mock treatment) or leukocyte activation cocktail (LAC; 5 ng/mL PMA and 500 ng/mL Ionomycin) and supernatants from triplicate wells were pooled and analyzed by Bio-Plex Human Cytokine Group-I 27-plex Assay (cat# L50-0KCAF0Y, BioRad Technologies, Hercules, CA) using Luminex100 (xMap Technologies, Austin, TX). B cells from healthy donors were isolated with CD19 microbeads (cat# 130-050-301, Miltenyi Biotec) the day of each assay and used as target cells in CRA. Antibodies specific for NKG2D (clone 1D11; BD Biosciences), DNAM1 (clone DX11; BD Biosciences), and TCRγδ (clone IM) were used for neutralization experiments at 0.3, 1.0, and 3.0 μg/mL in CRA at E:T ratio of 12:1. Normal mouse serum (NMS; Jackson ImmunoResearch) was used as a negative control at the same concentrations and wells without antibodies were used for purposes of data normalization.

Lentivirus packaging and transduction of CAOV3 cells

Lentivirus particles were packaged according to a modified version of a protocol described elsewhere (29) to introduce mKate red fluorescence protein and enhanced *firefly Luciferase* (e*ffLuc*) into tumor cells for non-invasive imaging by BLI (30). Briefly, packaging cells (293-METR) were plated on T125 flasks and transfected the following day with pCMV R8.2, VSV-G, and pLVU3G-e*ffLuc*-T2A-mKateS158A (**Supplemental Figure 2**) plasmids in conjunction with Lipofectamine 2000 transfection reagent according to manufacturer's instructions (Invitrogen). Viral particles were harvested 48 and 72 hours post-transfection and concentrated through 100 kDa NMWL filters (cat# UFC810096, MilliPore, Billerica, MA). CAOV3 cells were plated in a 6-well plate and the following day virus coding for e*ffLuc*-mKate was added with 8 μg/ml

polybrene. Plate was spun at 1,800 rpm for 1.5 hours and 6 hours later the viral-conditioned supernatant was replaced with DMEM complete media, which was changed the following day. Single-cell clones of transduced CAOV3 were derived by limiting dilution that displayed the same morphology as the parental cell line and clone 1C2 was chosen as it had uniform mKate fluorescence with high ($>10^6$ signal to noise ratio) e*ffLuc* activity.

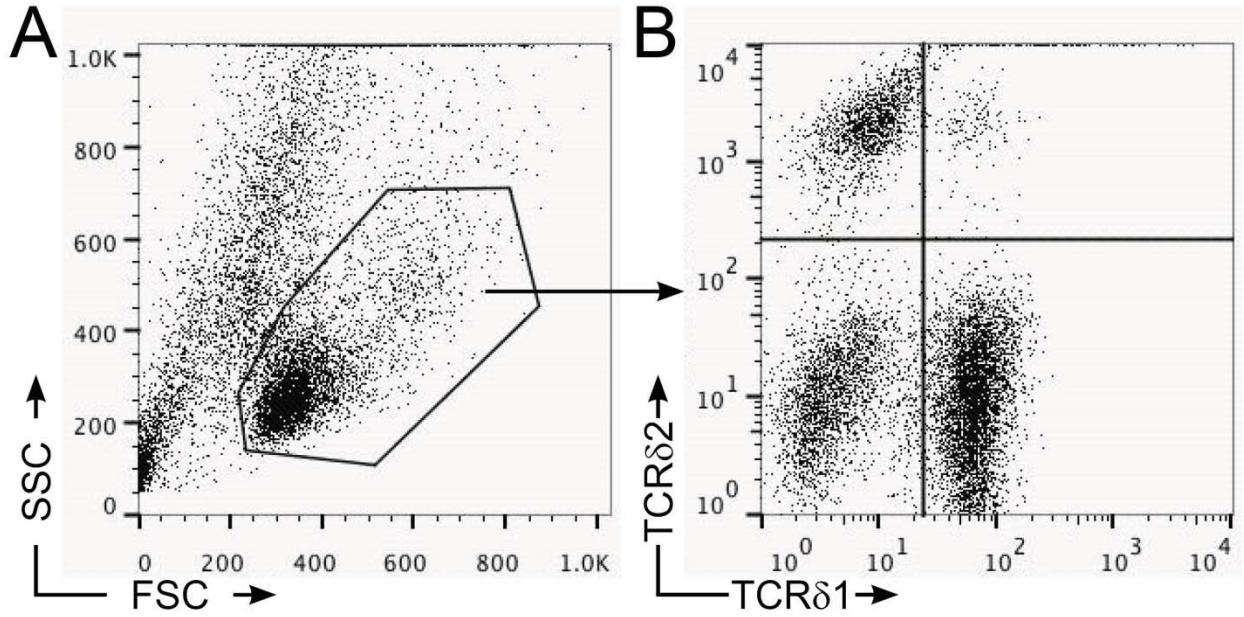

Supplemental Figure 1. An example of the gating strategy for γδ T-cell analyses. (A) Lymphocytes were gated by forward scatter (FSC) and side scatter (SSC) in the activated T-cell gate and were (B) analyzed for surface protein expression of markers of interest. A representative donor's expression of TCRδ1 and TCRδ2 are shown. Isotype controls were used to validate gating. Staining was performed as described (27).

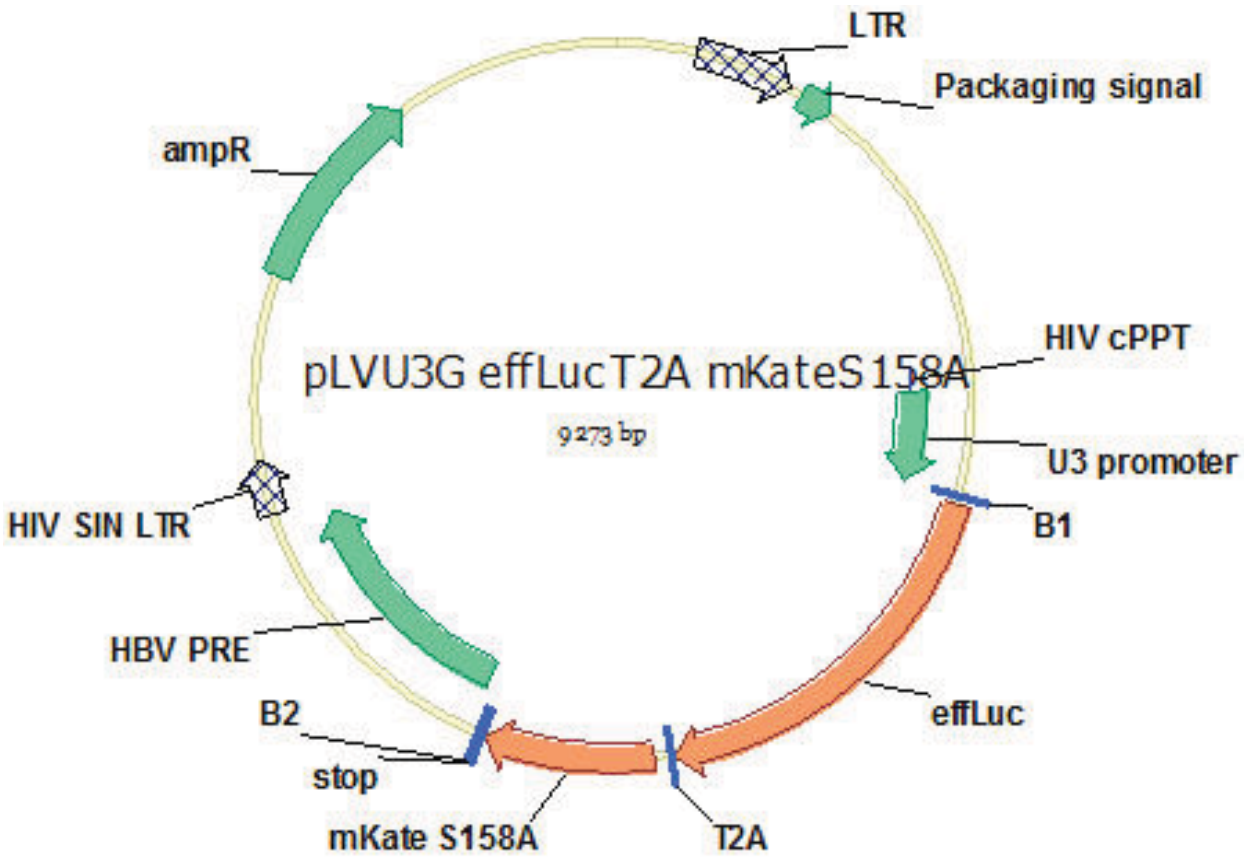

Supplemental Figure 2. Schematic of DNA plasmid pLVU3G-e*ffLuc*-T2A-mKateS158A used to co-express enhanced firefly luciferase (e*ffLuc*) and mKate. Annotations are, LTR: long terminal repeat; HIV cPPT: HIV central polypurine tract; B1: Gateway donor site B1; e*ffLuc*: enhanced *firefly Luciferase*; T2A: T2A ribosomal slip site; mKate S158A: enhanced mKate red fluorescence protein; B2: Gateway donor site B2; HBV PRE: Hepatitis B post-translational regulatory element; HIV SIN LTR: HIV self-inactivating long terminal repeat; ampR: ampicillin resistance (β-Lactamase).

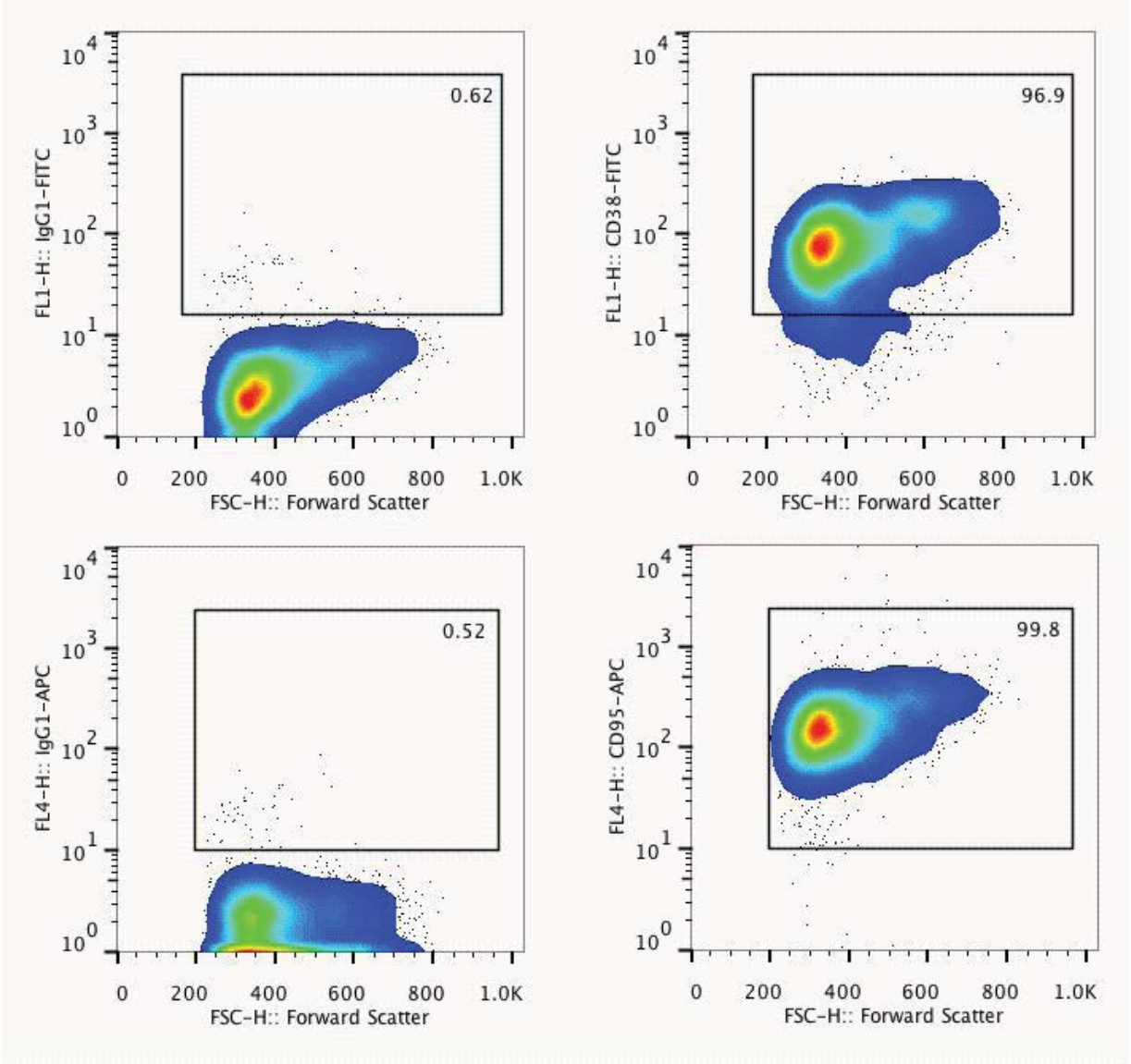

Supplemental Figure 3. Expression of activation markers CD38 and CD95 on propagated γδ T cells. Lymphocytes were gated by forward and side scatter and evaluated for expression of CD38 and CD95 (shown as a percentage). Left panels are isotype controls, upper right panel is CD38 expression, and bottom right panel is CD95 expression in one of four representative donors. Forward scatter is displayed on x-axes.

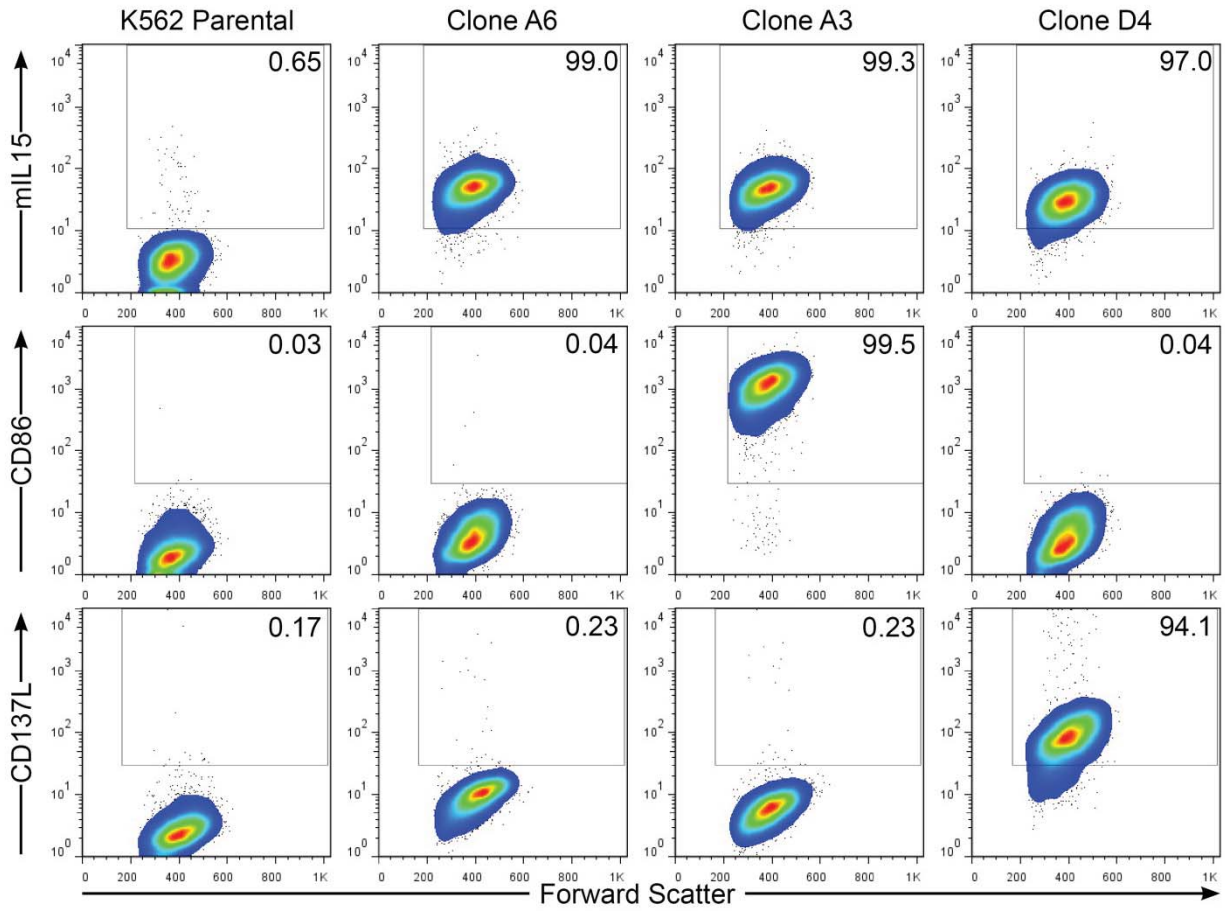

Supplemental Figure 4. aAPC developed for co-culture with γδ T cells to determine the impact of introduced co-stimulatory molecules. K562 cells were electroporated with SB transposase and transposon expressing a variant of membrane-bound IL-15 (mIL15), in which IL-15 cytokine/peptide is fused to IL-15 receptor-α. Genetically-modified cells were single-cell sorted by FACS to generate aAPC clone A6. Note that aAPC clone A6 uses a different variant of mIL15 than aAPC clone #4 (IL-15 cytokine is bound to surface of aAPC by IgG4 hinge/Fc stalk). Clone A6 was then electroporated with SB transposase and SB transposons containing either CD86 or CD137L and genetically modified cells were single cell sorted by FACS to generated aAPC clones A3 and D4. Cell surface immunophenotypes of aAPC are shown where forward scatter is displayed on x-axes and mIL15, CD86, and CD137L are displayed on top, middle, and bottom y-axes, respectively.

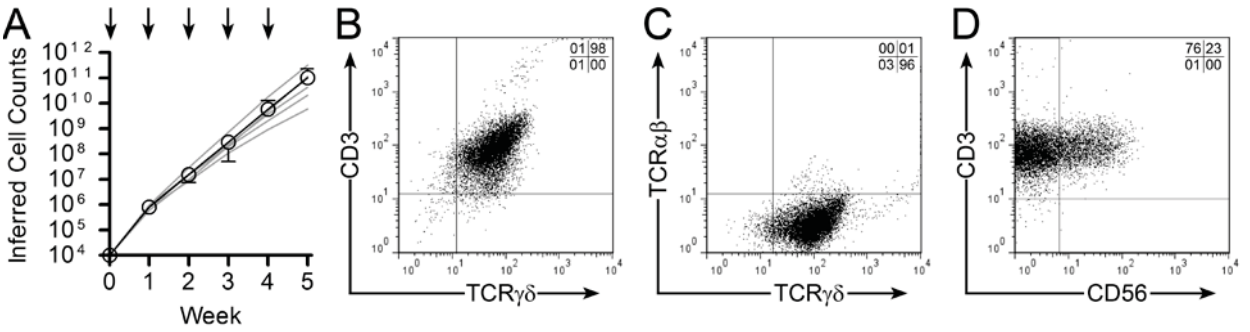

Supplemental Figure 5. Expansion of UCB-derived γδ T cells on aAPC with IL-2 and IL-21. γδ T cells from UCB units underwent FACS based on staining with CD3 and TCRγδ and were stimulated weekly with aAPC clone#4 in presence of soluble recombinant IL-2 and IL-21. (**A**) Total inferred cell numbers from co-cultures where black line represents the mean ± SD (n=5) pooled from 4 independent experiments and gray lines are the individual donors. Arrows represent the addition of γ-irradiated aAPC. Expression of (**B**) CD3 (y-axis) and TCRγδ (x-axis), (**C**) TCRαβ (y-axis) and TCRγδ (x-axis), and (**D**) CD3 (y-axis) and CD56 (x-axis) of a representative donor (1 of 5 from four independent experiments) by flow cytometry after 5 weeks of expansion on aAPC with IL-2 and IL-21. Quadrant frequencies (percentage) are displayed in upper right corners.

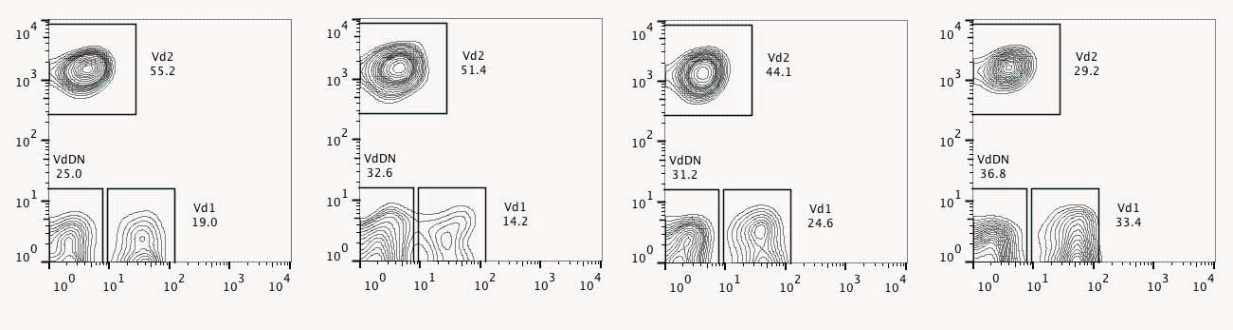

Supplemental Figure 6. Surface expression of TCRδ1 and TCRδ2 chains on γδ T cells derived from PBMC prior to propagation. Expression by flow cytometry of TCRδ2 (y-axes) and TCRδ1 (x-axes) on γδ T cells derived from PBMC prior to numeric expansion on aAPC. Each flow plot is an individual donor. Gate frequencies for each population (Vδ1, Vδ2, and $V\delta1^{neg}V\delta2^{neg}$ (VδDN)) are displayed next to gates. Gating strategy was lymphocytes, then $CD3^{+}TCR\gamma\delta^{+}$, then as shown.

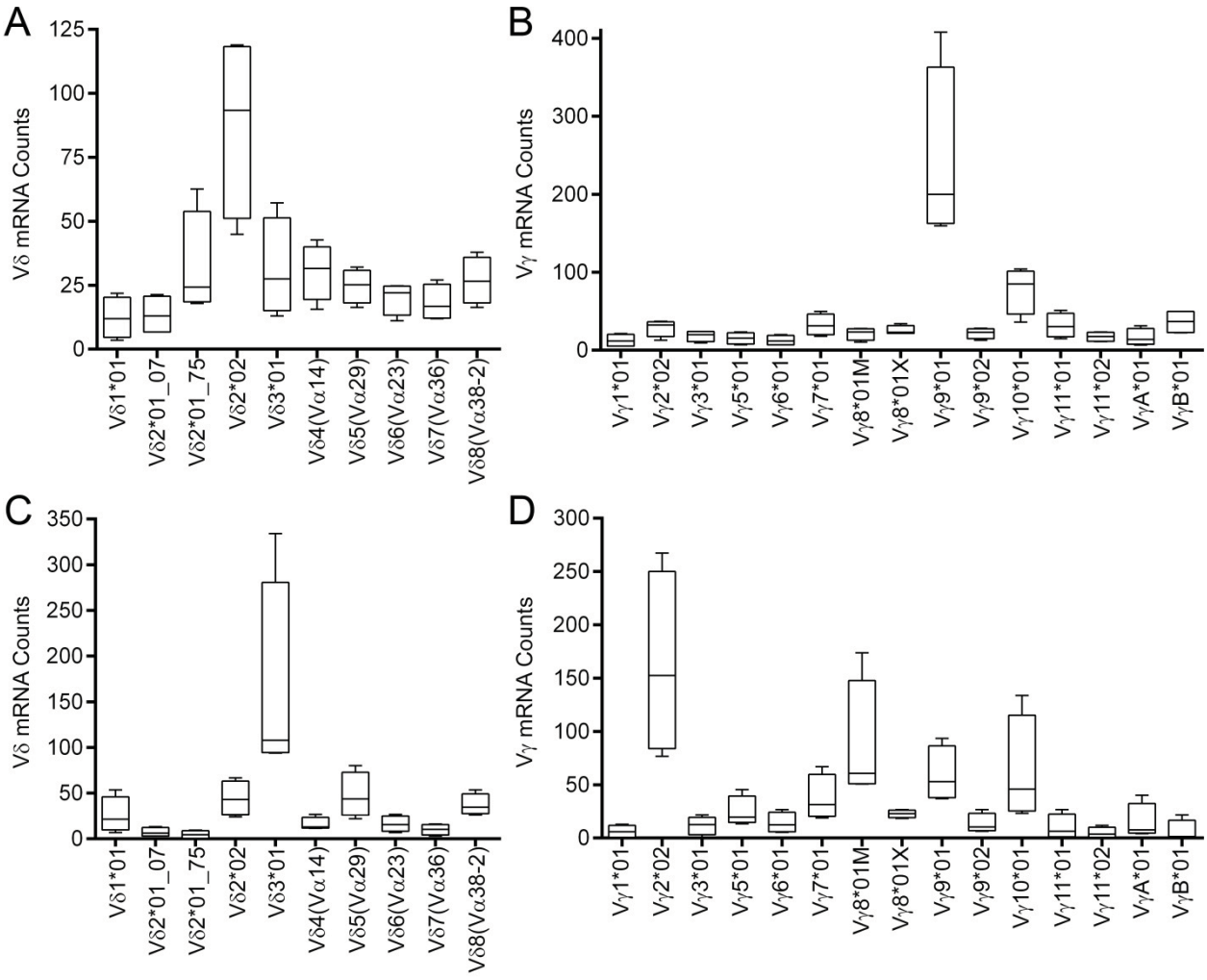

Supplemental Figure 7. Abundance of Vδ and Vγ mRNA species in γδ T cells prior to *ex vivo* numeric expansion. Quantification of mRNA species coding for (**A**) Vδ and (**B**) Vγ alleles in PBMC γδ T cells and (**C**) Vδ and (**D**) Vγ alleles in UCB γδ T cells by DTEA before co-culture (day 0) on aAPC/IL-2/IL-21. Box-and-whiskers plots display 25% and 75% percentiles where lines represent maximum, mean, and minimum from top to bottom (n=4).

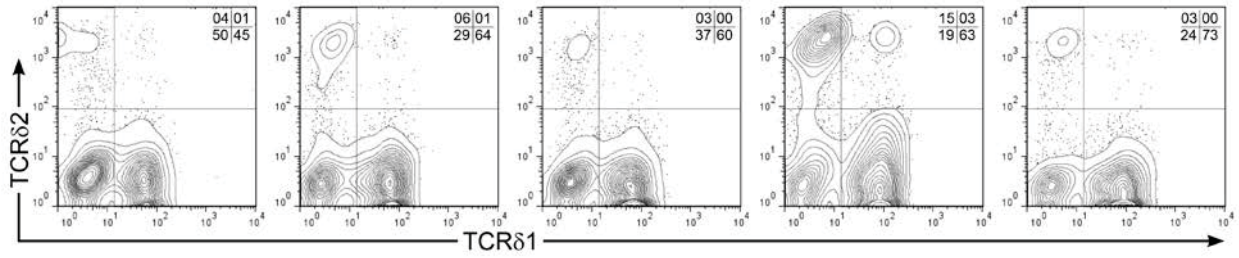

Supplemental Figure 8. Surface expression of TCRδ1 and TCRδ2 chains on γδ T cells derived from UCB and propagated on aAPC with IL-2 and IL-21. Expression by flow cytometry of TCRδ2 (y-axes) and TCRδ1 (x-axes) on γδ T cells derived from UCB following 35 days of co-culture on aAPC clone #4 in presence of IL-2 and IL-21. Quadrant frequencies (percentage) are displayed in upper right corners. T cells were propagated in 4 independent experiments.

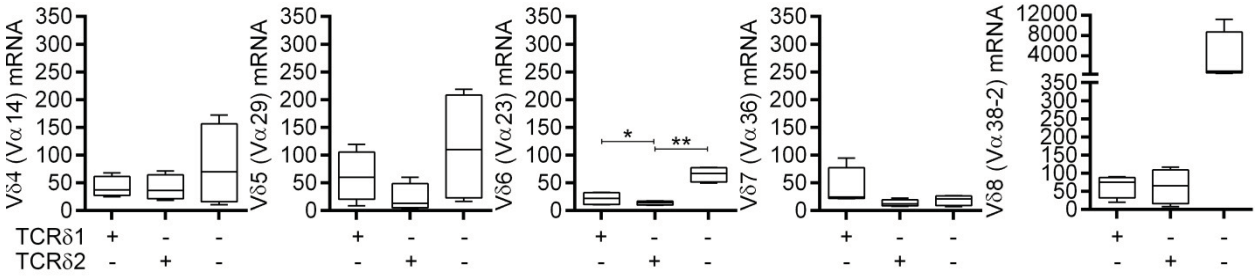

Supplemental Figure 9. mRNA expression of shared Vα/Vδ alleles in γδ T cells separated and then propagated on aAPC, IL-2, and IL-21. Expression of shared Vδ and Vα alleles by DTEA following 15 days of co-culture of Vδ1, Vδ2, and Vδ1^{neg}Vδ2^{neg} populations on aAPC clone #4 in presence of soluble IL-2 and IL-21. Detection of (from left to right) Vδ4 (Vα14), Vδ5 (Vα29), Vδ6 (Vα23), Vδ7 (Vα36), and Vδ8 (Vα38-2) in each separated subset. Student's paired two-tailed t-tests performed for statistical analysis between populations.

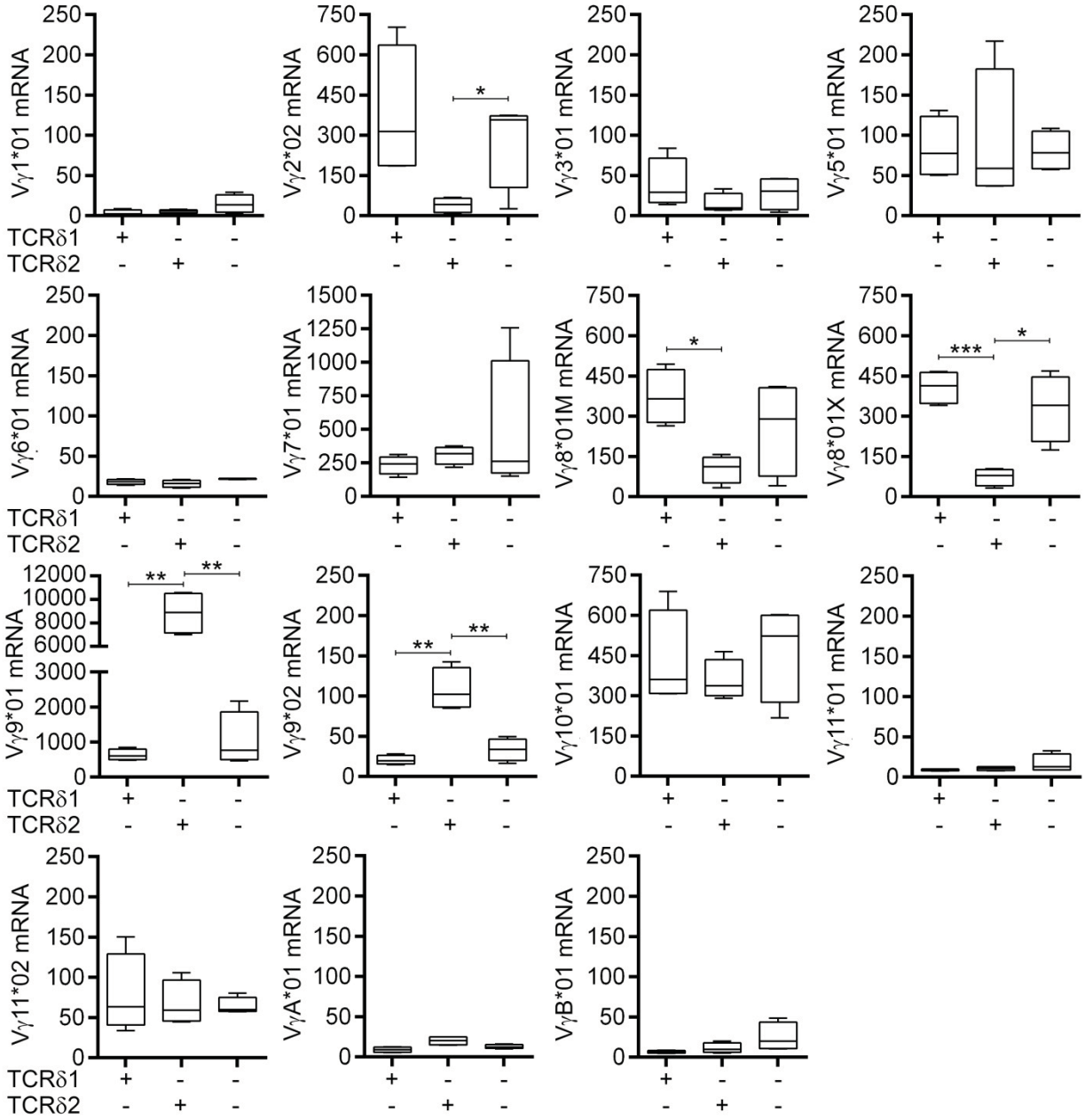

Supplemental Figure 10. Abundance of mRNA species coding for Vγ chains in γδ T-cell subsets. Polyclonal γδ T cells from PBMC were stimulated twice with aAPC clone #4 in presence of IL-2 and IL-21 and then FACS separated into TCRδ1^{+}TCRδ2^{neg}, TCRδ1^{neg}TCRδ2^{+}, and TCRδ1^{neg}TCRδ2^{neg} sub-populations. These were then stimulated as isolated subsets 2 more times with aAPC clone #4 in presence of IL-2 and IL-21. DTEA was used to identify and quantify mRNA coding for (from top left going left to right then top to bottom) Vγ1*01, Vγ2*02, Vγ3*01, Vγ5*01, Vγ6*01, Vγ7*01, Vγ8*01M, Vγ8*01X, Vγ9*01, Vγ9*02, Vγ10*01, Vγ11*01, Vγ11*02, VγA*01, and VγB*01. Box-and-whiskers plots display 25% and 75% percentiles where lines represent maximum, mean, and minimum from top to bottom (n=4). Student's paired two-tailed t-tests were performed for each allele between the Vδ-sorted populations. *p<0.05 and **p<0.01

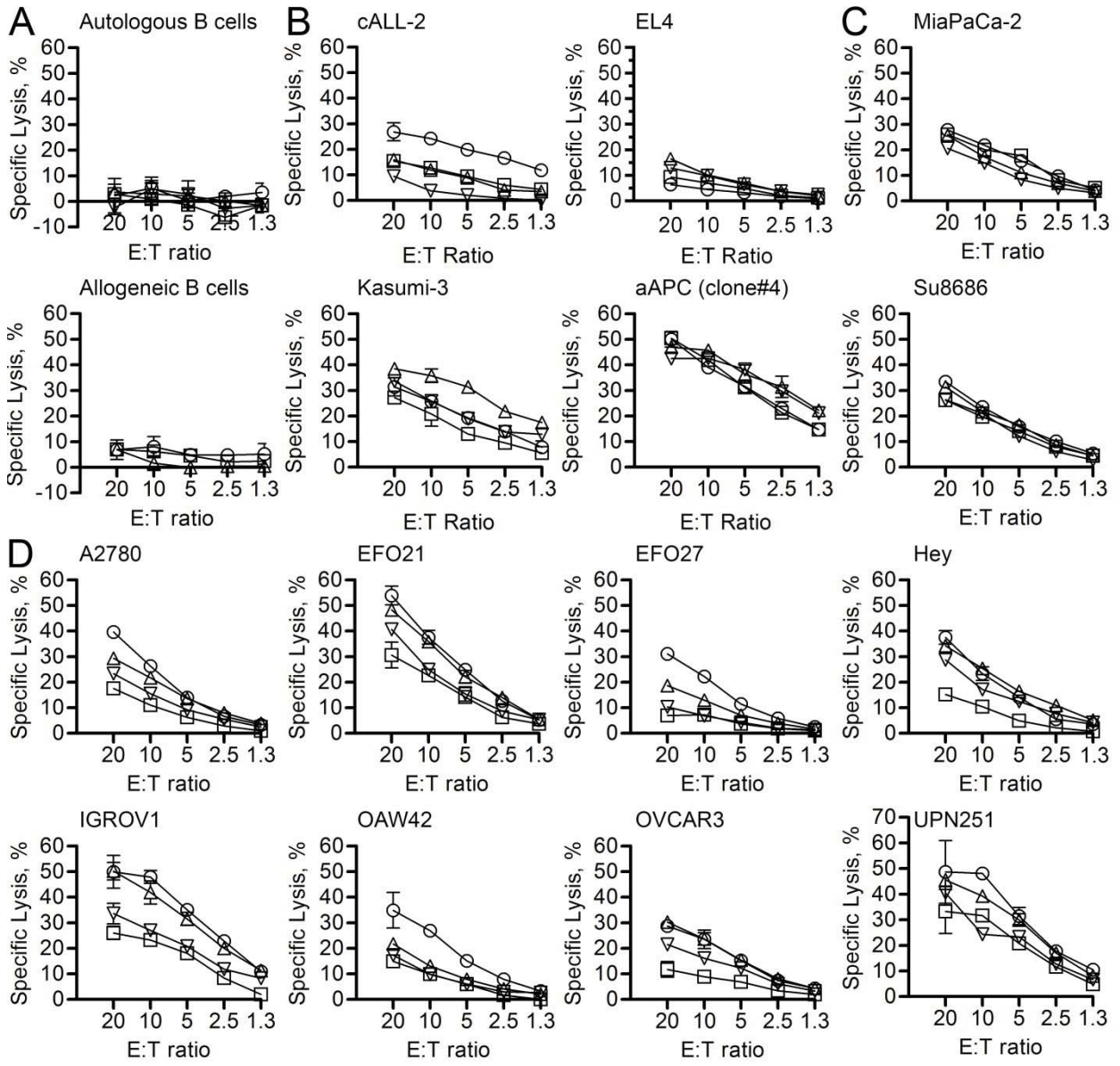

Supplemental Figure 11. *In vitro* lysis of tumor cell line panel by polyclonal γδ T cells. Standard 4-hour CRA were performed with increasing effector (polyclonal γδ T cells) to target (E:T) ratios against (**A**) healthy autologous and allogeneic (1 of 4 donors) B cells, (**B**) hematological cell lines derived from B-ALL: cALL-2, T-ALL (murine): EL4, undifferentiated leukemia: Kasumi-3, and K562-derived aAPC clone #4, (**C**) pancreatic cancer cell lines: MiaPaCa-2 and Su8686, and (**D**) ovarian cancer cell lines: A2780, EFO21, EFO27, Hey, IGROV1, OAW42, OVCAR3, and UPN251. Each line represents an individual γδ T-cell population derived from a PBMC donor and lysis data are presented as mean ± SD (n=3 wells per assay) pooled from 2 independent experiments.

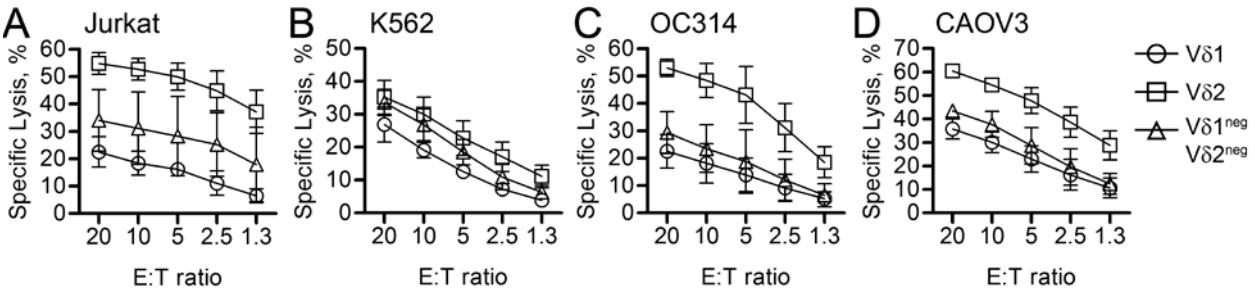

Supplemental Figure 12. Specific lysis of hematological and solid tumor cells by Vδ T-cell subsets. Standard 4-hour CRA with Vδ1 (circles), Vδ2 (squares), and $V\delta1^{neg}V\delta2^{neg}$ (triangles) γδ T-cell subsets effectors targeting (**A**) Jurkat, (**B**) K562, (**C**) OC314, and (**D**) CAOV3 cancer cell lines. Data were pooled from 2 independent experiments and are mean ± SD (n=4) of donor averages from triplicate measurements in CRA.

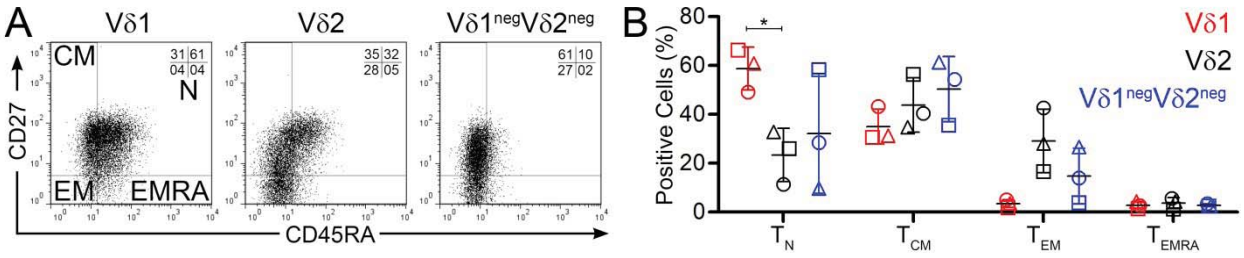

Supplemental Figure 13. Immunophenotypes associated with PBMC-derived Vδ T-cell subsets expanded on aAPC/IL-2/IL-21 (**A**) CD45RA and CD27 expression in Vδ1, Vδ2, and Vδ1^{neg}Vδ2^{neg} subsets (from left to right). (**B**) Assignment of γδ T cells to naïve (T_N), central memory (T_{CM}), effector memory (T_{EM}), and effector memory RA (T_{EMRA}) populations based on expression of CD27 and CD45RA, as indicated in part (**A**). Each shape represents a different donor and data are mean ± SD (n=3) pooled from 2 independent experiments. All flow plots are representative of 4 normal donors from 2 independent experiments. Quadrant frequencies (percentage) of flow plots are displayed in upper right corners.

Supplemental Table 1. Antibodies used.

Antibody specificity	Clone	Vendor
CD3	SK7	BD Biosciences
CD4	RPA-T4	BD Biosciences
CD8	RPA-T8	BD Biosciences
CD19	HIB19	BD Biosciences
CD25	M-A251	BD Biosciences
CD27	M-T271	BD Biosciences
CD28	L293	BD Biosciences
CD32	FLI8.26 (2003)	BD Biosciences
CD38	HB7	BD Biosciences
CD45RA	HI100	BD Biosciences
CD45RO	UCHL1	BD Biosciences
CD56	B159	BD Biosciences
CD57	NK-1	BD Biosciences
CD62L	Dreg 56	BD Biosciences
CD64	10.1	BD Biosciences
CD86	2331 FUN-1	BD Biosciences
CD95	DX2	BD Biosciences
CD122	TM-Beta 1	BD Biosciences
CD127	HIL-7R-M21	BD Biosciences
CD137L	C65-485	BD Biosciences
CCR7	TG8	eBiosciences
CXCR4	12G5	BD Biosciences
CLA	HECA-452	BD Biosciences
CCR4	1G1	BD Biosciences
ICOS	ISA-3	eBiosciences
PD-1	MIH4	BD Biosciences
TCRαβ	WT31	BD Biosciences
TCRγδ	B1	BD Biosciences
TCRγδ	IMMU510	Thermo Fisher
TCRδ1	TS-1	Thermo/Pierce
TCRδ2	B6	BD Biosciences
TCRγ9	B3	BD Biosciences
NMS	015-000-120	Jackson ImmunoResearch
DNAM1	DX11	BD Biosciences
NKG2D	1D11	BD Biosciences
IL15	34559	R&D Systems
IFNγ	4S.B3	BD Biosciences